March 2011

contact: qualif@mercator-ocean.fr

QuO Va Dis?
Quarterly Ocean Validation Display #3

Validation bulletin for October-November-December (OND) 2010

Edition:
Charles Desportes, Marie Drévillon, Charly Régnier
(MERCATOR OCEAN/Production Dep./Products Quality)

Contributions :
Eric Greiner, Benoît Tranchant, Hélène Etienne (CLS)
Jean-Michel Lellouche, Olivier Le Galloudec, Gilles Garric (MERCATOR OCEAN/ Production Dep./R&D)

Credits for validation methodology and tools:
Eric Greiner, Mounir Benkiran, Nathalie Verbrugge, Hélène Etienne (CLS)
Fabrice Hernandez, Laurence Crosnier (MERCATOR OCEAN)
Nicolas Ferry, Gilles Garric , Jean-Michel Lellouche (MERCATOR OCEAN)
Jean-Marc Molines (CNRS), Sébastien Theeten (Ifremer), the DRAKKAR and NEMO groups.
Nicolas Pene (ex-AKKA), Silvana Buarque (Météo-France), the BCG group (Météo-France, CERFACS)

Information on input data:
Christine Boone, Stéphanie Guinehut, Gaël Nicolas (CLS/ARMOR team)

Abstract

This bulletin gives an estimate of the accuracy of MERCATOR OCEAN's analyses and forecast for the season of ***October-November-December 2010****. It also provides a summary of useful information on the context of the production for this period. Diagnostics will be displayed for the global 1/12° (PSY4), global ¼° (PSY3) and the Atlantic and Mediterranean zoom at 1/12° (PSY2) monitoring and forecasting systems currently producing daily 3D temperature salinity and current products. In this issue, we focus on the Mercator Ocean products currently available via MyOcean V1 for the whole year 2010. Since the "calibration" of the global systems on the 2007-2009 period, regional biases have been identified and a series of improvements and corrections have been tested on the year 2010. As part of the continuous improvement process of MyOcean, we compare the results of these last R&D improvements to what was delivered through the MyOcean service in December 2010 (see data assimilation performance discussion). Apart from future quality updates, we verify that in OND 2010 the V1 forecast is already far more accurate than the V0 forecast (MyOcean V1 14-day forecast are available since December 2010). This issue's process study is performed with the global 1/12° system (PSY4) and shows the interest of global high resolution analyses and forecast, here in the Southern Ocean. Finally, Mercator Ocean systems are in constant evolution and many ideas are tested in the R&D team for their long term improvement. Those R&D sensitivity studies make use of the operational validation metrics in order to measure the eventual quality improvements. A short summary from a R&D study illustrates one of the ideas that has been tested for the improvement of the data assimilation scheme.*

Table of contents

I Executive summary

The Mercator Ocean global monitoring and forecasting system "MyOcean V1" is evaluated over the year 2010, with a focus on the October-November-December season. The system's description of the ocean water masses is very accurate on global average and almost everywhere between the bottom and 200m. Between 100 and 500m departures from *in situ* observations rarely exceed 0.4 °C and 0.04 psu (mostly in high variability regions like the Gulf Stream). Unfortunately, large biases appear locally in the surface layers of the North Sea, Celtic Sea and in the western Mediterranean Sea. A fresh bias also appears in the tropics in response to overestimated precipitations in the atmospheric forcings. These biases were not present in the previous systems and are currently under evaluation. Modifications were made before the operational launch of V1 that partially reduce the bias in the Mediterranean. A correction of the atmospheric forcings will be implemented in the coming months. The biases in the North and Celtic seas were diagnosed more recently and are still under investigation.

The monitoring system is generally very close to altimetric observations (global average of 6cm RMS error). Future updates of the Mean Dynamic Topography will correct the local biases that are currently observed for instance in the Banda Sea, and hopefully will prevent the degradation of the subsurface currents at the Equator. Another scientific update to expect in 2011 is the assimilation of Reynolds AVHRR-AMSRE SST products in place of RTG-SST.

The surface currents are underestimated with respect to *in situ* measurements of drifting buoys. The underestimation ranges from 20% in strong currents to 60% in weak currents. On the contrary the orientation of the current vectors is well represented.
The temperature and salinity forecast have significant skill in many regions of the ocean in the 0-500m layer, but a longer period of operational forecast is needed to properly interpret the forecast scores.

The sea ice cover is very realistic in the global monitoring systems compared to previous versions, especially for the Arctic in winter. Sea ice drift velocities have to be evaluated too in the next issues of QuO Va Dis.

II Status and evolutions of the systems

New versions of the PSY3 and PSY2 (see Table 1 and Table 2) systems are operated at MERCATOR OCEAN since 2010 December, 15th. These systems provide the version 1 products of the MyOcean global monitoring and forecasting centre. The atmospheric forcing is updated daily with the last analyses and forecast from the ECMWF, and a new oceanic forecast is run every day for both PSY3 and PSY2. This daily update of the forcing (referred to as PSY3QV3 and PSY2QV4) is not yet broadcasted by MyOcean.

The scientific evolution of the systems is described in QuO Va Dis #2 and will not be detailed here. The system is started in October 2006 from a 3D climatology of temperature and salinity (Levitus 2005). After a short 3-month spin up of the model and data assimilation, the performance of the system has been evaluated on the 2007-2009 period (MyOcean internal calibration report, which results are synthesised in QuO Va Dis#2). The performance of the system over the year 2010 is now described in this issue.

PSY2: Atlantic and Mediterranean at 1/12°			
System name	Model	Assimilation	status
PSY2V3R1	NATL12 LIM2 NEMO 1.09 (Tropical, North Atlantic and Mediterranean Sea, 1/12° horizontal resolution, 50 vertical levels) Daily atmospheric forcing, bulk CLIO.	Assimilating RTG-SST, SLA from Jason 1, Jason 2 and Envisat, in situ profile from CORIOLIS with SAM2 (SEEK Kernel)	Operated weekly with daily update of atmospheric forcings until 2011 January, 20th.
PSY2V4R1	NATL12 LIM2 EVP NEMO 3.1 (Tropical, North Atlantic and Mediterranean Sea, 1/12° horizontal resolution, 50 vertical levels) 3-hourly atmospheric forcing, bulk CORE.	Assimilating RTG-SST, SLA from Jason 1, Jason 2 and Envisat, in situ profile from CORIOLIS with SAM2 (SEEK Kernel) + IAU and bias correction	Operated weekly since 2010 December, 15th, with daily updates of atmospheric forcing since January 2011.

Table 1: synthetic description of the PSY2 system, in yellow the main improvements included in the new version

PSY3: global at ¼°			
System name	Model	Assimilation	status
PSY3V2R2	ORCA025 LIM2 NEMO 1.09 (Global, 1/4° horizontal resolution, 50 vertical levels) Daily atmospheric forcing, bulk CLIO	Assimilating RTG-SST, SLA from Jason 1, Jason 2 and Envisat, in situ profile from CORIOLIS with SAM2 (SEEK Kernel)	Operated weekly
PSY3V3R1	ORCA025 LIM2 EVP NEMO 3.1 (Global, 1/4° horizontal resolution, 50 vertical levels) 3-hourly atmospheric forcing, bulk CORE	Assimilating RTG-SST, SLA from Jason 1, Jason 2 and Envisat, in situ profile from CORIOLIS with SAM2 (SEEK Kernel) + IAU and bias correction	Operated weekly since 2010 December, 15th, with daily updates of atmospheric forcing since January 2011.

Table 2: Synthetic description of the PSY3 system. In yellow the main improvements included in the new version

PSY4: global at 1/12°			
System name	Model	Assimilation	status
PSY4V1R3	ORCA12 LIM2 NEMO 1.09 (Global, 1/12° horizontal resolution, 50 vertical levels) Daily atmospheric forcing, bulk CLIO	Assimilating RTG-SST, SLA from Jason 1, Jason 2 and Envisat, in situ profile from CORIOLIS with SAM2 (SEEK Kernel) + IAU	Operated weekly, broadcasted since January 2011

Table 3: Synthetic description of the PSY4 system

During the OND 2010 season, the **PSY2V4R1 and PSY3V3R1 hindcast were reprocessed** on the year 2010 (April to November) adding several corrections:

- The mean dynamic topography (MDT) has been updated in closed seas (correction of the long term bias in the CNES/CLS09 MDT). It was hybridized with a model MDT in the Baltic Sea, the Hudson Bay and the Black Sea. Finally the MDT was shifted in Mediterranean Sea.
- The diurnal cycle of SST has been taken into account in the observation operator (innovation is now computed at night).
- Jason 1 along track data were assimilated in PSY3V3R1 (pre-processing errors prevented these data from being assimilated in the first numerical experiment from November 2009 to August 2010)

This experiment was used as a restart for the beginning of real time production of V1, on 2010 December, 15th.

No major technical problem was encountered with PSY3V2R2 and PSY2V3R1 during the OND quarter.
The PSY4V1R3 system is available for users since the end of February 2011. It will be visible on the Mercator Ocean web site at the end of March 2011. The scientific assessment of this system was made on the 2009-2010 period (see section VIII). In October a correction was made on the sea ice model LIM: update of the ocean current velocity computation under the ice.

IBI: regional at 1/36°			
System name	Model	Assimilation	status
IBI (temporary)	NEATL36 NEMO 2.3 (North East Atlantic and West Mediterranean Sea, 1/36° horizontal resolution, 50 vertical levels) 3-hourly atmospheric forcing, bulk CORE.	None. Restarted every week with initial conditions from PSY2V4R1	In transition to weekly operation.

Table 4 : synthetic description of the IBI system

The IBI system (Table 4) is now initialized weekly and forced at the boundaries with PSY2V4R1 outputs. The operational scenario is to produce weekly a 14-day spin-up and then a 5-day forecast updated each day. This system is currently being "calibrated" on the year 2008 in order to begin MyOcean V1 production in June. The nominal MyOcean production unit for IBI is Puertos Del Estado (Spain) while Mercator Océan will produce the back up products.

III Summary of the availability and quality control of the input data

III.1. Observations available for data assimilation

III.1.1. In situ observations of T/S profiles

system	PSY3V2R2	PSY3V3R1	PSY4V1R3	PSY2V3R1	PSY2V4R1
Min/max nb of T profiles per DA cycle	2000/4600	2000/4600	2000/4600	200/800	200/800
Min/max nb of S profiles per DA cycle	2000/3900	2000/3900	2000/3900	100/600	100/600

Table 5: minimum and maximum number of observations (orders of magnitude) of temperature and salinity assimilated weekly in OND by the Mercator Ocean monitoring and forecasting systems.

We note in Table 5 that there is no longer a discrepancy between the global systems whereas in JAS PSY3V3R1 allowed a larger number of observations for a given analysis than the current version of PSY4V1R3. This was not due to the different tuning of the systems as was first guessed but was simply due to the use of delayed time dataset for PSY3V3R1 (not already operated with the real time operational suite in JAS 2010).

The maximum number of observations occurs in December. If we look back at the whole year 2010 (Figure 1) we can note that two periods were particularly well observed: February and December, in temperature as well as in salinity, and from the surface to 2000m.

The quality check procedure that is performed by the ARMOR team prior to data assimilation in the Mercator Océan systems (from “Rapport trimestriel de suivi des observations T/S – Octobre/Décembre 2010”). The temperature and salinity profiles provided by Coriolis are first validated and then undersampled, to meet assimilation’s needs and keep, at the most, one profile per 0.1° box every 24 hours.

The ARMOR team also regularly performs preliminary studies for the use of various observational datasets in the Mercator Ocean systems. In the following a brief summary of a study on SST products is displayed.

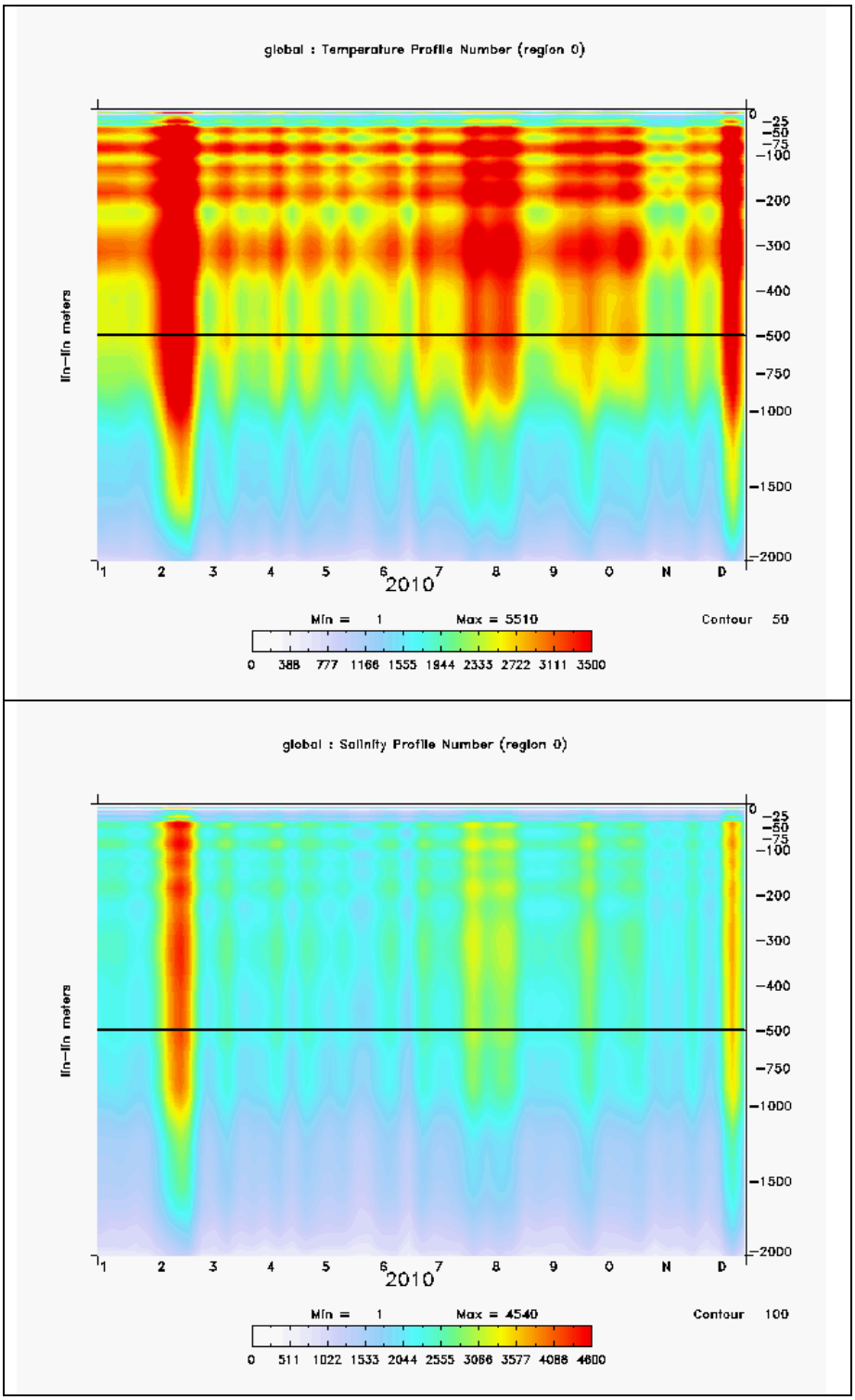

Figure 1 : number of observations assimilated weekly in function of depth and time for temperature profiles (upper panel) and salinity profiles (lower panel).

III.1.2. Sea Surface Temperature

system	PSY3V2R2	PSY3V3R1	PSY4V1R3	PSY2V3R1	PSY2V4R1
Min/max nb (in 10^3) of SST observations	163/168	174/182	170/178	32/34	30/33.5

Table 6: minimum and maximum number (orders of magnitude in thousands) of SST observations (from RTG-SST) assimilated weekly in OND by the Mercator Ocean monitoring and forecasting systems.

As shown in Table 6, PSY3V3R1 and PSY2V4R1 assimilate more SST observations on average than the other systems.

The ARMOR team has performed a study on SST products in "Rapport de synthèse pour le Service Données ATD-O" (reference: CLS-DOS-NT-10-327) and "Validation of different SST products using Argo dataset" (reference: CLS-DOS-NT-10-264).

The objective of the study was to assess the quality of new SST fields, with respect to Reynolds or RTG (currently assimilated at Mercator Ocean). One level-3 SST product and seven level-4 SST products have been compared over the year 2008:

- Reynolds 1°
- Reynolds AVHRR (1/4°)
- Reynolds AVHRR+AMSR (1/4°)
- OSTIA (1/20°)
- RTG (1/2°)
- RTG-HR (1/12°)
- Odyssea-L4 (1/10°)
- Odyssea-L3 (1/10°).

Many assessments and comparisons have been performed:

- resolution of the spatial structures, variability between two consecutive analyses
- difference between OSTIA and the other products
- time series of the global mean
- comparison to independent *in situ* data from Argo network

The main results are summarized hereafter. The global mean averaged time series (Figure 2) over the year 2008 show very consistent and similar results for the seven L4 SSTs, except for Odyssea that shows a drift at the beginning of the period (production is then interrupted for about 2 months and the drift is corrected). The zonal means of the differences between Ostia and the other SSTs (Figure 3) show where are located the main differences. At high latitudes the differences can reach 0.2 to 0.3 °C (RTG are colder than OSTIA, Reynolds and Odyssea are warmer).

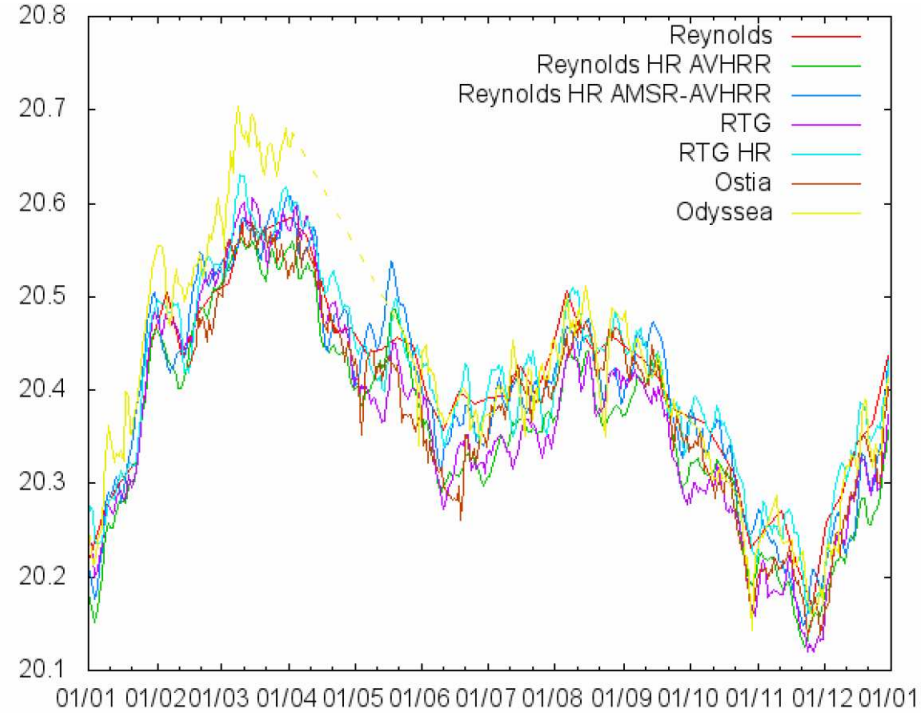

Figure 2: time series of different SSTs global means over year 2008

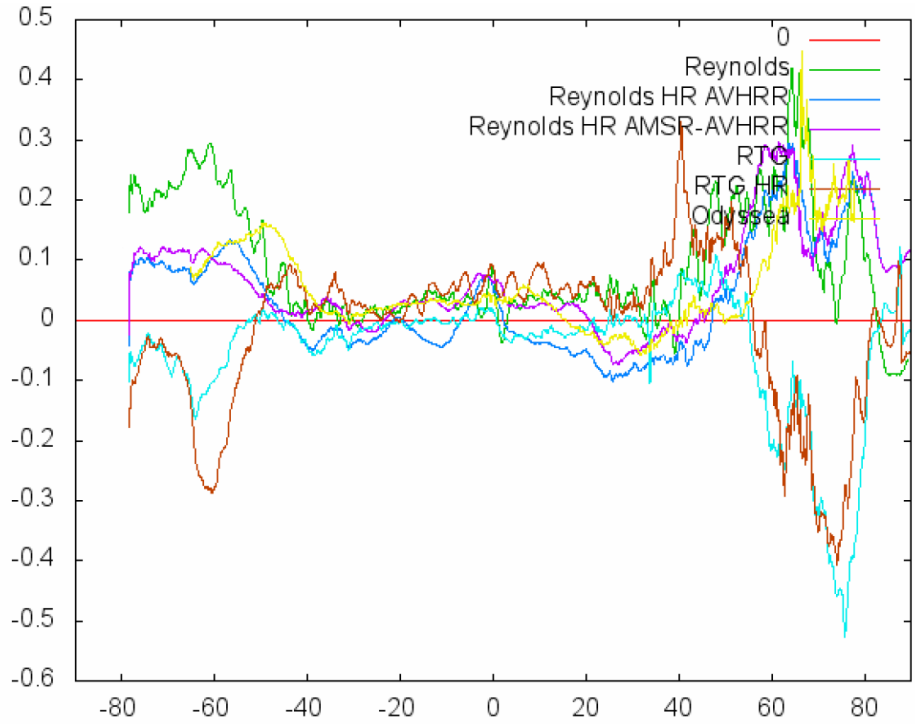

Figure 3: differences between OSTIA SST and other SSTs, zonal means over year 2008

Compared to Argo data, RTG-HR show the worst results with too cold temperature (T) at high latitudes (~0.8 °C), too warm T in the South Subtropical gyre (~0.15°C) and too cold T in the North Subtropical gyre (~0.25 °C). Compared to Argo data, RTG is also too cold at high latitudes but to a lesser extent (~0.4 °C).

Reynolds 1° weekly analysis show noisier results due to the lack of spatial and temporal resolution compared to more recent higher temporal and spatial resolution products. Reynolds 1/4° AVHRR and Reynolds 1/4° AVHRR-AMSR lead to very similar results.

Odyssea L3 product also shows noisier results compared to Odyssea L4 with larger differences compared to Argo temperature.

Ostia and Odyssea SST are comparing very well between 30°S and 30°N. Differences increase at higher latitudes with too warm T in winter in Odyssea for latitudes south of 40°S (~0.2°C), and too cold T in spring in Ostia (~0.2°C). At high latitudes of the Northern Hemisphere, Ostia T are too cold (~0.2 to 0.4°C) for all seasons and Odyssea T are too cold in winter and autumn and too warm in spring (~0.2 to 0.3°C).

Finally Reynolds HR AVHRR-AMSR (SST used in ARMOR3D), OSTIA (MyOcean nominal product) and RTG (SST used in Mercator Ocean systems) are comparing very well with again too cold T in RTG mainly in winter at high latitudes. Winter temperatures are also too cold in OSTIA but mainly at high latitudes of the Northern Hemisphere.

The podium is thus:

1. OSTIA
2. Reynolds AVHRR-AMSR
3. Odyssea
4. RTG

Nevertheless, OSTIA SSTs (defined on a 1/20° grid) only solve structures at 1/2°.

The Mercator Ocean R&D team currently evaluates the use of Reynolds AVHRR-AMSR observations in the operational systems data assimilation process. Reynolds AVHRR analyses have been assimilated in GLORYS2V1 reanalysis for the 1992-2009 period and the preliminary results are satisfactory (summary to be published in QuO Va Dis #4).

III.1.3. Sea Level Anomalies

system	PSY3V2R2	PSY3V3R1	PSY4V1R3	PSY2V3R1	PSY2V4R1
Min/max nb (in 10^3) of Jason 2 SLA observations	58/86	77/91	60/91	11/16	14/16
Min/max nb (in 10^3) of Envisat SLA observations	0/79	0/80	0/80	0/16	0/16
Min/max nb (in 10^3) of Jason 1 SLA observations	55/84	73/86	50/86	9/15	14/15

Table 7: minimum and maximum number (orders of magnitude in thousands) of SST observations (from RTG-SST) assimilated weekly in OND by the Mercator Ocean monitoring and forecasting systems.

There was no Envisat data assimilated in the analyses since October, 20th during the change of orbit performed on the satellite (now referred to as enn "Envisat new orbit"). The new Envisat data were assimilated in PSY3V2R2 and PSY2V3R1 starting from November, 17th, in PSY4V1R3 and PSY2V4R1 starting from November 24th and finally in PSY3V3R1 starting from December, 1st.

III.2. Observations available for validation

Both observational data and statistical combinations of observations are used for the real time validation of the products. All were available in real time during the OND 2010 season and no incidents were reported:

- T/S profiles from CORIOLIS
- OSTIA SST (with one problem on July 21st) from UKMO
- Arctic sea ice concentration and drift from CERSAT
- SURCOUF surface currents from CLS
- ARMOR-3D 3D temperature and salinity fields from CLS
- Drifters velocities from Météo-France reprocessed by CLS

IV Information on the large scale climatic conditions

Mercator Ocean participates in the monthly seasonal forecast expertise at Météo-France. This chapter summarizes the state of the ocean and atmosphere during the OND 2010 season, as discussed in the "Bulletin Climatique Global" of Météo-France.

This OND 2010 season was characterized by mature La Niña atmospheric and oceanic conditions. In the ocean (Figure 4), the Eastern Tropical Pacific Ocean is colder than the climatology, with negative temperature anomalies at depth (we show here the 0-300m layer) extending from the dateline to the South American coasts. The activity of Tropical instability waves is important in the centre of the basin (see EKE on Figure 40). Warm anomalies strengthened between 0 and 300m in the Pacific warm pool.
Cyclones and strong precipitation events were observed in Australia and in the western tropical Pacific. Precipitations were above average over Indonesia, the Caribbean Sea and Gulf of Mexico, the Eastern Tropical Atlantic and were below average in the eastern Tropical Pacific.

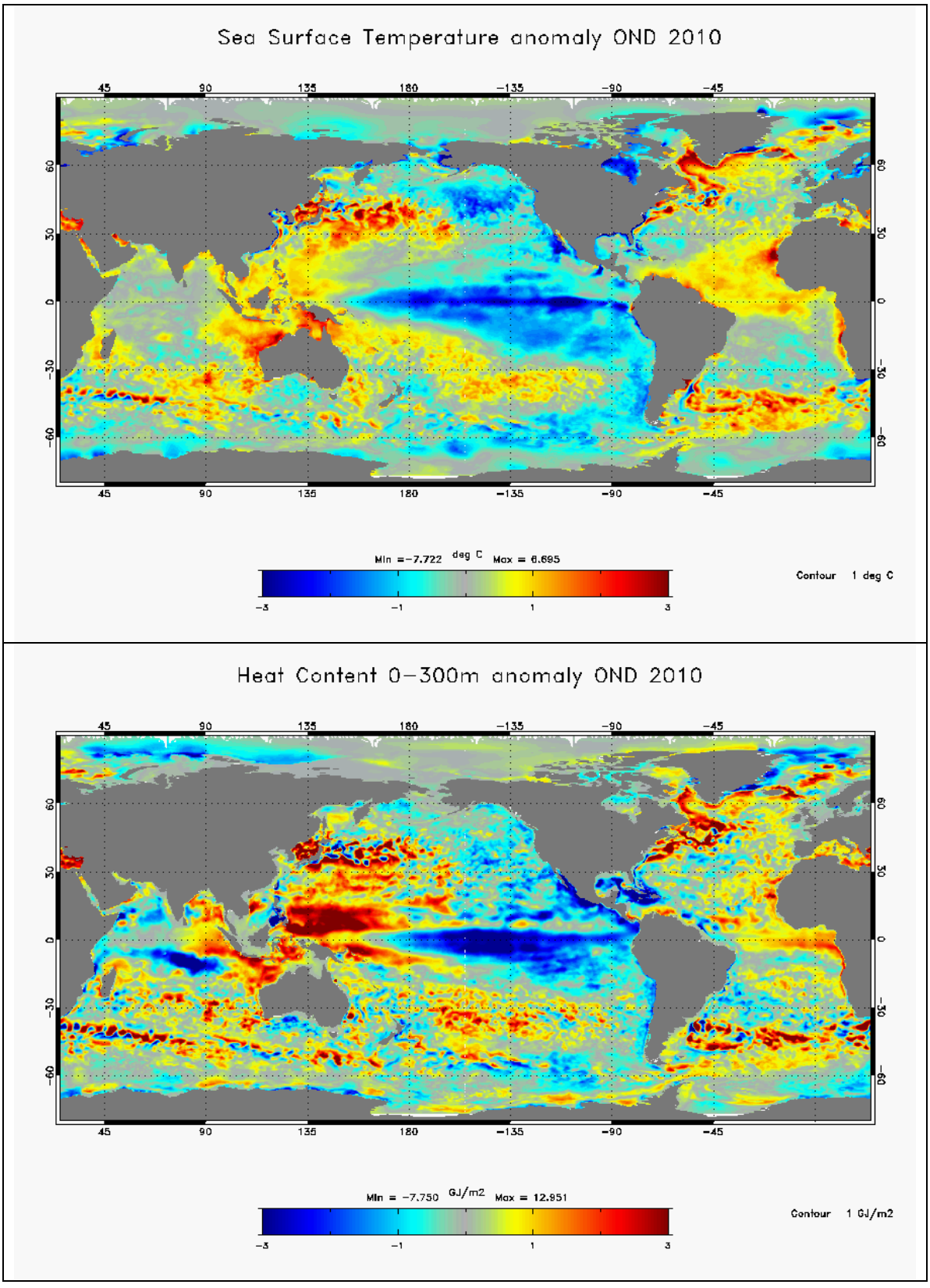

Figure 4: Seasonal OND 2010 temperature anomalies with respect to Levitus (2005) climatology. Upper panel: SST anomaly (°C) at the global scale from the 1/4° ocean monitoring and forecasting system PSY3V3R1. Lower panel heat content anomaly ($\rho_0 C_p \Delta T$, with constant ρ_0=1020 kg/m3) from the surface to 300m.

The Tropical Atlantic and the North Atlantic Sub-polar gyre surface temperatures were anomalously warm over the whole season. The North Atlantic oscillation is still negative (it has been negative since November 2009), but the negative anomaly in the centre of the North Atlantic basin tends to disappear (probably due to the dominant Atlantic Ridge or East Atlantic mode positive phases: anticyclonic anomalies over the North East Atlantic).
The Mediterranean Sea is anomalously warm in the eastern parts.

As can be seen in Figure 5, the sea ice extent in the Arctic Ocean is less than the winter 2007-2008 minimum in November and December.

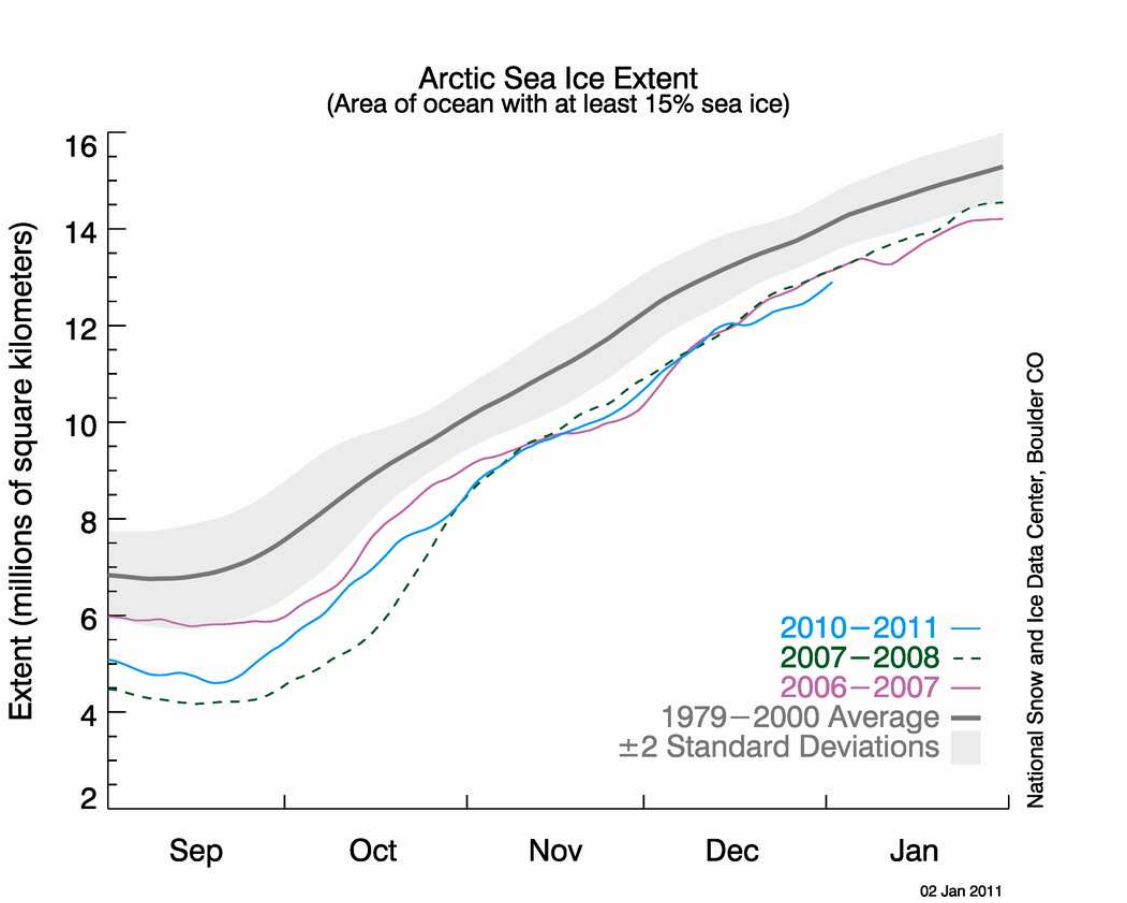

Figure 5: Arctic sea ice extent from the NSIDC:
http://nsidc.org/data/seaice_index/images/daily_images/N_stddev_timeseries.png

V Accuracy of the products

V.1. Data assimilation performance

V.1.1. Introduction

As explained in chapter III PSY2V4R1 and PSY3V3R1 hindcast were reprocessed since April 2010. The new runs include several corrections such as a modification of the MDT which was corrected from a long term bias and modified in several "closed seas" such as the

Mediterranean and Baltic Seas. These new runs were not delivered early enough to be considered as MyOcean V1 *1 year hindcast*. Nevertheless they were used as initial conditions for the operational MyOcean V1 *real time delivery* on December, 15th. In the following we will comment the usual data assimilation statistics on the OND 2010 season for the official "MyOcean products", and in parallel we will check if there is a further improvement in the new experiment (referred to as "best experiment") performed for the year 2010.

V.1.2. Sea surface height

V.1.2.1. North Atlantic Ocean and Mediterranean Sea

The impact of the corrections in the Mediterranean is not significant when comparing mean SLA innovations from MyOcean products and from the best experiment over the year 2010 (Figure 6). In the Baltic, the mean innovation is reduced in the Northern part of the domain, whereas it is larger in the Labrador Sea. The same patterns can be observed when comparing the old and new runs of PSY3V3R1 for 2010 (not shown).

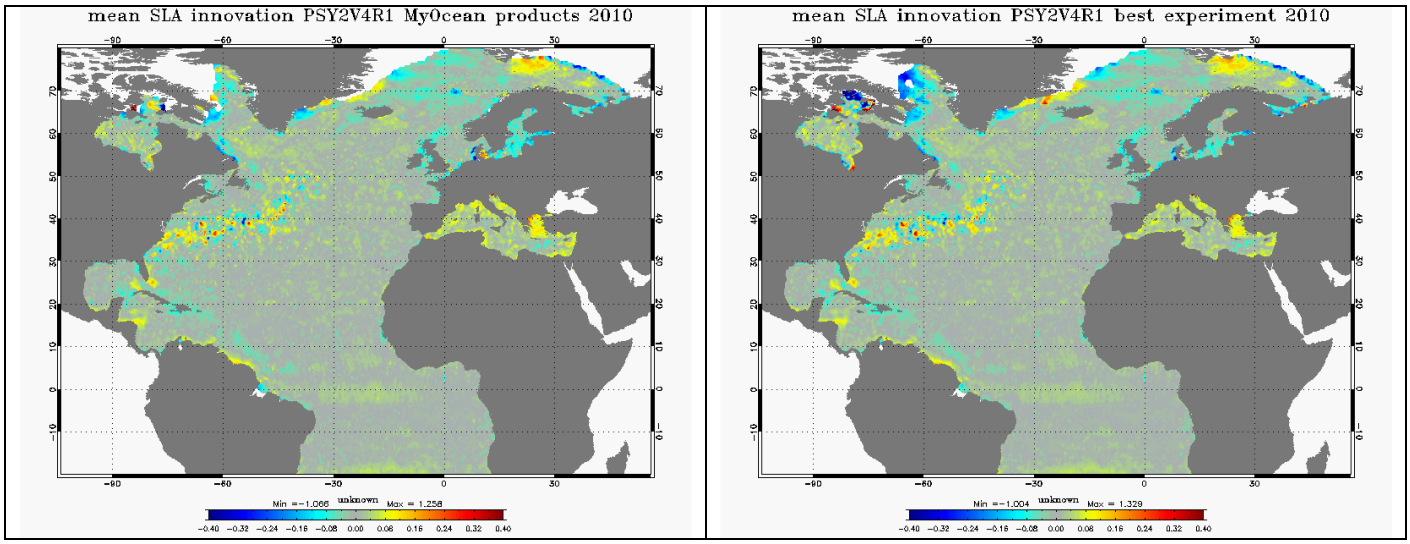

Figure 6: Mean innovation (observation-forecast) of SLA (m) averaged on the year 2010, in the MyOcean 1-year hindcast (left panel) and in the updated experiment (right panel) for PSY2V4R1.

The Tropical and North Atlantic Ocean Sea SLA assimilation scores for all systems in OND 2010 are displayed in Figure 7. The most recent systems' performance (PSY4V1R3, PSY3V3R3, PSY2V4R1) is still very close to the previous versions'. The biases generally decrease in the new systems, except in the tropical regions like Belem XBT or SEC regions. These tropical biases may be in link with the fresh anomaly that can be diagnosed in the tropics (see section V.1.4). The RMS errors are almost identical in all systems except in the regions of high mesoscale variability like the Gulf Stream.

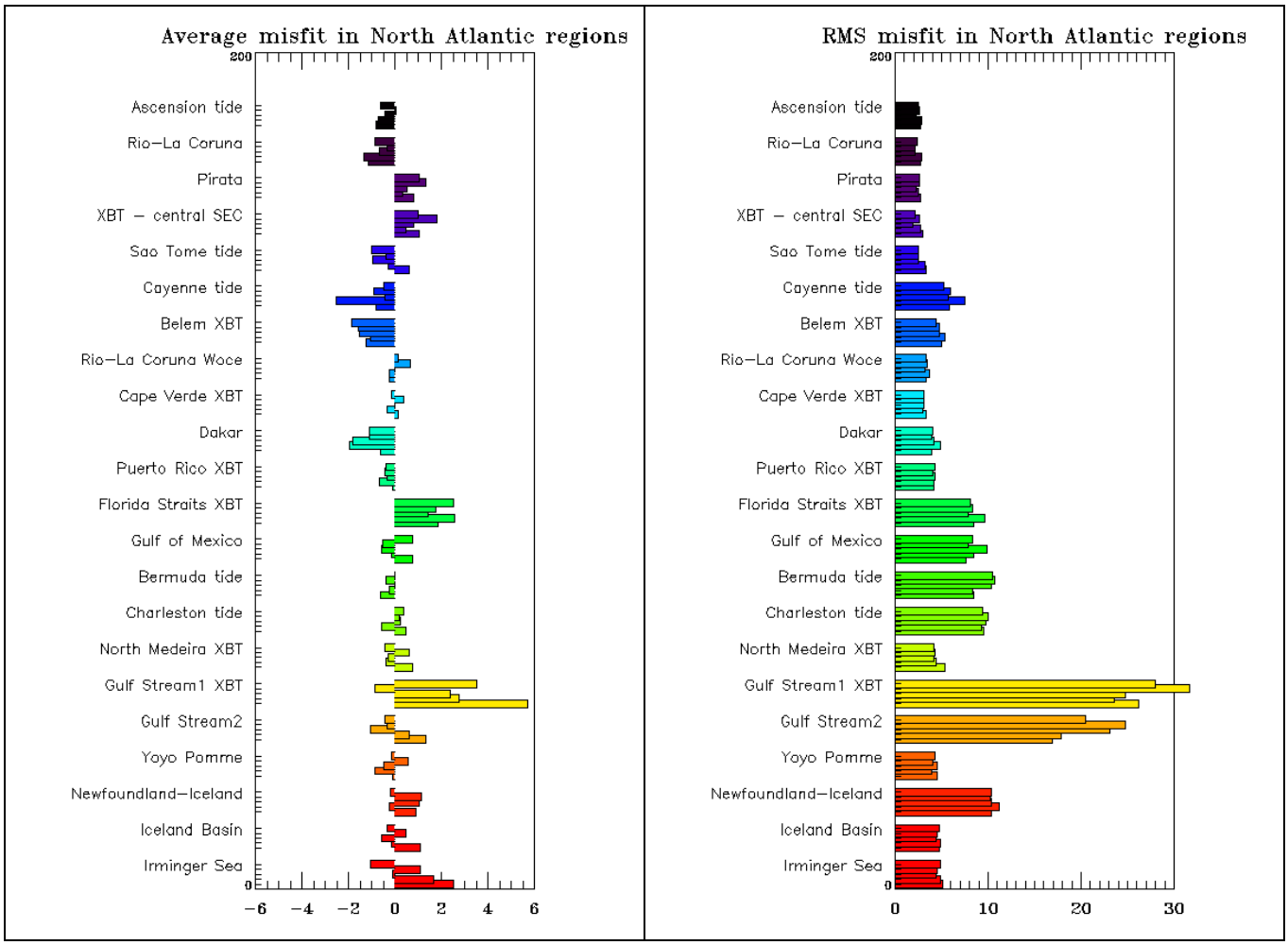

Figure 7: Comparison of SLA data assimilation scores (left: average misfit in cm, right: RMS misfit in cm) in OND 2010 and between all available Mercator Ocean systems in the Tropical and North Atlantic. The scores are averaged for all available satellite along track data (Jason 1, Jason 2 and Envisat). For each region from bottom to top, the bars refer respectively to PSY3V2R2, PSY2V3R1, PSY3V3R1, PSY2V4R1, PSY4V1R3. The geographical location of regions is displayed in annex A.

In the Mediterranean Sea the bias is reduced in PSY2V4R1 with respect to PSY2V3R1 as can be seen in Figure 8, except in the Aegean Sea and Adriatic Seas and in the western Mediterranean Sea (regions Alboran, Lyon, Algerian). The PSY2V3R1 and PSY2V4R1 RMS misfit have very similar levels, with regional differences. The RMS increases where the bias increases, while it decreases slightly elsewhere.

The impact of the corrections made in August (mainly shift of the MDT) is not as clear in the RMS of misfit as it is in the "NMS" score (Figure 9). The latter indicates that the RMS error (order of magnitude 5-8 cm) is generally lower than the intrinsic variability of the observations in the North Atlantic and Mediterranean. This result characterizes a good performance of the system in the region, provided that the scores of the other assimilated observations are also good (see newsletter Mercator #9). We note that this score is significantly improved in OND 2010 in the Mediterranean Sea compared to the previous season JAS.

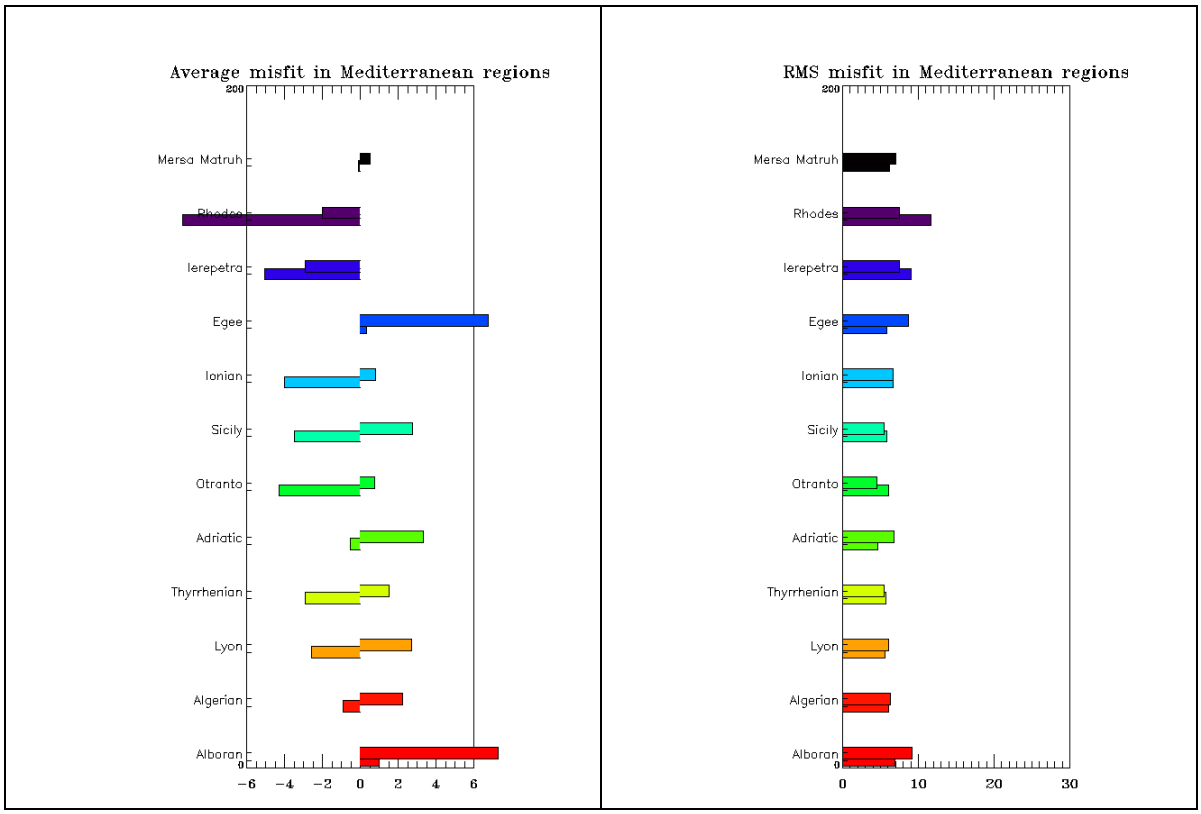

Figure 8: Comparison of SLA data assimilation scores (left: average misfit in cm, right: RMS misfit in cm) in OND 2010 and between both PSY2 systems in the Mediterranean Sea. For each region from bottom to top: PSY2V3, and new version PSY2V4. The scores are averaged for all available satellite along track data (Jason 1, Jason 2 and Envisat). The geographical location of regions is displayed in annex B.

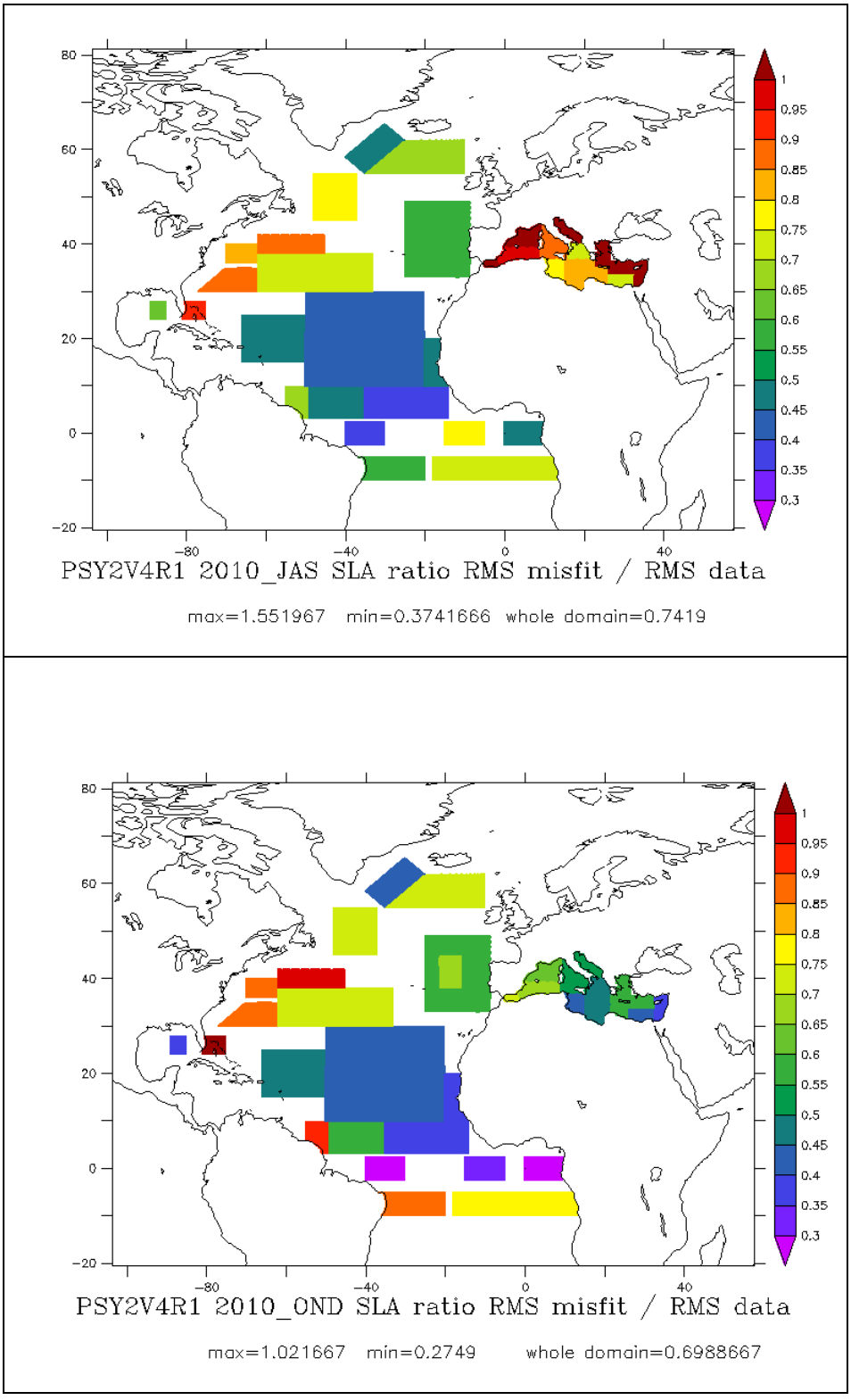

Figure 9: Synthetic map of regional ratio of RMS misfit over RMS of SLA data in the Atlantic Ocean and Mediterranean Sea for the new system PSY2V4 in JAS 2010 (upper panel) and OND 2010 (lower panel). The scores are averaged for all available satellite along track data (Jason 1, Jason 2 and Envisat).

V.1.2.2. Performance at global scale in PSY3 (1/4°) and PSY4 (1/12°)

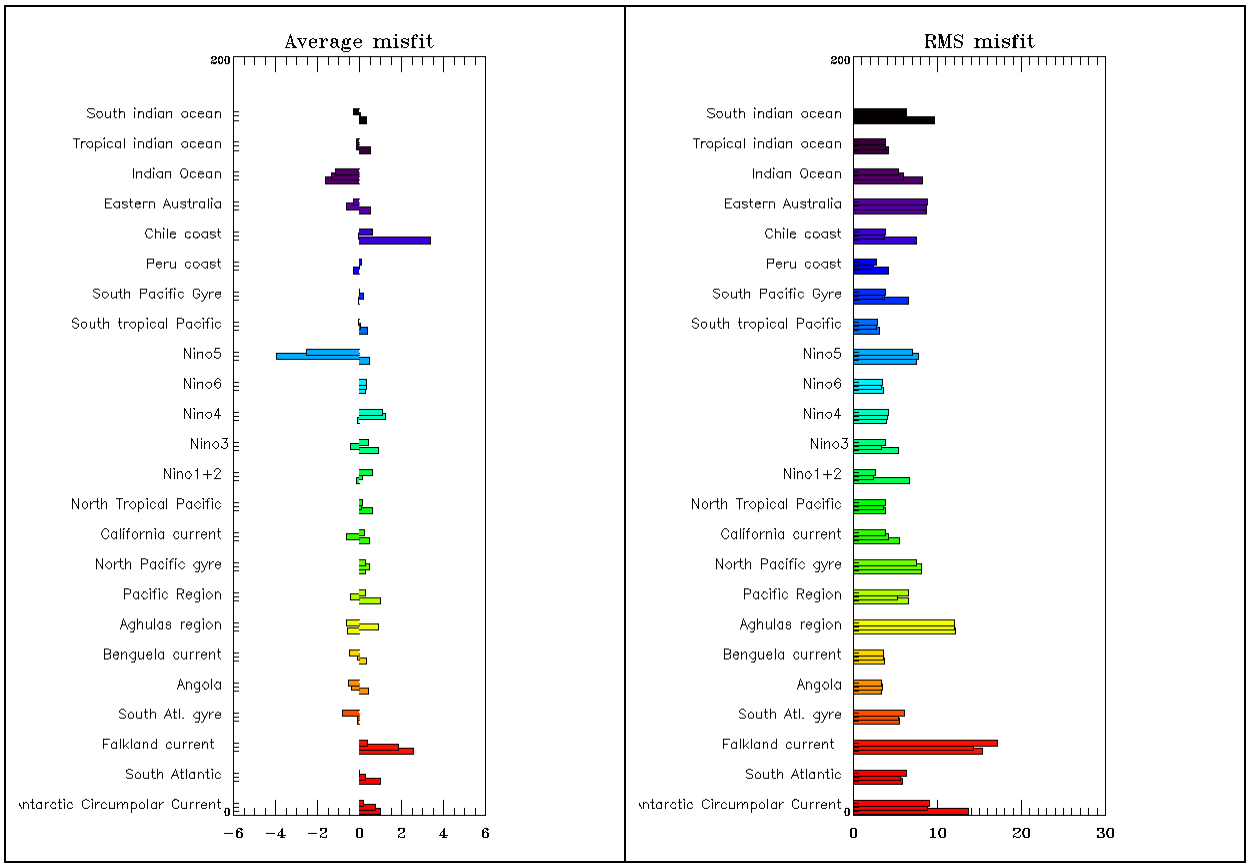

Figure 10: Comparison of SLA data assimilation scores (left: average misfit in cm, right: RMS misfit in cm) in OND 2010 and between all available Mercator Ocean systems in all basins but the Atlantic and Mediterranean. For each region from bottom to top: PSY3V2R2, PSY3V3R1, and PSY4V1R3. The geographical location of regions is displayed in annex B.

As can be seen on Figure 10 both new systems PSY3V3R1 and PSY4V1R3 perform significantly better than PSY3V2R2 in terms of SLA assimilation, especially in the southern oceans. Either the bias or the RMS error is reduced, except in the “Nino 5” box centred on the Banda Sea, in Indonesia.

NB: The RMS error has been increasing regularly in the Antarctic Ocean in PSY3V2R2 since April, which is not the case in the new systems. This problem is under investigation and might be due to aliasing phenomena in the observation operator of PSY3V2R2.

V.1.3. Sea surface temperature

V.1.3.1. North and Tropical Atlantic Ocean and Mediterranean Sea in all systems

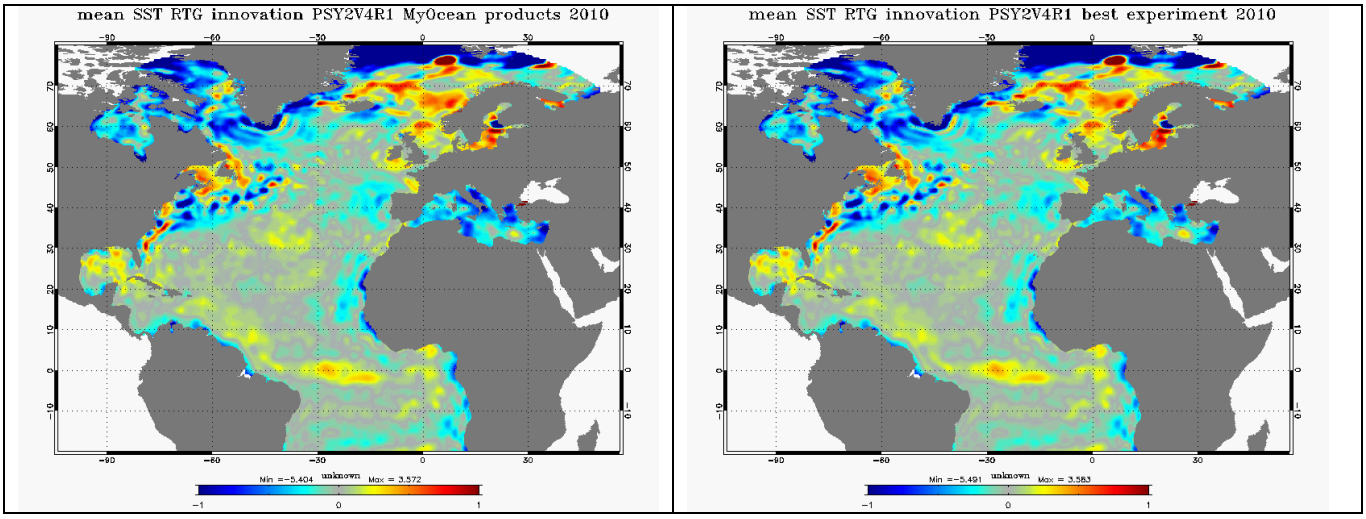

Figure 11: Mean innovation (observation-forecast) of SST (°C) averaged on the year 2010, in the MyOcean 1-year hindcast (left panel) and in the updated experiment (right panel) for PSY2V4R1.

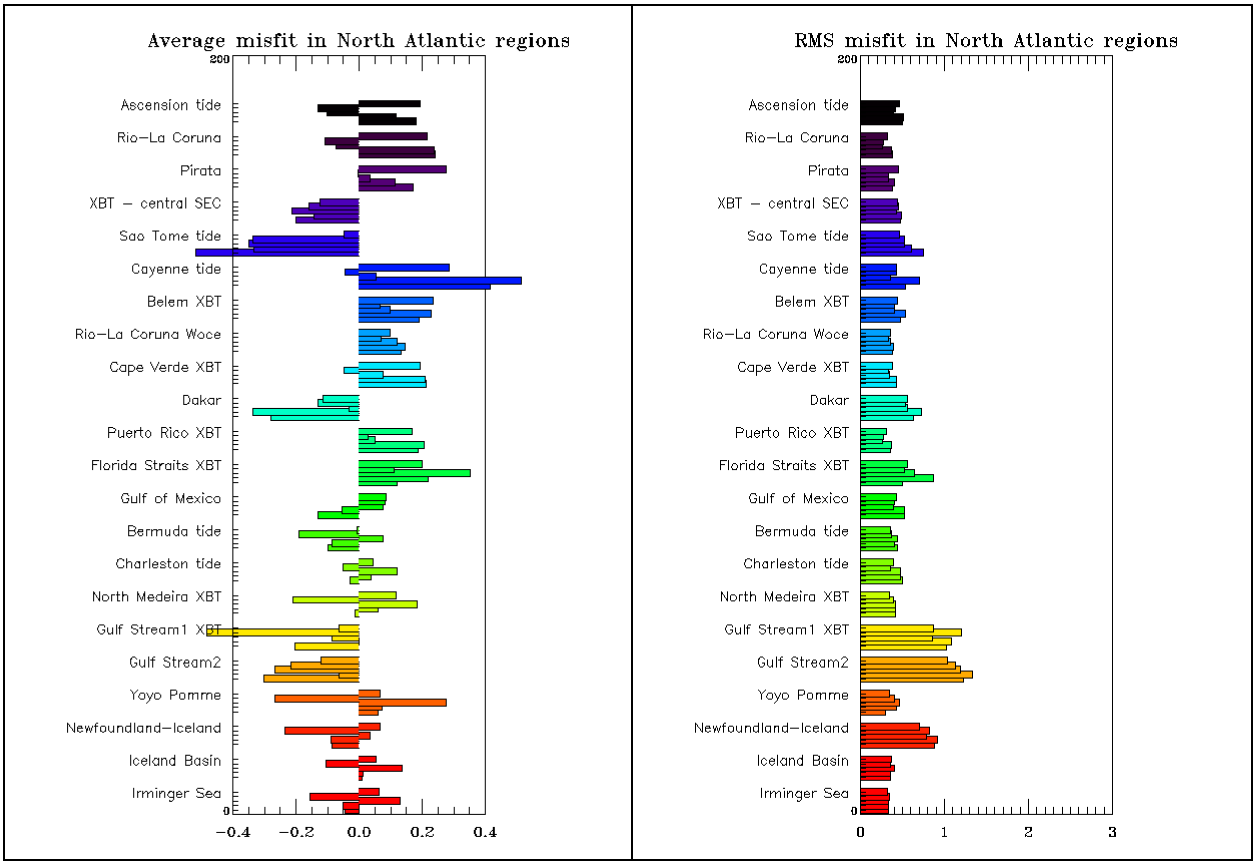

Figure 12: Comparison of RTG-SST data assimilation scores (left: average misfit in °C, right: RMS misfit in °C) in OND 2010 and between all available Mercator Ocean systems in the Tropical and North Atlantic. For each region from bottom to top: PSY3V2, PSY2V3, PSY3V3, PSY2V4, PSY4V1.

The updates of the systems in the best experiment runs of the year 2010 do not have a major impact on SST data assimilation statistics as can be seen in Figure 11. Nevertheless we note a slight decrease of the mean error in the Western Mediterranean and an increase in the Baltic Sea.

In the Atlantic the new systems SST RMS error is significantly lower than in the current systems' as illustrated on Figure 12. Over all systems, PSY2V4R1 is the closest to RTG-SST satellite observations in terms of RMS. PSY4V1R3 which has IAU and daily average atmospheric forcings (instead of IAU and 3-hourly forcings for PSY2V4R1 and PSY3V3R1) is the less biased of all system in the Northern part of the basin. There is a cold bias in PSY3V3R1 north of 30°N of about 0.5°C (for instance in yoyo Pomme and north Madeira XBT regions, Figure 12). The calibration of the system over the 2007-2009 period shows that this bias is seasonal and is maximum during boreal summer (JAS season). The change of the observation operator (which now considers only night-time SSTs to compare with RTG-SST) does not reduce significantly this bias in OND. PSY2V4R1 exhibits on the contrary a warm bias in the northern seas (Irminger Sea, Iceland Basin) but it is close to in situ observations in these regions (not shown) and RTG-SST are known to be too cold in these regions (see section III.1.2).

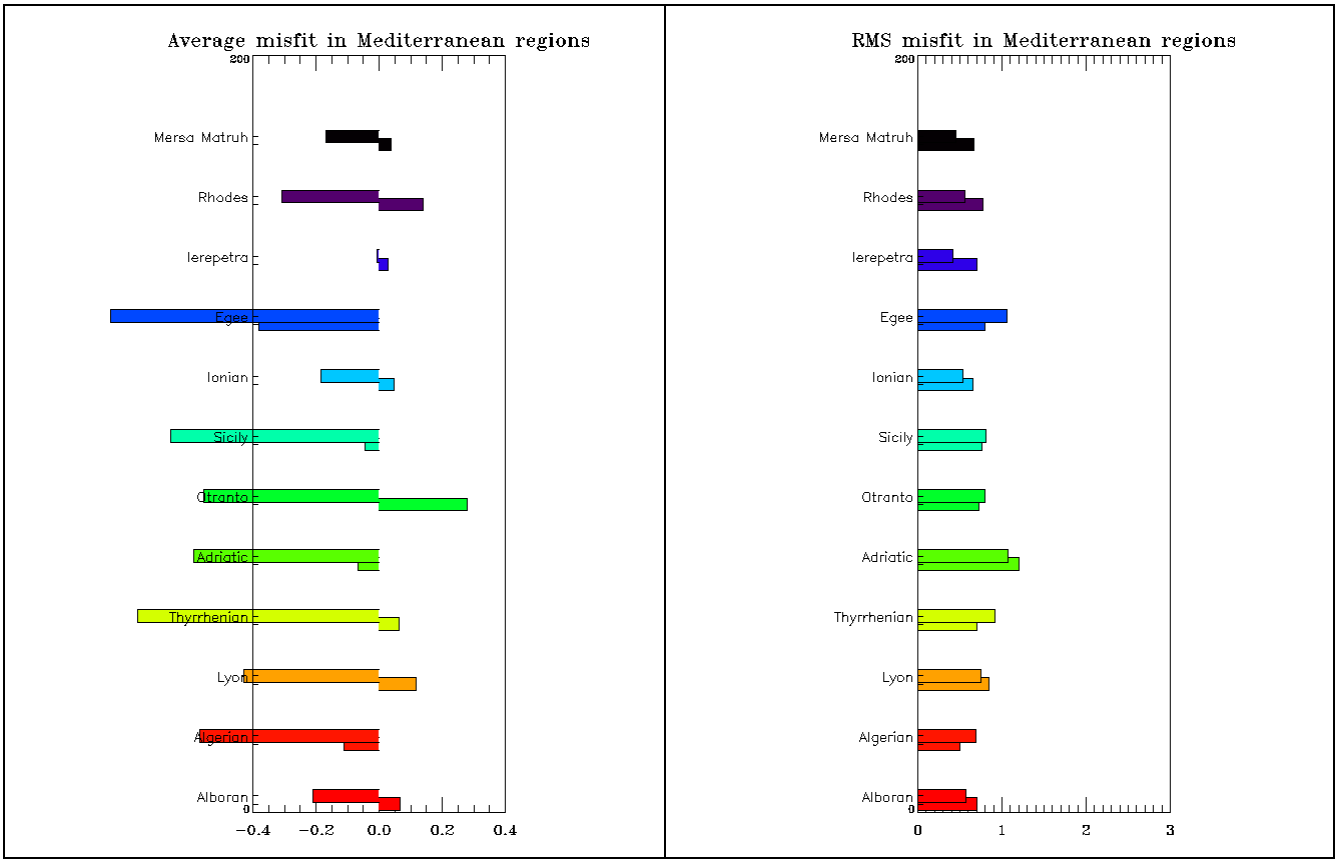

Figure 13: Comparison of RTG-SST data assimilation scores (left: average misfit in °C, right: RMS misfit in °C) in OND 2010 and between both PSY2 systems in the Mediterranean Sea. For each region from bottom to top: PSY2V3, and new version PSY2V4.

In the Mediterranean Sea the departures from RTG-SST are larger in PSY2V4R1 than in PSY2V3R1 (Figure 13). Only the most eastern regions exhibit smaller errors than in

PSY2V3R1. The Western part of the Mediterranean is thus too warm with respect to RTG-SST. This bias is slightly reduced in the new experiment on average over the whole year 2010 (Figure 11). Not many in situ observations are available to analyse this bias but statistics in the Gulf of Lion (not shown) suggest that part of these departures from observations can be due to a cold bias of RTG-SST in the Mediterranean (to be confirmed on a longer period).

V.1.3.2. Performance at global scale in PSY3 (1/4°) and PSY4 (1/12°)

A bias seems to develop in the North Pacific in PSY3V3R1 (Figure 14, Pacific region). Nevertheless the RMS error stays in the expected range. The Antarctic Ocean and Southern Oceans in general are closer to the observations in PSY3V3R1 than in PSY3V2R2. The bias and RMS error is significantly reduced in PSY3V3R1 in the Niño regions 3, 4 and 6, with respect to RTG-SST as well as with respect to in situ data. Peru and Chile regions, as well as the East Australia region are also closer to the observations in PSY3V3R1 than in PSY3V2R2. In general PSY3V3R1 performs better than PSY4V1R3; however the higher resolution of PSY4V1R3 can contradictorily lead to poorer forecast scores (with few observations leading to few innovations). We note that in nino5 region the RMS error is higher in PSY3V3R1 than in PSY3V2R2, as for the SLA RMS error. Biases in this region probably come from errors in the MDT CNES-CLS09 (under investigation).

NB: the number of in situ SST data in the statistics has not been considered here, but in situ statistics in the smallest regions should be considered with caution.

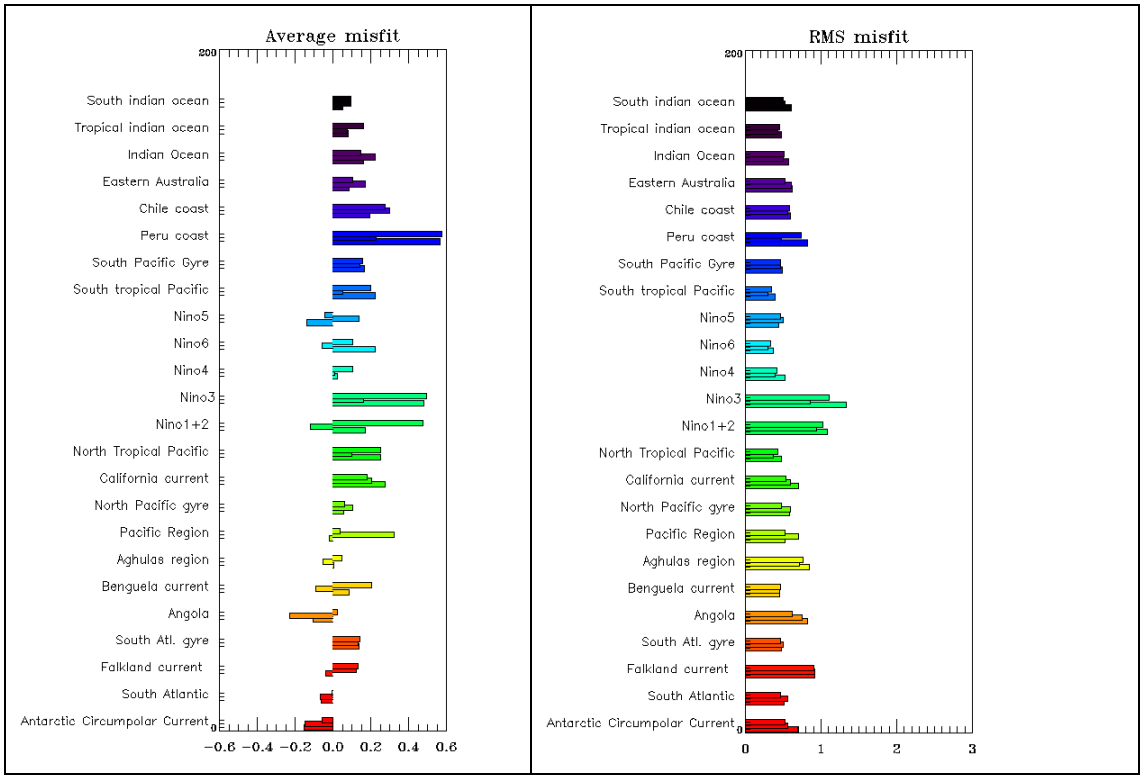

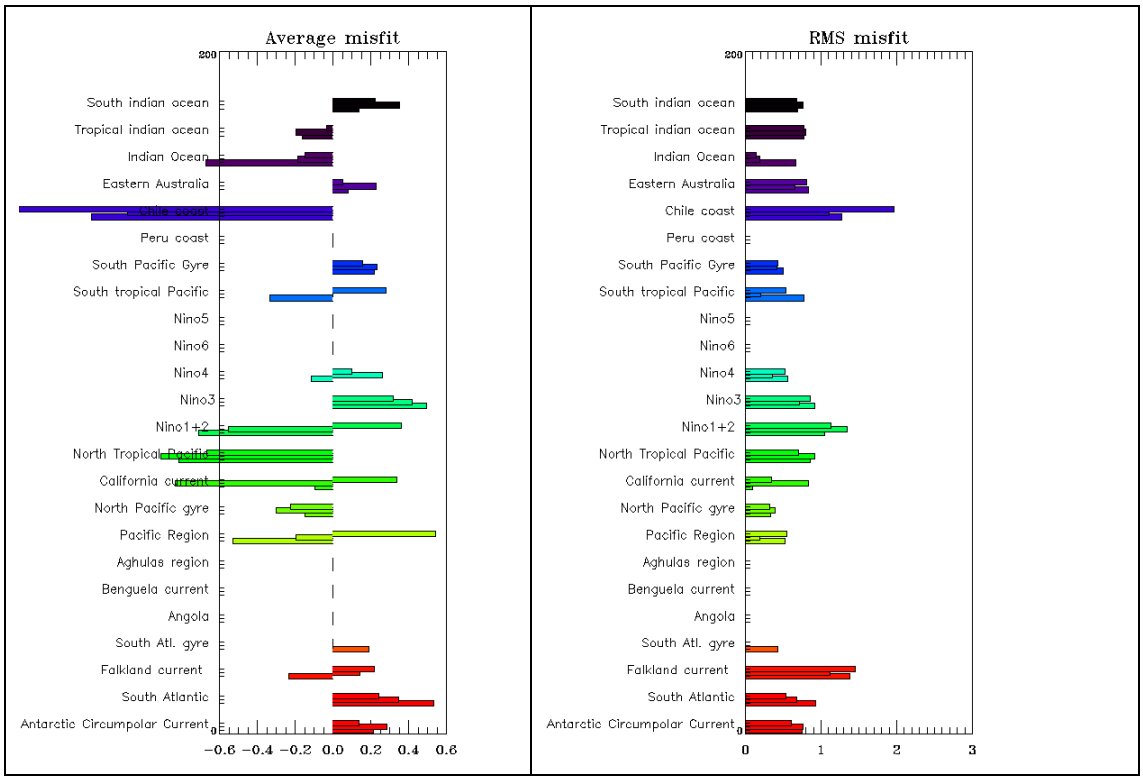

Figure 14: Comparison of SST data assimilation scores (left: average misfit in °C, right: RMS misfit in °C) in OND 2010 and between all available Mercator Ocean systems in all basins but the Atlantic and Mediterranean. Upper panel: RTG-SST data assimilation scores, lower panel: in situ SST data assimilation scores. For each region from bottom to top: PSY3V2R2, PSY3V3R1, and PSY4V1R3.

V.1.4. Temperature and salinity profiles

V.1.4.1. Performance at global scale of PSY3 (1/4°) and PSY4 (1/12°)

As can be seen in Figure 15 PSY3V2R2 is generally too cold over 100 m, and too warm (0.3 °C) between 100 and 200 m. A warm bias can be detected under 1500m. PSY4V1R3 is too cold (0.2 °C) over the 0-500m water column, and too warm under 1500m. The warm bias at depth is equivalent to PSY3V2R2. In both systems the RMS error nearly reaches 1.2°C between 100 and 200 m at the average thermocline position. Under 1000m the RMS error is lower in PSY4V1R3 (0.1 °C) than in PSY3V2R2 (0.15 °C).

The latest system PSY3V3R1 displays the best performance as the bias at depth disappears. A cold bias of 0.2°C is still visible in the surface layer, as well as a warm bias of 0.1 °C near 100m and a cold bias of 0.1°C or less between 100 and 500m. The RMS error is reduced by at least 0.1°C on the whole water column, and is lower than in PSY4V1 in the 0-200m layer. *These same comments were made for the previous JAS season which shows the stability of the performance of the systems.*

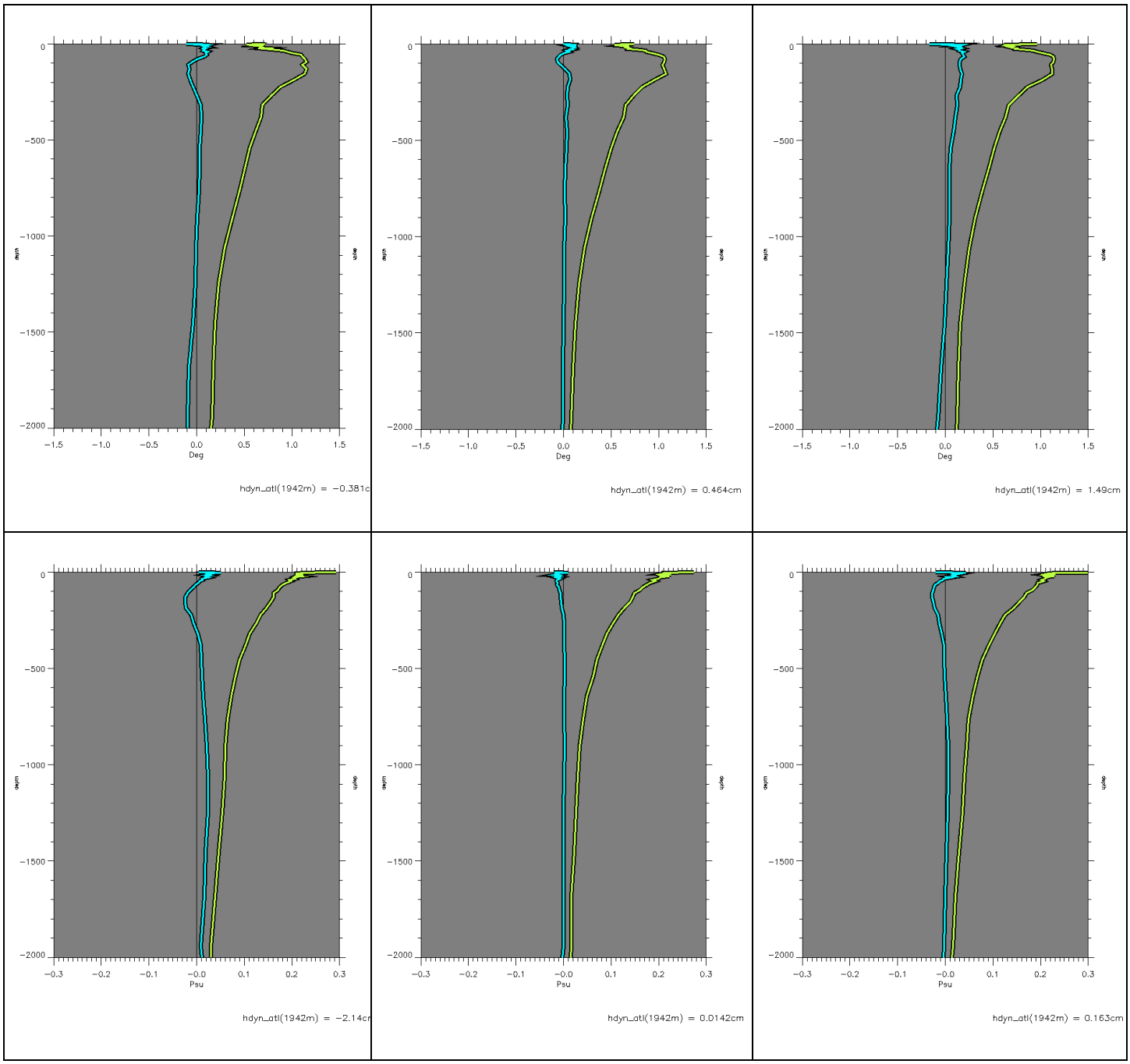

Figure 15: Profiles of OND 2010 global mean (blue) and rms (yellow) innovations of temperature (°C, upper panel) and salinity (psu, lower panel) in PSY3V2R2 (left column) PSY3V3R1 (centre column) and PSY4V1R3 (right column).

PSY3V2R2 and PSY4V1R3 display a salty bias near 100m and a fresh bias near the surface (also on Figure 15). PSY3V3R3 seems to have reduced the surface bias but these apparent good results on global average mask a fresh bias that has appeared in the tropics. A well known bias of ECMWF atmospheric forcing fields is that the precipitations are too strong in the tropics. PSY3V2R2 compensate this bias with a nudging to GPCP observations which is not applied in PSY3V3R1, and PSY2V4R1. This correction is not applied either in PSY4V1R3 but the fresh bias does not develop. Tests are currently performed in order to evaluate the necessity to go on applying a correction of the precipitations in the new systems. The fresh bias in the tropics also results in an apparent amplification of the

Amazon runoff. At depth the fresh bias visible in PSY3V2R2 below 1000m disappears in PSY3V3R1 and PSY4V1R3, with consequently a division by 2 of the RMS error from 0.03 psu in PSY3V2R2 to 0.015 in PSY4V1R3 and PSY3V3R1. The bias at 100m is reduced in the most recent system PSY3V3 compared to PSY4V1R3, thus PSY4 water masses still can be improved in future versions.

V.1.4.2. Tropical and North Atlantic Ocean, Mediterranean Sea by PSY2 (1/12°)

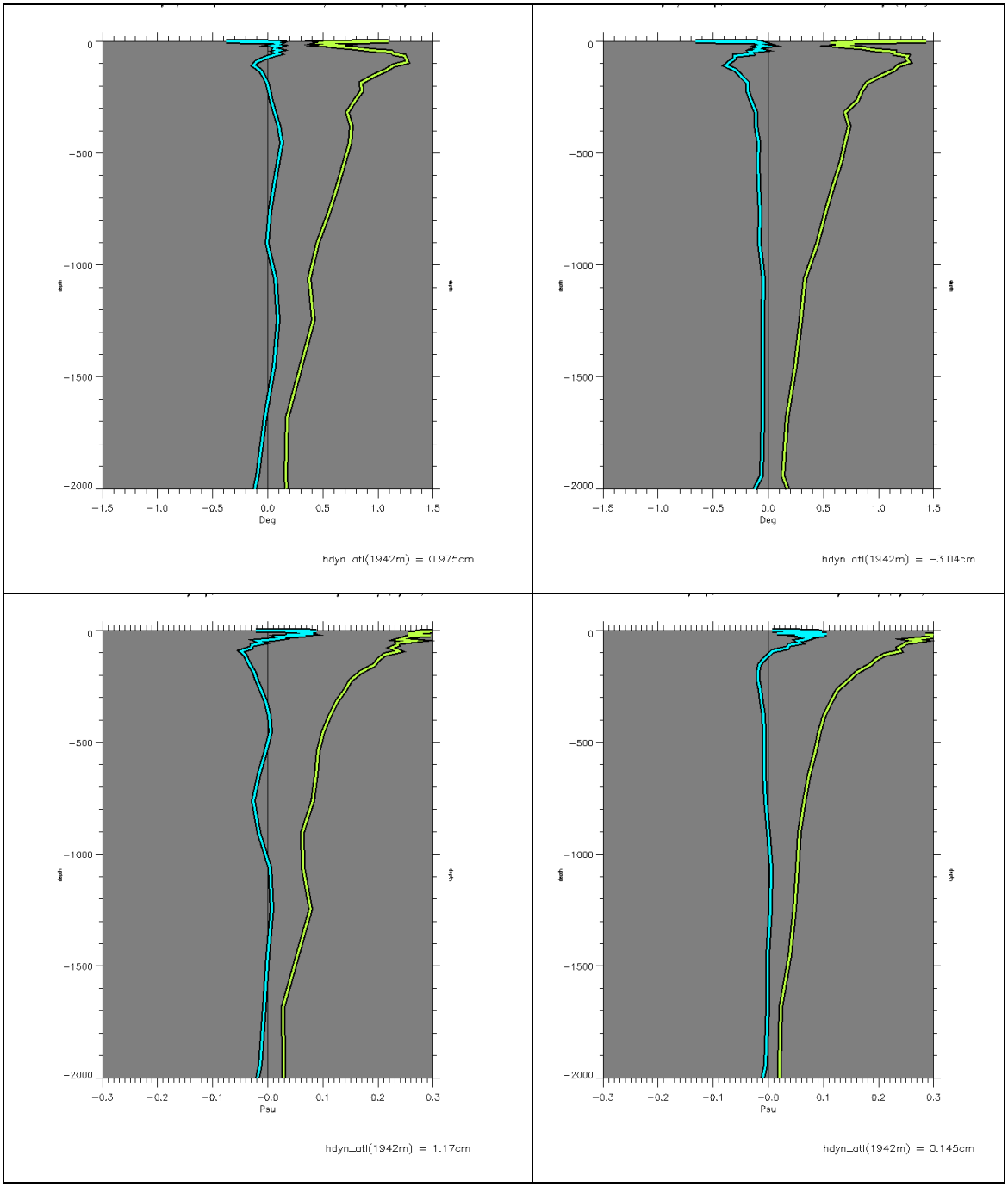

Figure 16 : mean OND 2010 temperature profiles (°C, upper panel) and salinity profiles (psu, lower panel) of average of innovation (blue) and RMS of innovation (yellow) on the whole domain of PSY2V3R1 (left column) and PSY2V4R1 (right column).

Due to a smaller sample PSY2 temperature and salinity biases are amplified with respect to the global domain averages of PSY3 and PSY4. A salty anomaly appeared in PSY2V3R1 between 500 and 1000m due to the ill positioned Mediterranean outflow in the Atlantic, as well as the cold bias near 500 and between 1000 and 1500m. These anomalies are strongly reduced in the new systems and especially in PSY2V4R1 as can be seen in Figure 16 (see also Figure 39).

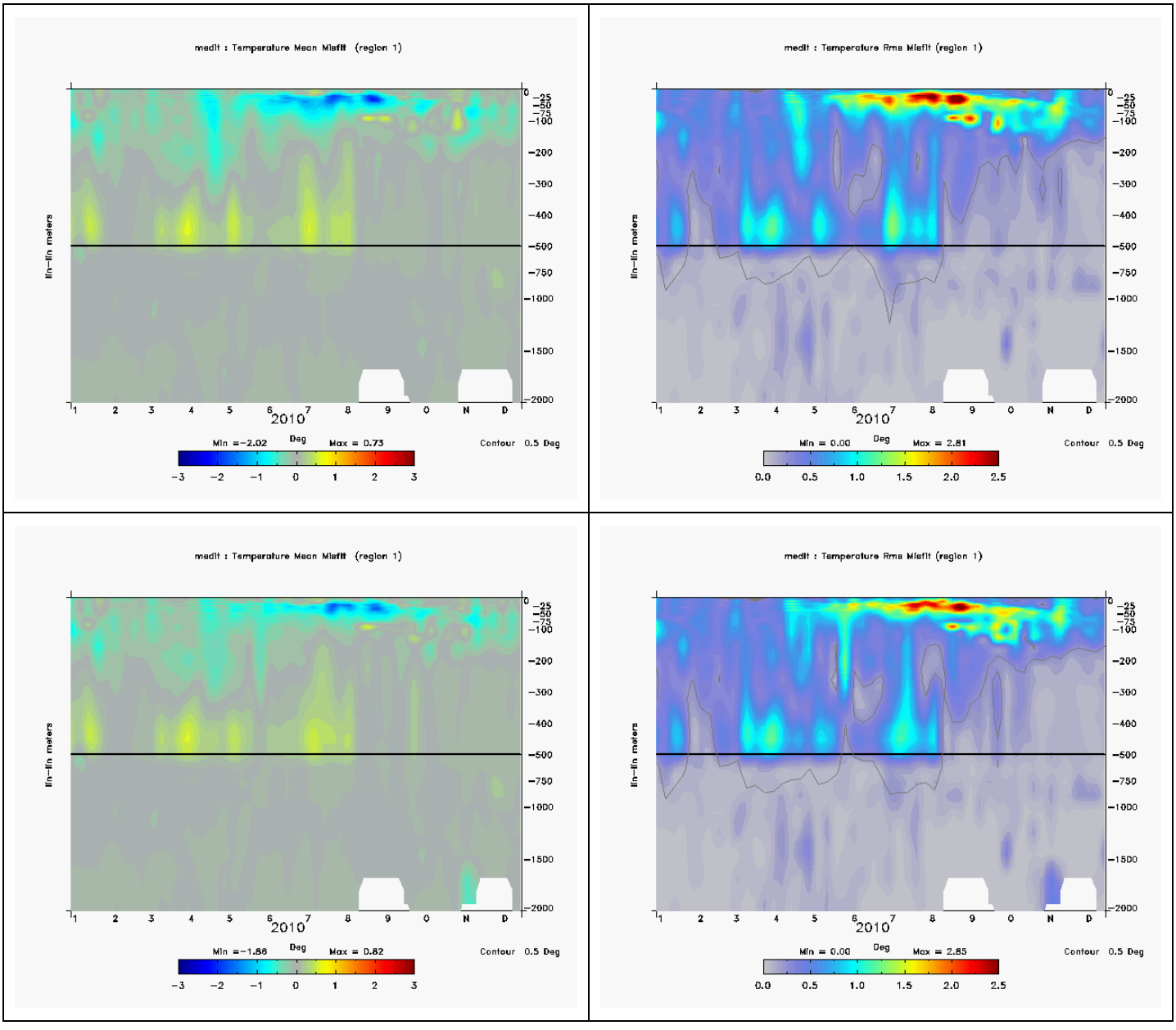

Figure 17: Time evolution of the mean (left column) and rms (right column) of temperature innovation (observatio-forecast) (°C) averaged over the whole Mediterranean Sea, for PSY2V4R1 MyOcean V1 products (upper panel) and for the best experiment (lower panel).

The RMS error in the 0-200m layer is not reduced in the new PSY2V4R1 with respect to PSY2V3R1. In the Atlantic in PSY2V4R1 and PSY3V3R1 a warm bias appears in JAS, strengthens and propagates in the 0-500m layer during the OND season. The maximum amplitude of this bias (around 1°C) occurs in the western part of the extra-tropical Atlantic

(not shown). This seasonal bias occurs mostly during boreal autumn and winter and explains most of the negative innovations observed from 0 to 1000m in the North Atlantic and Mediterranean Sea.

A warm and fresh bias in the 0-100m layer in the Mediterranean Sea partly explains the positive salinity innovation in this layer. The fresh anomaly in the tropical Atlantic (Amazon runoff and too much precipitations) also contributes to these positive innovations on average.

The modifications that were implemented in the systems before re-processing the year 2010 have a moderate positive impact the temperature and salinity biases of the Mediterranean Sea. Most of the improvements take place during summer (June and July) when the bias is maximum, as can be seen on Figure 17 and Figure 18.

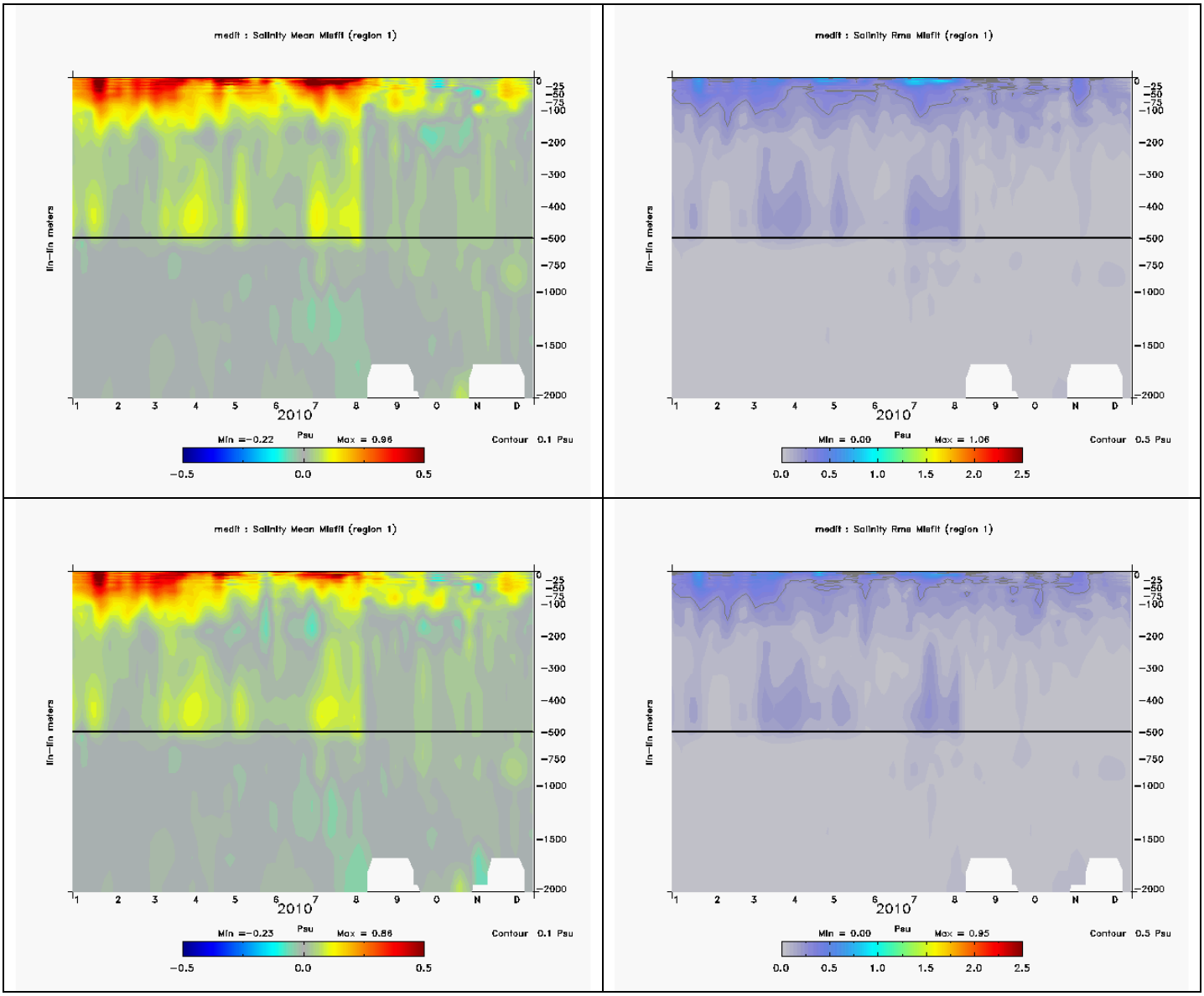

Figure 18: Time evolution of the mean (left column) and rms (right column) of salinity innovation (observation-forecast) (psu) averaged over the whole Mediterranean Sea, for PSY2V4R1 MyOcean V1 products (upper panel) and for the best experiment (lower panel).

While most of the deep biases disappear in the new systems, seasonal biases appear. One of the hypotheses is that the SST assimilation is not as efficient as it used to be. The Incremental Analysis Update together with the bulk rejects part of the increment. There is too much mixing in the surface layer inducing a cold (and salty) bias in surface and warm (and fresh) bias in subsurface. The bias is intensifying with the stratification and the winter mixing episodes reduce the bias. The bias correction is not as efficient on reducing seasonal biases as it is on reducing long term systematic biases. The R&D team currently evaluates possible corrections and the potential use of another L4 SST product for data assimilation (OSTIA, Reynolds AVHRR+AMSRE or CMC). Important departures from the temperature and salinity observations take place on the European Marginal seas, which could lead to further updates of the SLA data assimilation (MDT shifts, tuning of errors) in these regions.

V.2.Accuracy of the daily average products with respect to observations

Note that in the following all diagnostics are computed for the "best experiment" available in 2010 for PSY3V3R1 and PSY2V4R1.

V.2.1. T/S profiles observations

V.2.1.1. 2010 summary for all products on common regions

Comparisons with in situ observations from CORIOLIS within the overlapping regions of the systems (North Atlantic and Mediterranean) are displayed on Figure 19 and Figure 20. PSY3V3R1 and PSY2V4R1 significantly improve the Mercator Ocean analyses in the North and Tropical Atlantic. Both the temperature and salinity errors are reduced, of approximately 0.2 °C and 0.02 psu respectively. PSY3V3R1 is more accurate in terms of salinity than PSY2V4R1, in coherence with a stronger tropical fresh bias in PSY2V4R1 than in PSY3V3R1.

Biases accumulated In the Mediterranean Sea since the beginning of the hindcast run (2007) are still visible in 2010 after the various corrections were implemented. Nevertheless in the second part of the year the new systems reach the performance of PSY2V3R1, except in salinity at the surface.

Geographical maps of the temperature and salinity biases of PSY2V4R1 are displayed on Figure 21. Most temperature errors are located in the Gulf Stream due to high variability in this region, in the main thermocline in the tropical Atlantic and in the Mediterranean sea. Under 100m a temperature bias appears in the western equatorial Atlantic. Salinity biases appear at the surface in the Tropical Atlantic and Gulf of Guinea, in the Gulf Stream and in the Mediterranean. Biases are still strong in subsurface in the western Mediterranean and western tropical Atlantic. Errors deeper than 100m are restricted to the high variability region of the Gulf Stream and off the Amazon runoff. One can notice significant errors along a line between Rio and Dakar. The error here is due to uncorrected observations as the "CLASS4" data used for these statistics (and defined during Mersea) is less quality controlled than the assimilated observations.

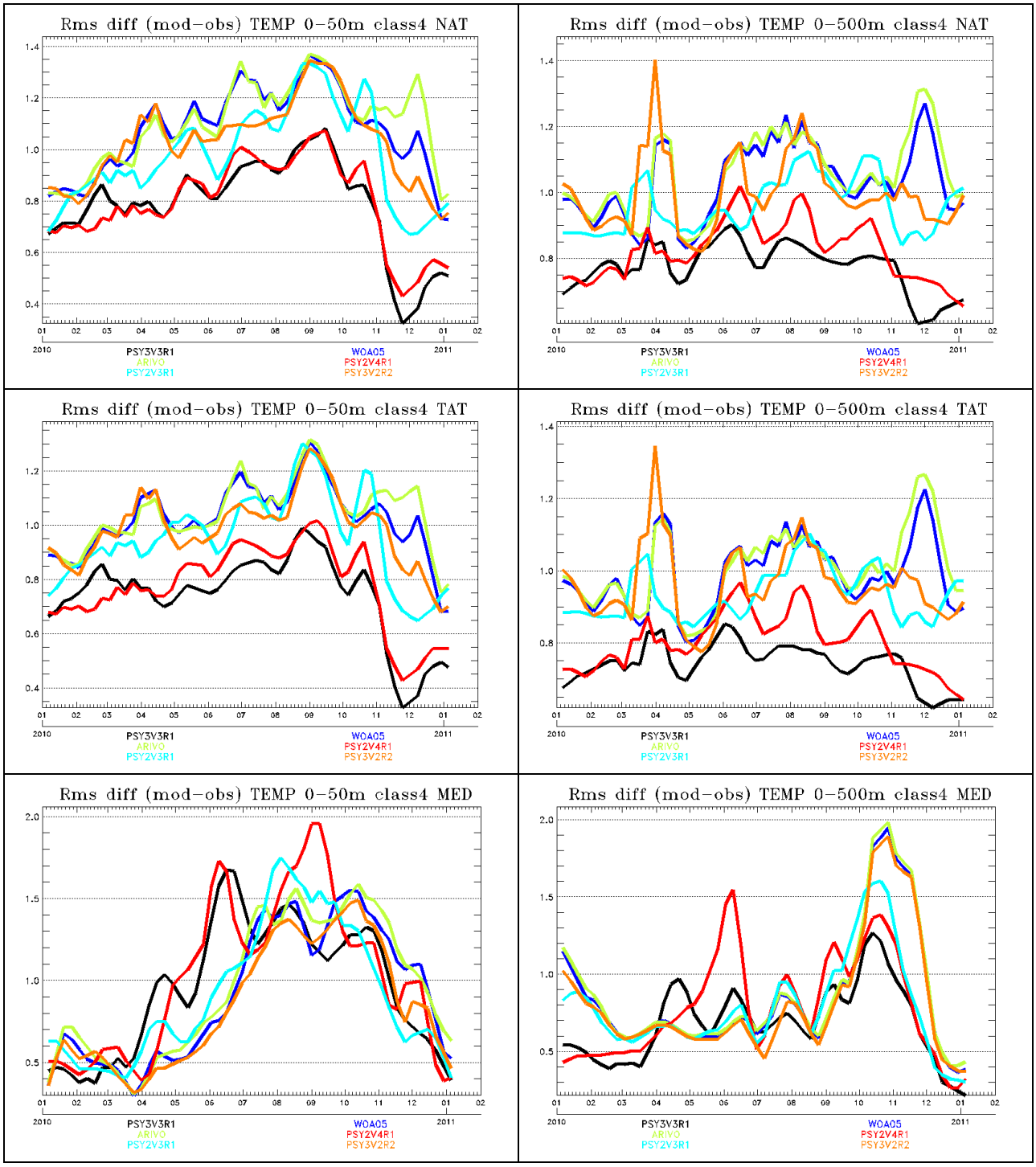

Figure 19: stability of the temperature RMS errors (°C) over the year 2010 for PSY3V2R2 (orange), PSY3V3R1 (black), PSY2V3R1 (cyan), PSY2V4R1 (red), Levitus WOA05 climatology (blue) and Ifremer ARIVO climatology (green). From top to bottom for the North Atlantic, Tropical Atlantic and Mediterranean regions, averaged between 0 and 50m (left panel) and averaged between 0 and 500m (right panel)

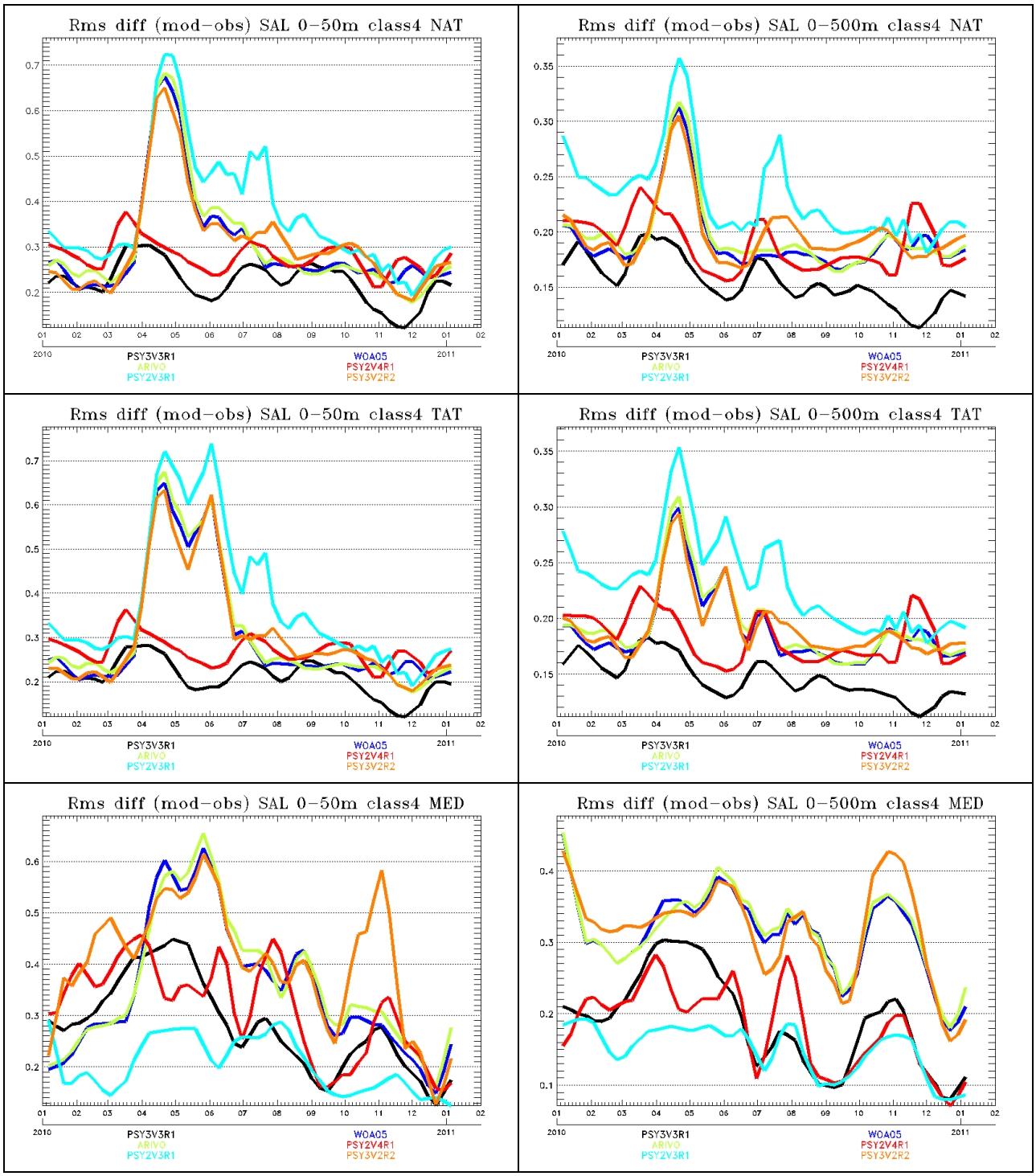

Figure 20: stability of the salinity RMS errors (psu) over the year 2010 for PSY3V2R2 (orange), PSY3V3R1 (black), PSY2V3R1 (cyan), PSY2V4R1 (red), Levitus WOA05 climatology (blue) and Ifremer ARIVO climatology (green). From top to bottom for the North Atlantic, Tropical Atlantic and Mediterranean regions, averaged between 0 and 50m (left panel) and averaged between 0 and 500m (right panel)

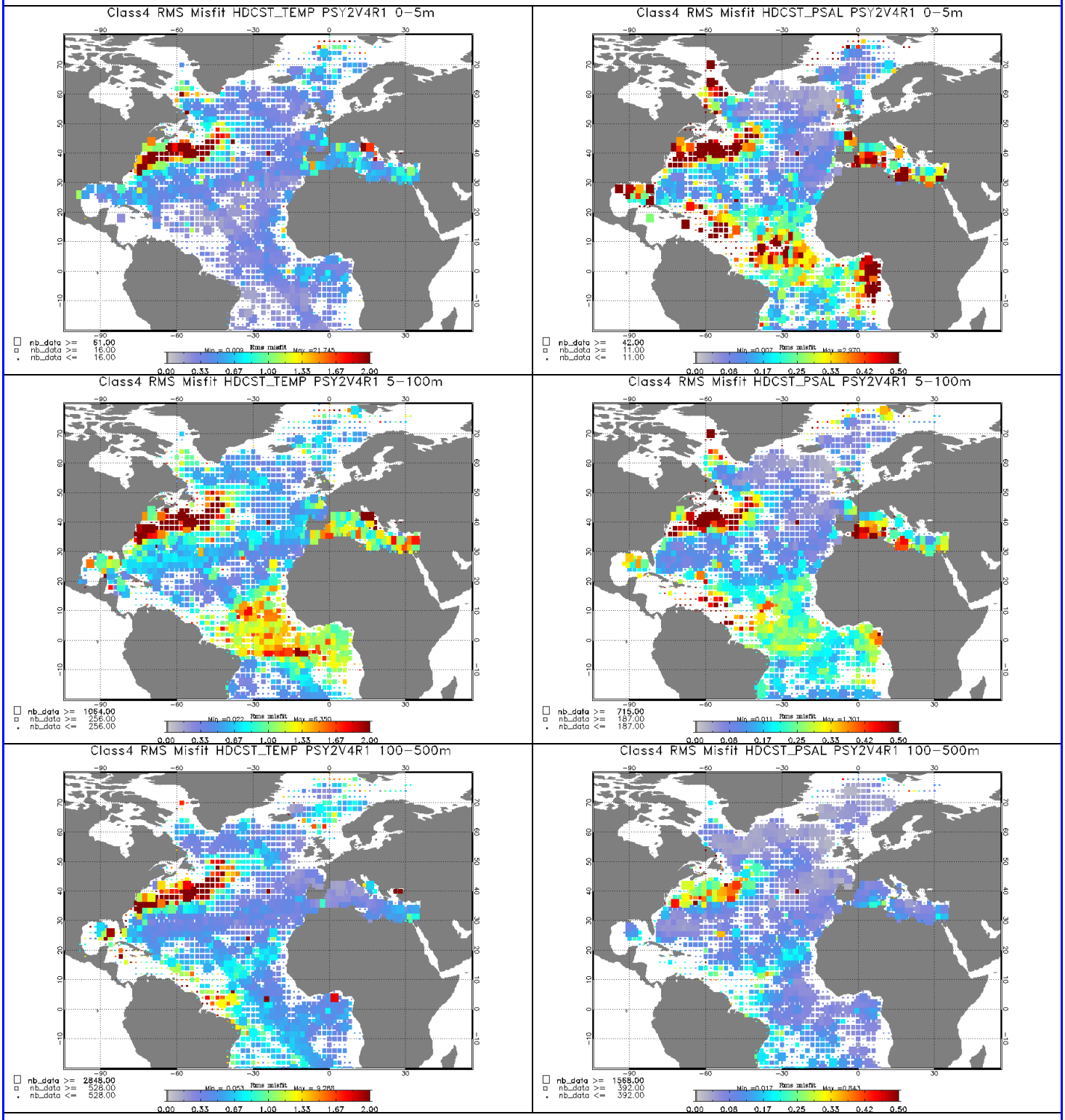

Figure 21: Spatial distribution of the temperature (left, °C) and salinity (right, psu) RMS error departures from the observations in the PSY2V4R1 system in 2007-2010. From top to bottom: averaged in the 0-5 m layer, in the 5-100m layer and in the 100-500m layer. The size of the pixel is proportional to the number of observations used to compute the RMS in 2°x2° boxes.

V.2.1.2. Global statistics for OND 2010

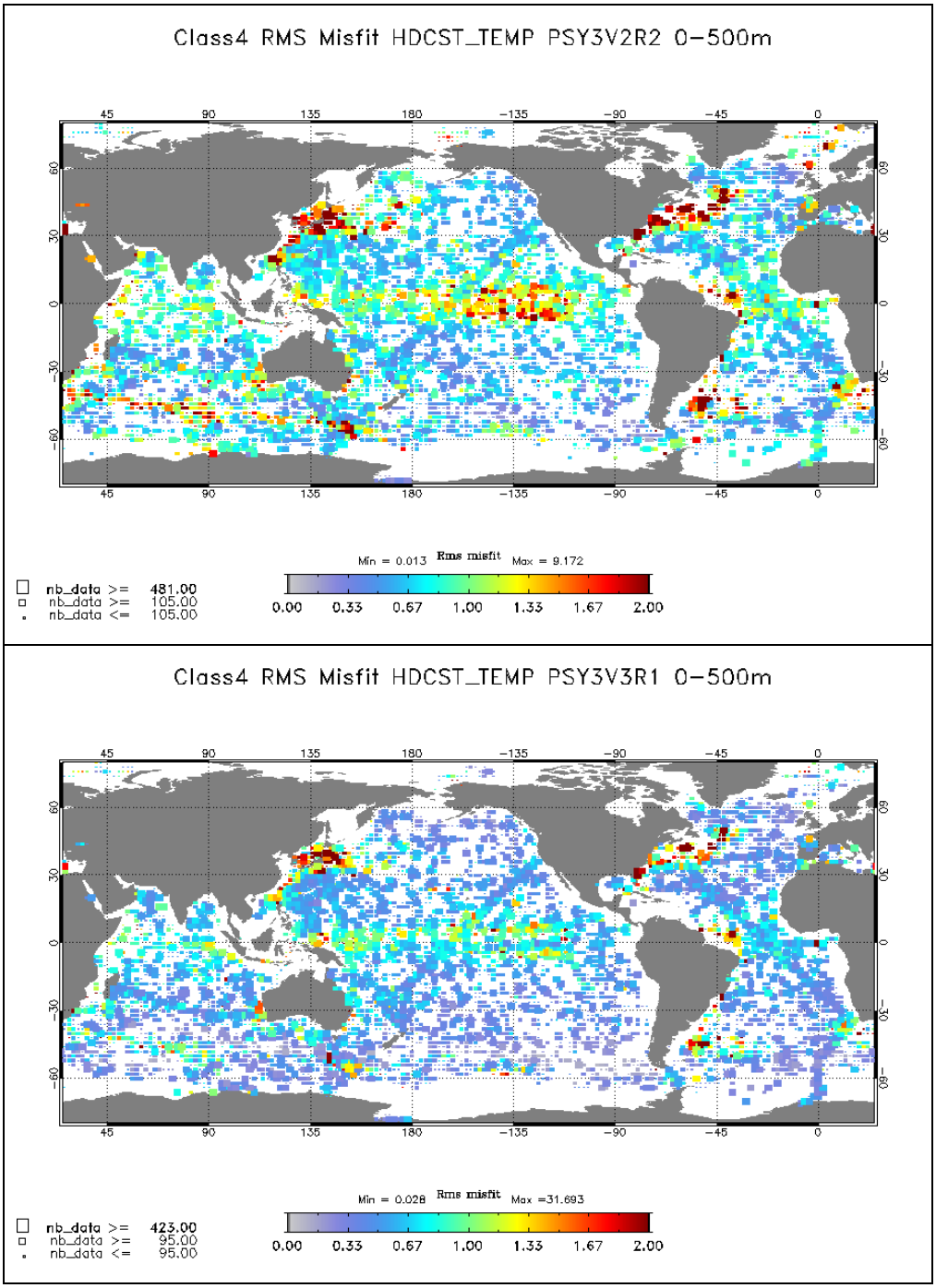

Figure 22: RMS temperature (°C) difference (model-observation) OND 2010 between all available T/S observations from the Coriolis database and the daily average PSY3V2R2 (upper panel) and PSY3V3R1 (lower panel) products (here the nowcast run) colocalised with the observations. The size of the pixel is proportional to the number of observations used to compute the RMS in 2°x2° boxes.

As can be seen in Figure 22, temperature errors in the 0-500m layer stand between 0.5 and 1°C in most regions of the globe in both PSY3V2R2 and PSY3V3R1. Regions of high

mesoscale activity and regions of Sea Ice melting experience higher values (up to 3°C). PSY3V3R1 is clearly closer to the observations in the tropical oceans. The signal is very clear in the Pacific where PSY3V3 will describe the Niña signal and associated instability waves in the central pacific with more accuracy. A bias in the Southern Indian Ocean basin present in PSY3V2R2 (and probably linked with the bias in SLA) disappears in PSY3V3R3. We note that for a given region a minimum of 90 measurements is used to compute the statistics for this three months period.

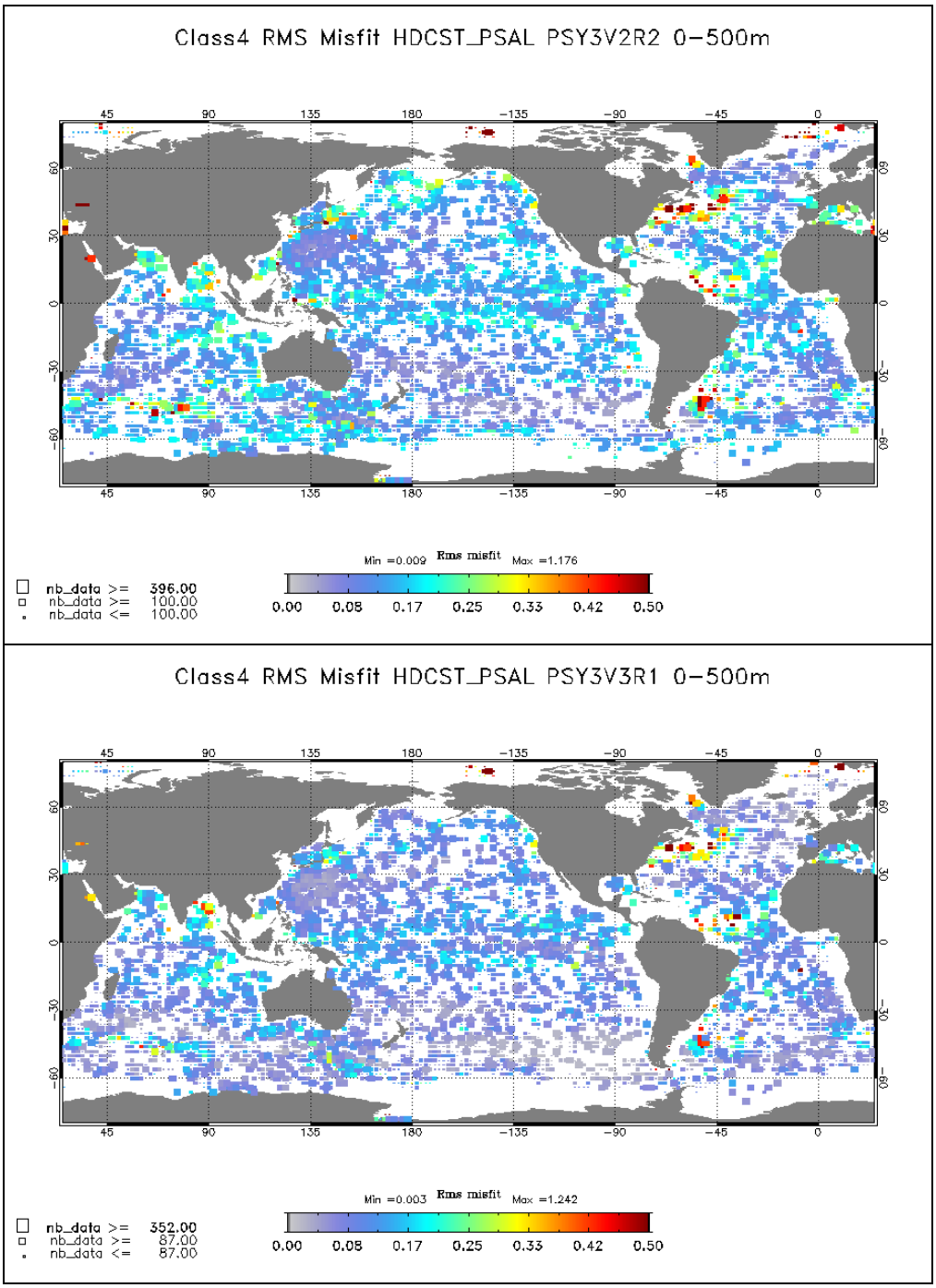

Figure 23: RMS salinity (psu) difference (model-observation) between all available T/S observations from the Coriolis database and the daily average PSY3V2 (upper panel) and PSY3V3 (lower panel) products colocalised with the observations. The size of the pixel is proportional to the number of observations used to compute the RMS in 2°x2° boxes.

The salinity RMS errors (Figure 23) are usually less than 0.2 psu but can reach high values in regions of high runoff (Amazon, Sea Ice limit) or precipitations (SPCZ), and in regions of high mesoscale variability. The salinity error is globally reduced in PSY3V3R1 with respect to PSY3V2R2. As in PSY2V4R1 for the whole hindcast period (2007-2010, Figure 21) the salinity error is important in PSY3V3R1 off the Amazon runoff.

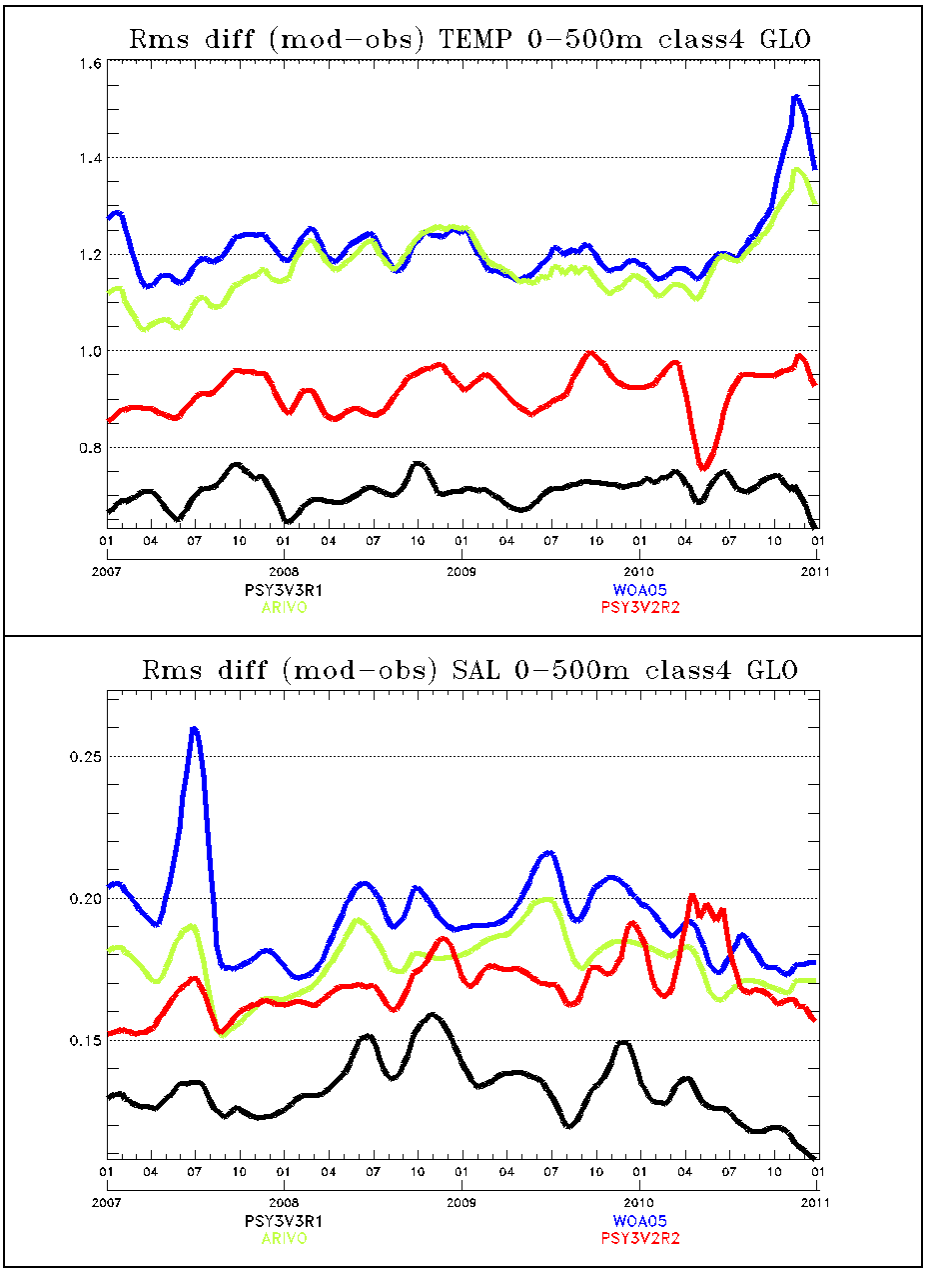

Figure 24: stability of the temperature (upper panel) and salinity (lower panel) RMS errors over the 2007-2010 period for PSY3V2R2 (red line), PSY3V3R1 (black line), Levitus WOA05 climatology (blue line) and Ifremer ARIVO climatology (green line).

Figure 24 illustrate the stability in time of the new system PSY3V3R1, as well as the improvement of in situ profile data assimilation. A gain of 0.2°C and 0.02 psu RMS error can be observed on average in the new system.

In April 2010 the PSY3V2R2 system is very close to temperature observations, and symmetrically drifts away from salinity observations, giving poor performance on average (the climatology is closer to the observations). This phenomenon is not observed in PSY3V3R1. Note that in PSY3V3R1, pseudo observations of salinity are used near estuaries and under sea ice (where error covariances are not trusted) in order to avoid error compensation phenomena.

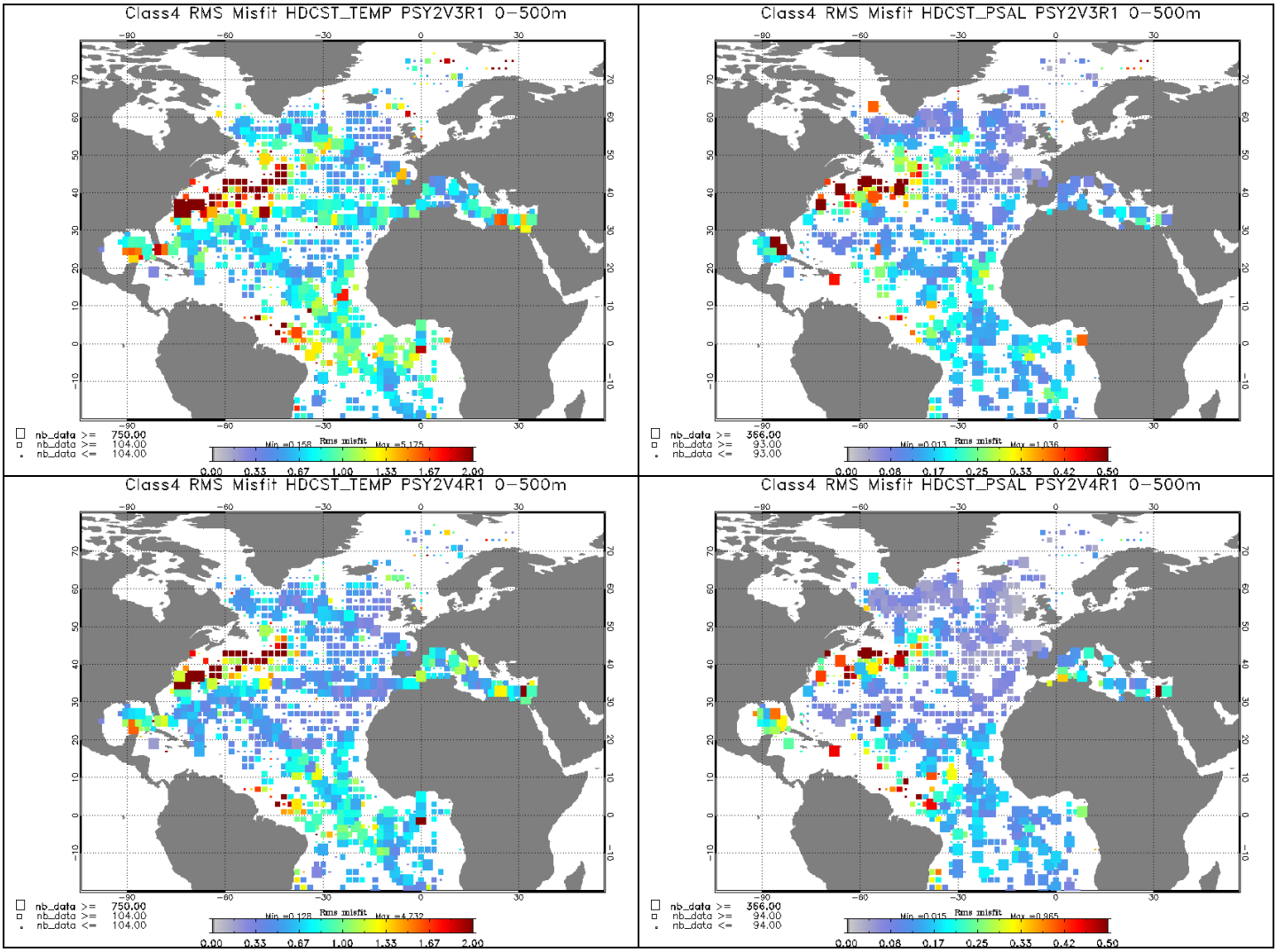

Figure 25: Upper panel: RMS temperature (left column) and salinity (right column) difference (model-observation) in OND 2010 between all available T/S observations from the Coriolis database and the daily average PSY2V3R1 products colocalised with the observations. Lower panel: same with PSY2V4R1.

PSY2V4R1 is closer to the in situ profiles than PSY2V3R1, mainly in the tropics and the subtropics (Figure 25). In the Mediterranean Sea on average, PSY2V3R1 is still closer to the observations than the new version PSY2V4R1.

V.2.1.3. Water masses diagnostics

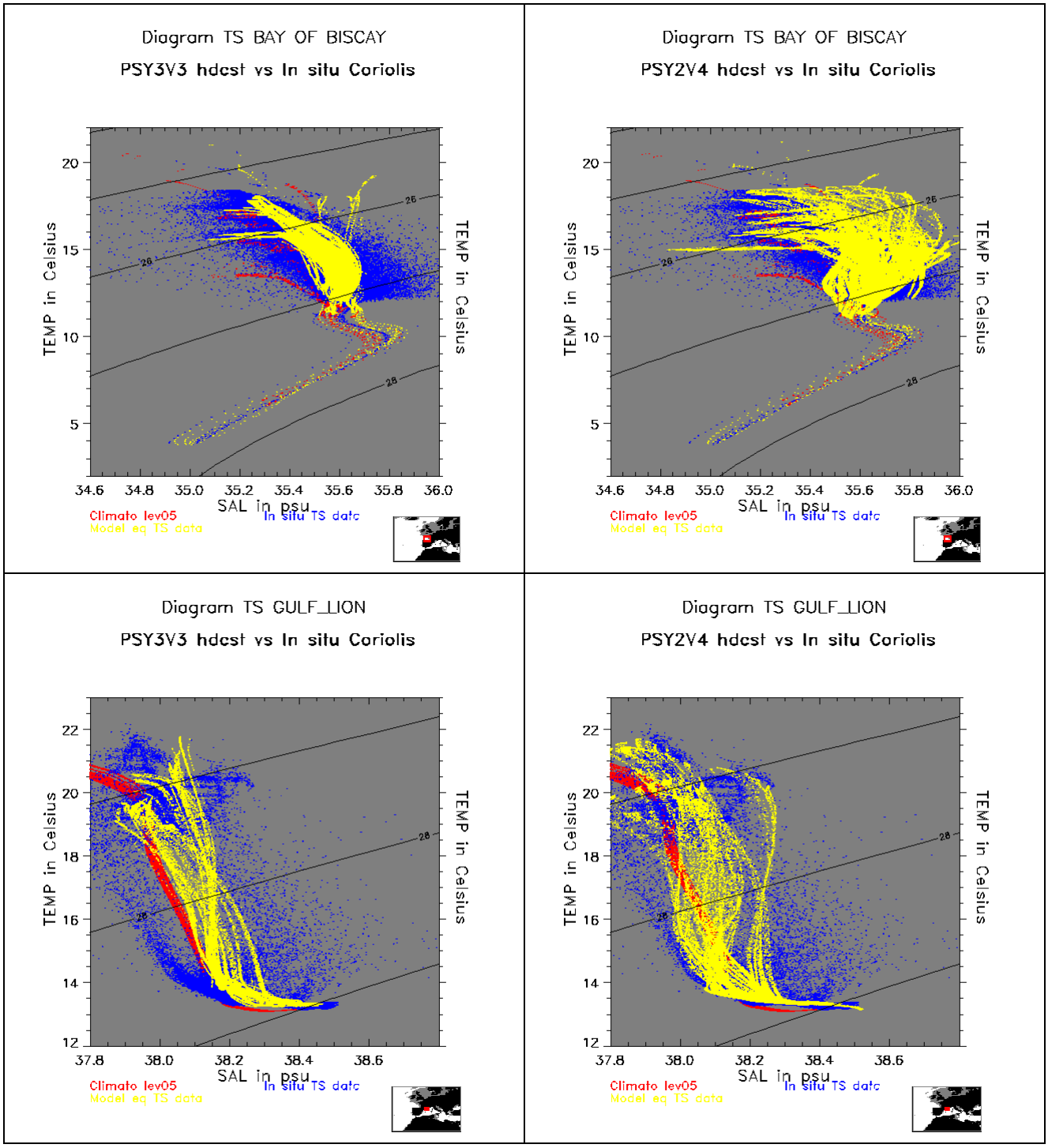
Diagram TS BAY OF BISCAY
PSY3V3 hdcst vs In situ Coriolis
TEMP in Celsius
SAL in psu
Climato lev05
Model eq TS data
In situ TS data
Diagram TS BAY OF BISCAY
PSY2V4 hdcst vs In situ Coriolis
TEMP in Celsius
SAL in psu
Climato lev05
Model eq TS data
In situ TS data
Diagram TS GULF_LION
PSY3V3 hdcst vs In situ Coriolis
TEMP in Celsius
SAL in psu
Climato lev05
Model eq TS data
In situ TS data
Diagram TS GULF_LION
PSY2V4 hdcst vs In situ Coriolis
TEMP in Celsius
SAL in psu
Climato lev05
Model eq TS data
In situ TS data

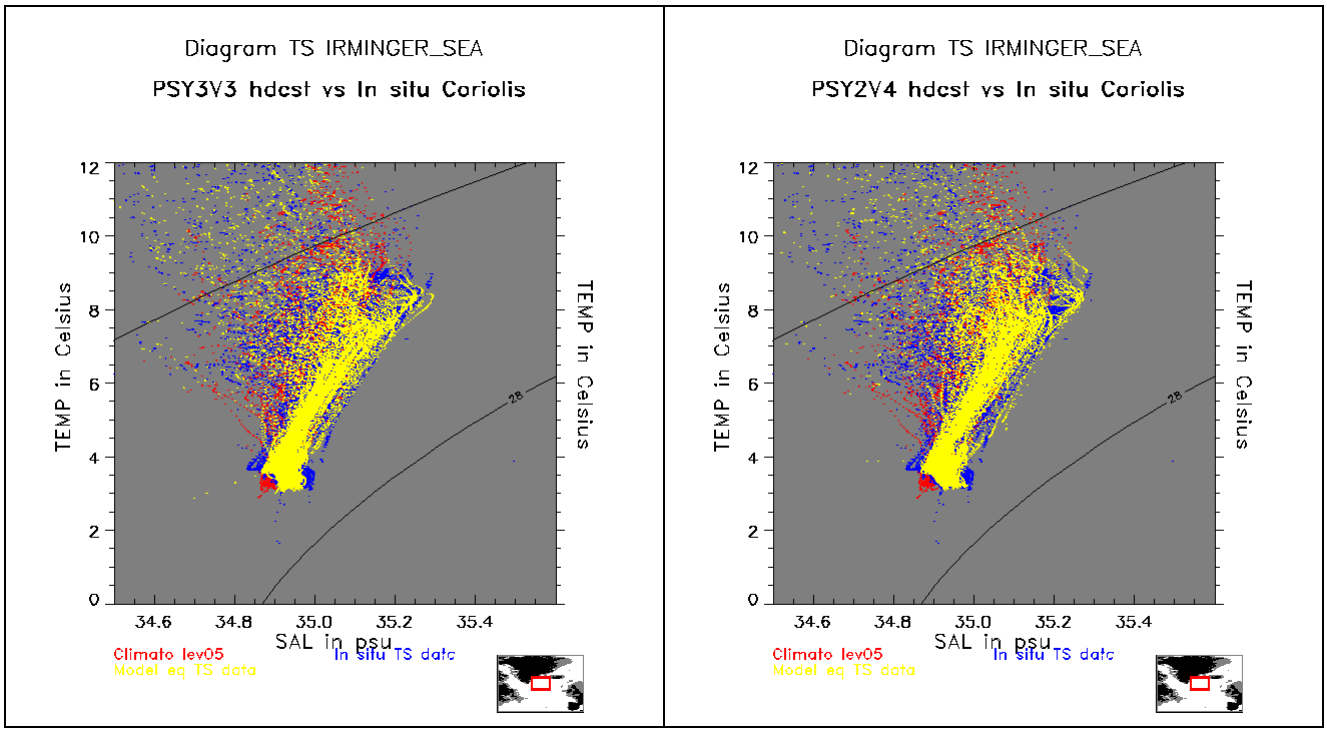

Figure 26: Water masses (Theta, S) diagrams in the Bay of Biscay (upper panel), Gulf of Lyon (middle panel) and Irminger Sea (lower panel), comparison between PSY3V3R1 (left column) and PSY2V4R1 (right column). PSY2 and PSY3: yellow dots, Levitus WOA05 climatology : red dots, in situ observations : blue dots.

We use here the daily products (analyses) collocated with the T/S profiles to draw "theta, S" diagrams. PSY2V4R1 better represents water masses characteristics than PSY2V3R1, especially in the Bay of Biscay (Figure 26). Nevertheless warm surface waters are too salty in in PSY2V4R1. On the contrary PSY3V3R1 surface characteristics stay within the observed envelope. The spread of the PSY3V3R1 water masses characteristics is not as large as in the observations and in PSY2V4R1, probably due to larger variability scales in the global at ¼°. An improvement is also visible in the Gulf of Lyon, despite the bad statistical results in the Mediterranean Sea. The Tropical Atlantic is at least as realistic as in PSY2V3R1. We note the possibly (fresh) biased observations in the tropical Atlantic (Figure 27).

In the tropics the systems stick to the climatology (Figure 27). PSY3V3R1 and PSY2V4R1 have very similar behaviours except in the surface layer where PSY2V4R1 fresh bias is more pronounced.

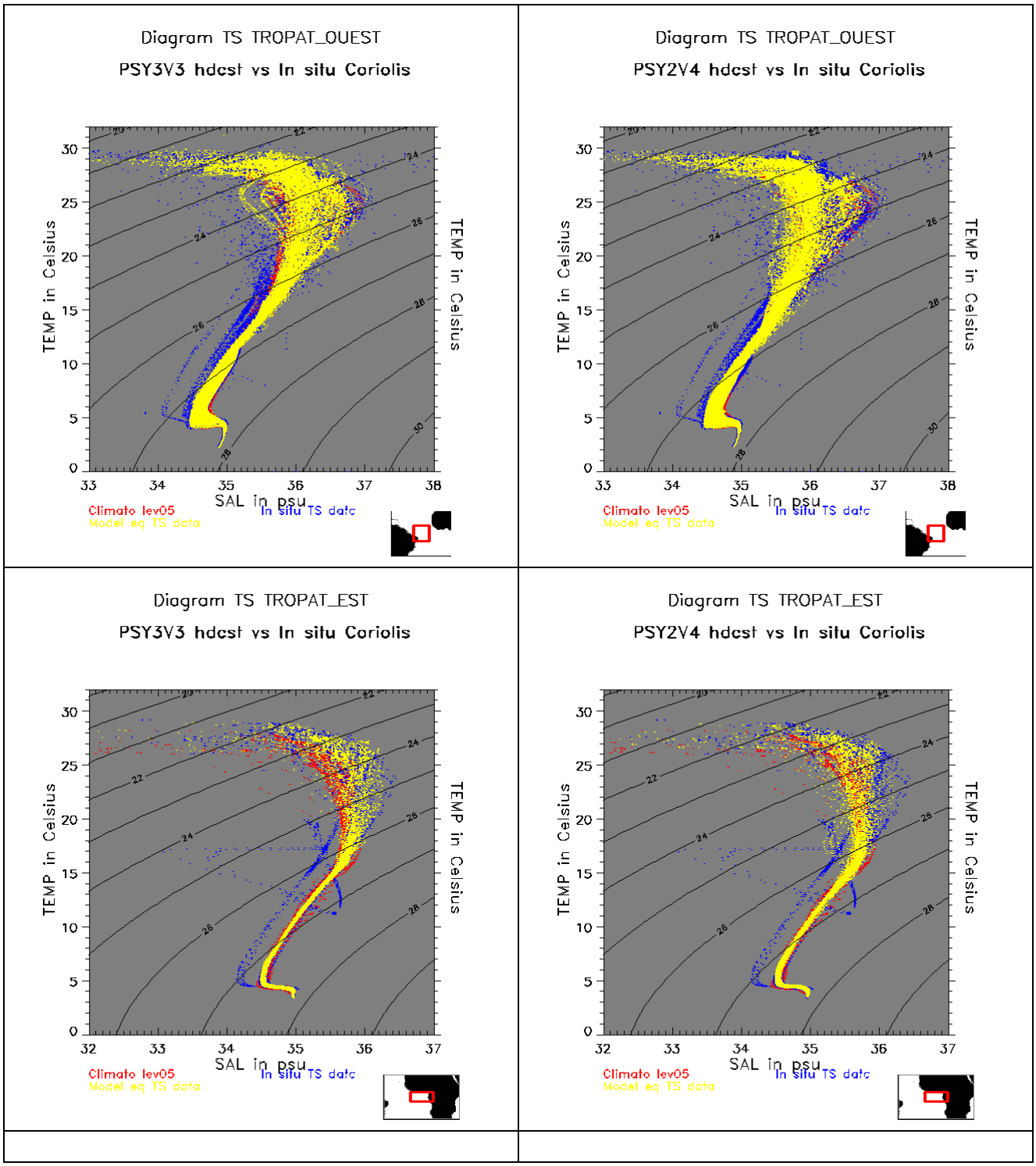

Figure 27 : Water masses (Theta, S) diagrams in the Western Tropical Pacific (upper panel) for PSY3V3R1 (left) and PSY2V4R1 (right) and in the Eastern Tropical pacific (lower panel) for PSY3 (left) and PSY2 (right). PSY2 and PSY3 : yellow dots, Levitus WOA05 climatology : red dots, in situ observations : blue dots.

In the Benguela current and Kuroshio current (Figure 28) PSY3V3R1 gives realistic descriptions of water masses. Regions of the North Atlantic are also displayed such as the Gulf Stream, where the model misses some cold and fresh waters of the Labrador current. In the Gulf of Cadiz the signature of the Mediterranean outflow is well reproduced.

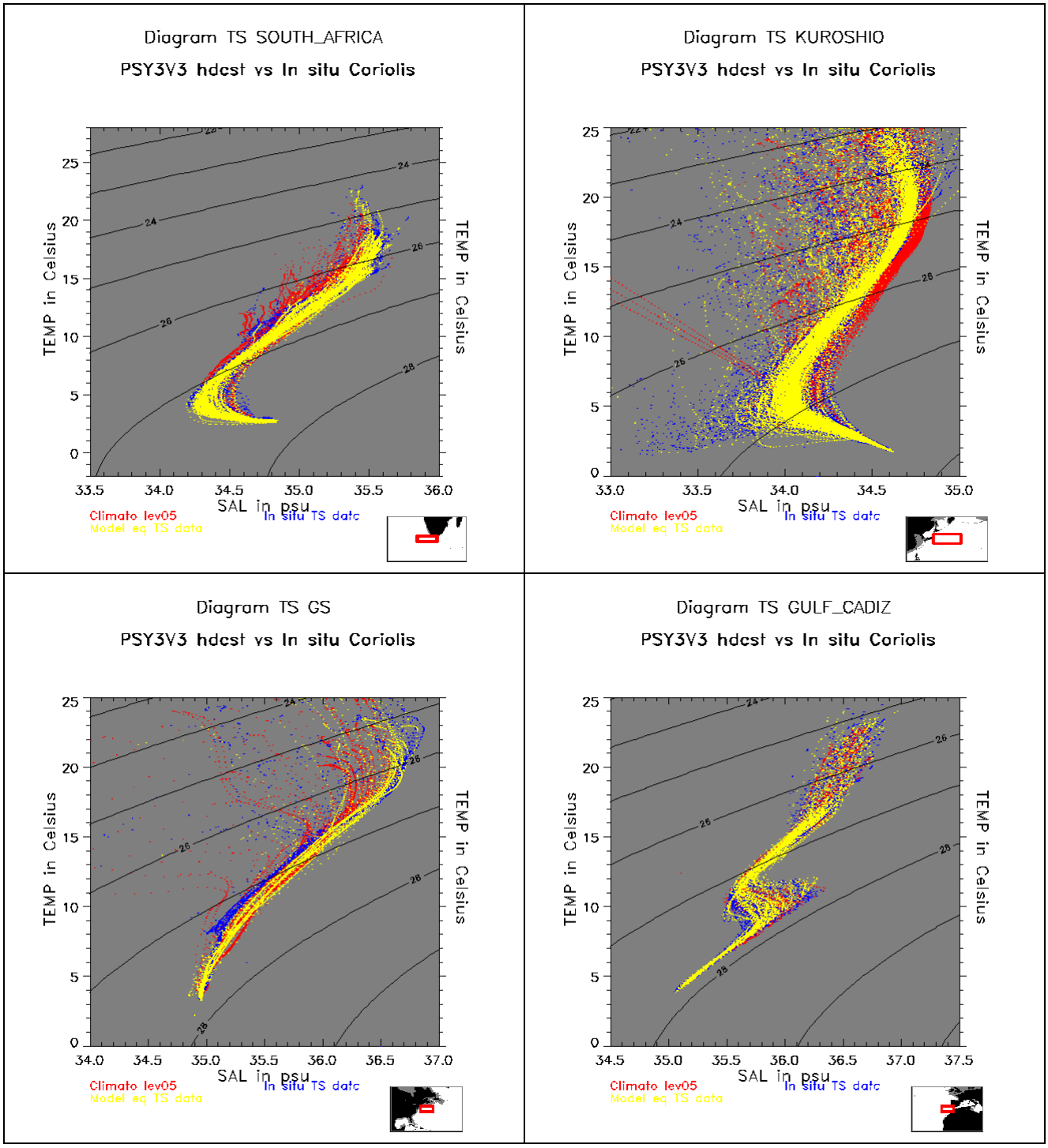

Figure 28: Water masses (Theta, S) diagrams in South Africa and Kuroshio (upper panel) and Gulf Stream region and Gulf of Cadiz (lower panel) in PSY3V3R1

V.2.2. Drifting buoys velocity measurements

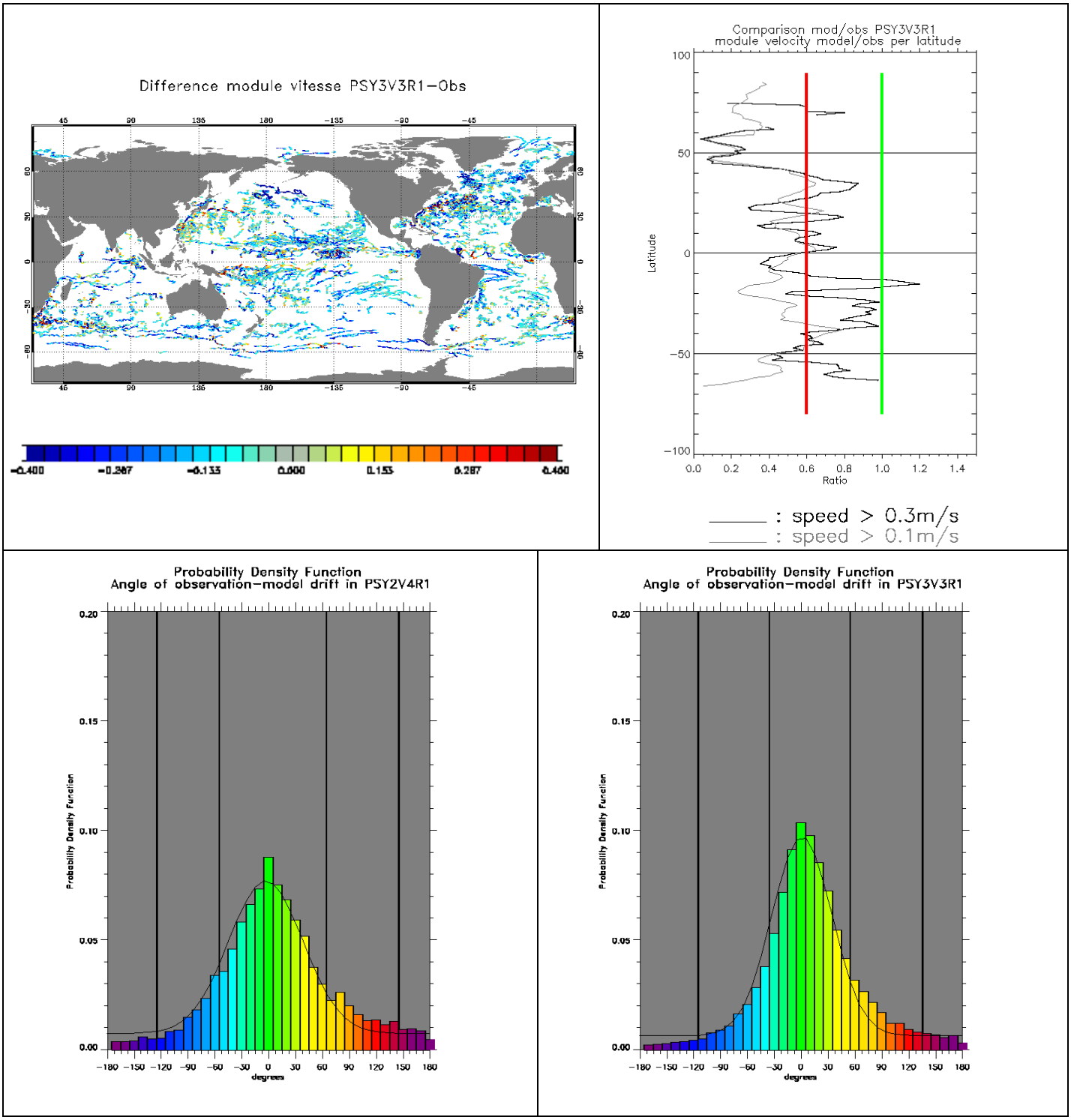

Figure 29: PSY3V3R1 analyses of velocity (m/s) collocated with drifting buoys velocity measurements. Upper left panel: difference model - observation of velocity module. Upper right panel: ratio model/observation per latitude. Lower panel: distribution of the velocity vector direction errors (degrees) for PSY2V4R1 (left panel) and PSY3V3R1 (right panel)

The surface velocity is globally underestimated by the new systems, as well as in the former PSY3V2R2 and PSY2V3R1, and as illustrated in Figure 29. Comparisons of surface

drifter velocity measurements with PSY3V3R1 velocities (comparisons done at 15m) show that the relative error is approximately 20 % and reaches locally more than 50 % (not shown). The zonal averaged ratio between modelled and observed velocities shows a latitudinal dependency of this bias which appears to be stronger north of 20°N. High velocities (> 30 cm/s) are better represented, which indicates that this bias is mainly due to small velocity values in the centre of gyres for instance. The large direction errors are localized and generally correspond to ill positioned mesoscale structures. The PDF of angle errors is sharper in PSY3V3R1 than in PSY2V4R1 due to a larger (global) sample in PSY3V3R1 (regional comparisons to be done in the next issue).

V.2.3. Sea ice concentration

In PSY3V3R1 the Arctic sea ice fraction is well reproduced on average. It is underestimated in the Denmark Strait in OND (Figure 30). Slight departures from the observations are visible in marginal seas. The calibration on years 2007 to 2009 has shown that the system tends to melt too much ice during the summer, while the winter sea ice covers are much more realistic in PSY3V3R1 than in previous versions of PSY3 or even GLORYS1V1 reanalysis. See Figure 41 for monthly averages time series over the last 12 months. GLORYS2V1 also exhibits realistic sea ice fractions in both hemispheres (results to come in the next issue).

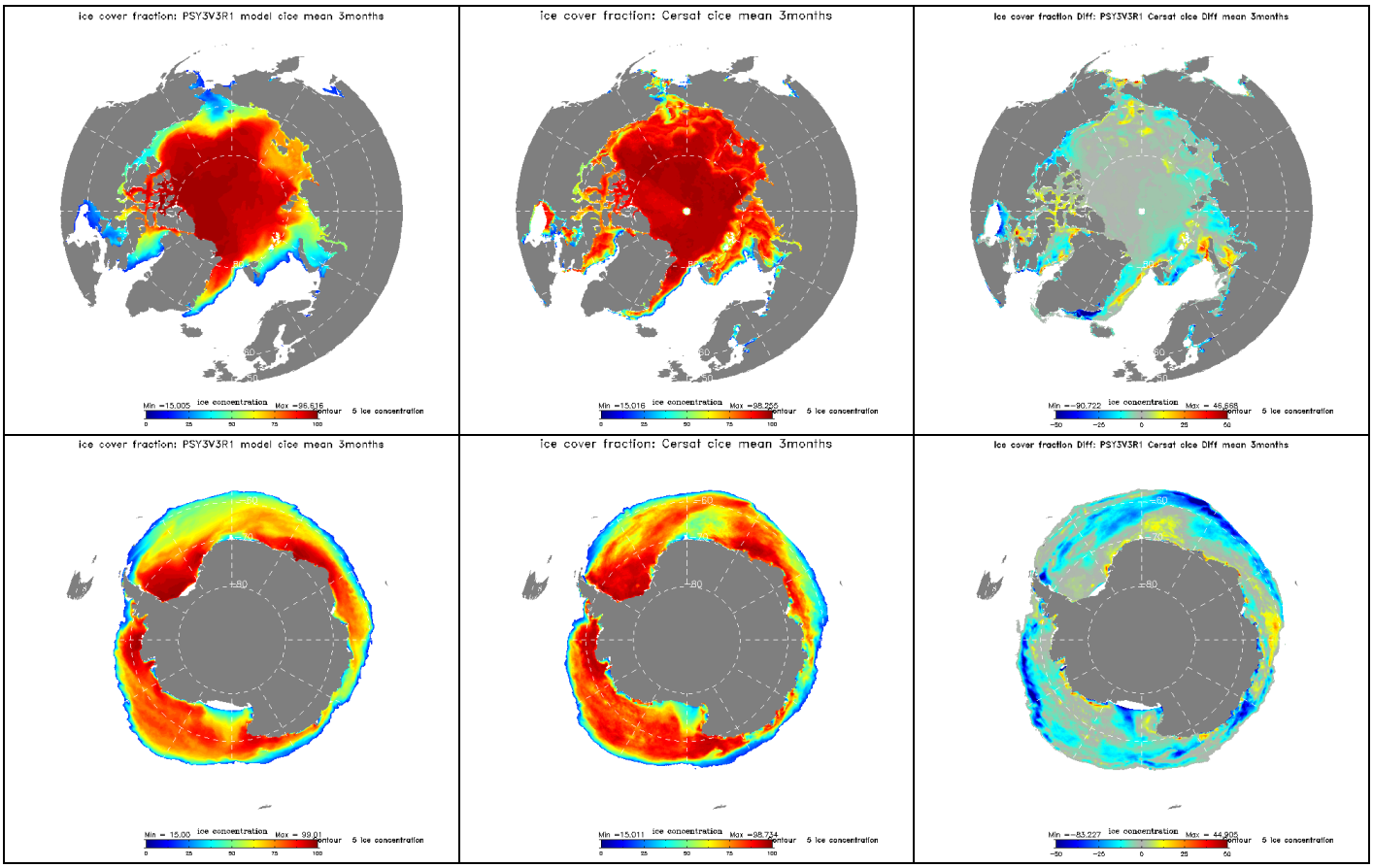

Figure 30: Comparison of the sea ice cover fraction mean for OND 2010 for PSY3V3 in Arctic (upper panel) and Antarctic (lower panel), for each panel the model is on the left the mean of Cersat dataset in the middle and the difference on the right.

In the Antarctic the sea ice concentration is underestimated near the sea ice limit but the extent is well reproduced.

Figure 31 illustrates the fact that sea ice cover in OND 2010 is well under the past years climatology.

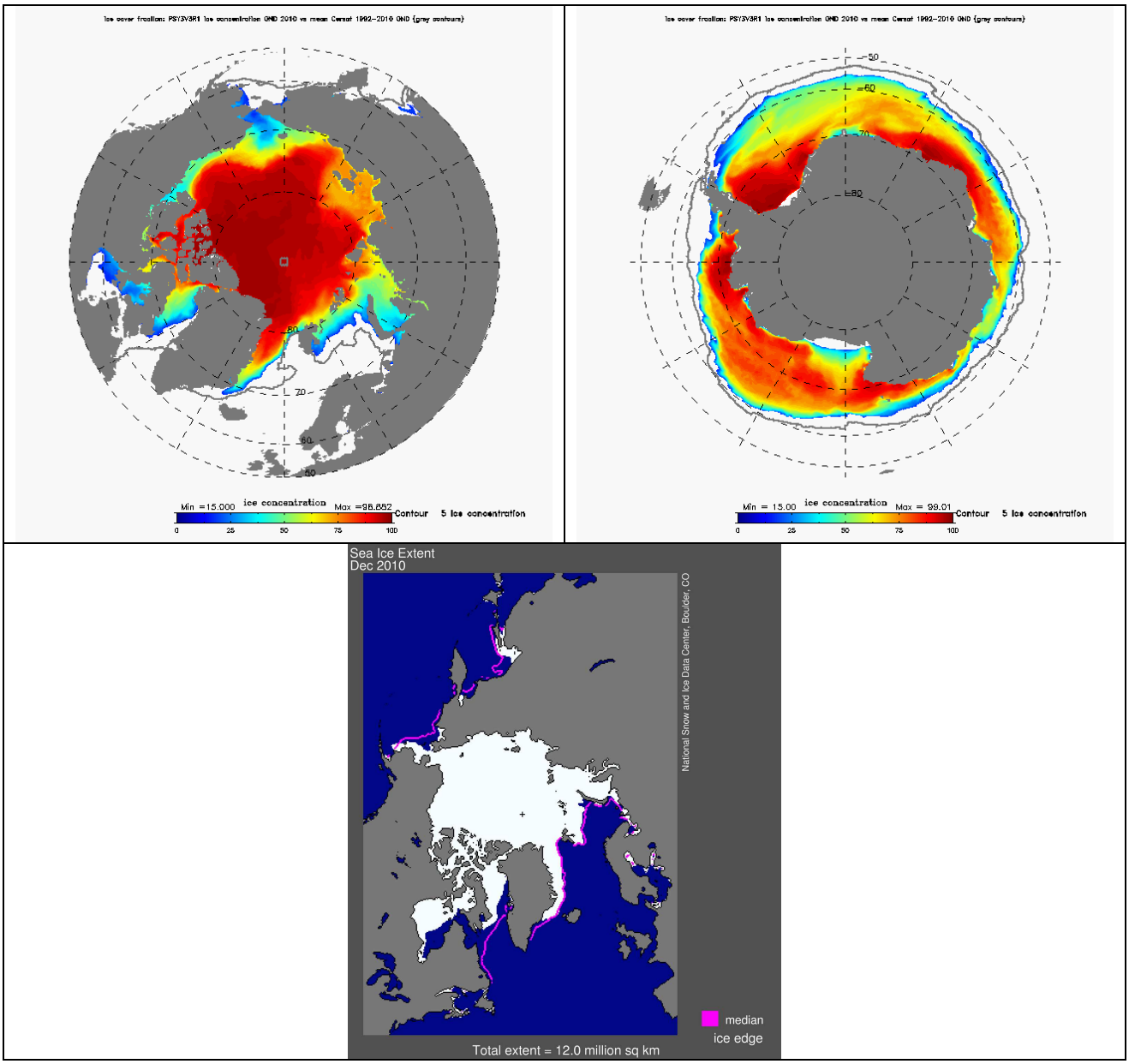

Figure 31: Upper panel: OND 2010 sea ice extend in PSY3V3R1 with overimposed climatological OND 1992-2010 sea ice fraction (grey line, > 15% ice concentration) for the Arctic (left) and Antarctic (right) areas. Lower panel: NSIDC map of the sea ice extend in the Arctic for December 2010 in comparison with a 1979-2000 median extend (magenta line).

VI Forecast error statistics

VI.1. Forecast accuracy: comparisons with observations when and where available

Not many PSY2V4R1 and PSY3V3R1 forecast are available in 2010 to perform significant statistics. Forecasts are only available since December, 15th. Nevertheless as can be seen in Figure 32 the PSY2V4R1 products have a better accuracy than the climatology in the North Atlantic region in OND 2010. The accuracy is better in the near surface layer (0-50m) than in the 0-500m layer.

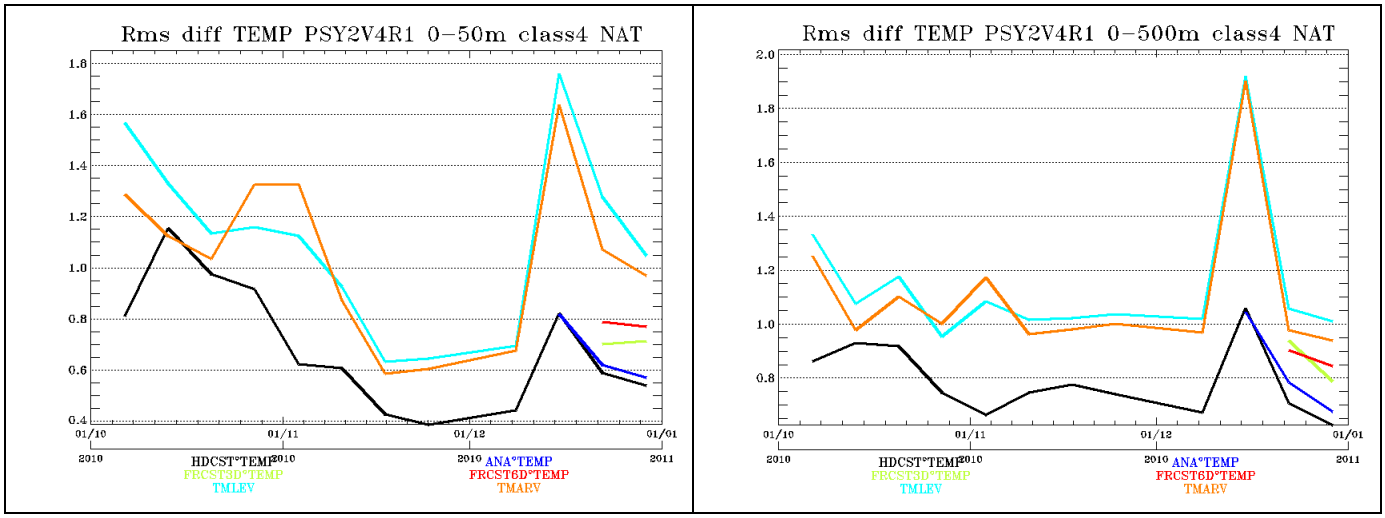

Figure 32: In the North Atlantic region for PSY2V4R1, time series of forecast (FRCST) accuracy at 3 (green line) and 6 (red line) days range, together with analysis (ANA in blue and HDCST in black), and climatology (TMLEV Levitus (2005) in cyan and in orange TMARV Arivo from Ifremer). Accuracy as measured by a RMS difference with respect to all available temperature (°C) observations from the CORIOLIS database.

In the Mediterranean Sea (Figure 33), the PSY2V4R1 salinity analyses do not beat the climatology in November, while the temperature analyses are useful through the whole season. The forecast beat the climatology in December.

PSY3V3R1 statistics in the Atlantic, Pacific and Indian basin in the 0-500m layer (Figure 34) display a generally good accuracy and added value of the analyses and forecast with respect to climatology, especially in the Tropical Pacific and Indian Ocean. In these regions the system is controlled by the TAO/TRITON and RAMA arrays of T/S moorings. In November the accuracy of the South Atlantic analyses fall below the climatology probably partly due the seasonal bias. We note that accuracy differences between the hindcast and the nowcast analyses are visible in December in PSY3V3R1 (to be followed in time).

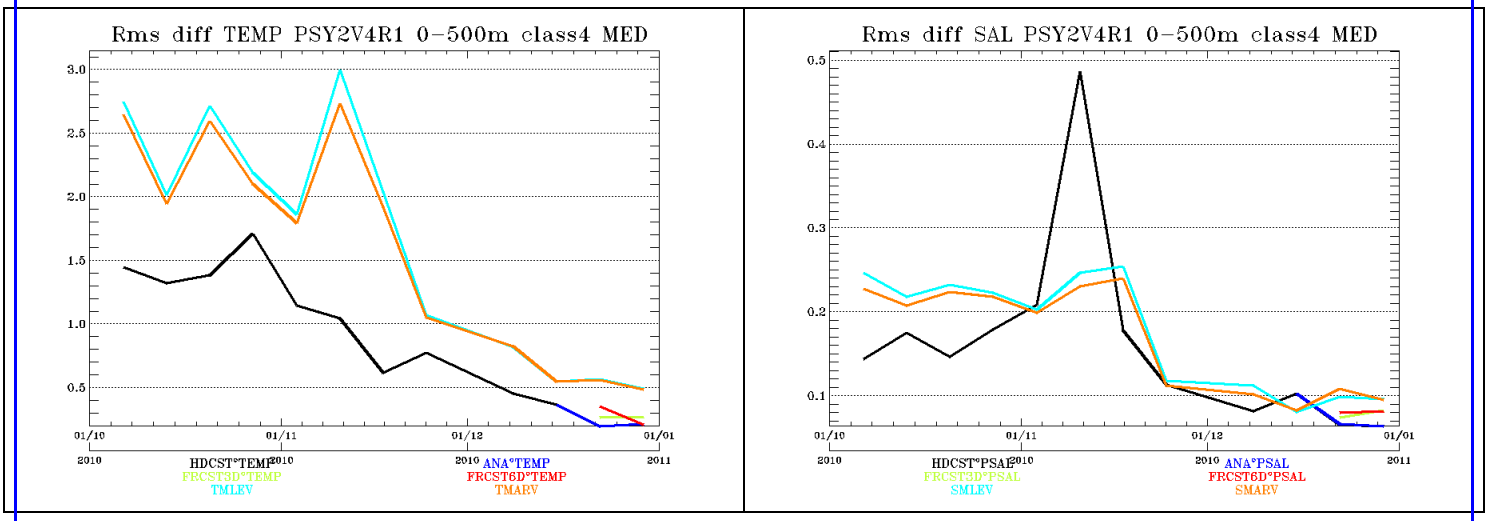

Figure 33: same as Figure 32 for the Mediterranean Sea in the PSY2V4R1 system (upper panel) and comparison with the old system PSY2V3 (lower panel), the old system PSY3V2R2 and the new PSY3V3 R1 in the 0-500m layer. On the left temperature (°C) and on the right salinity (psu)

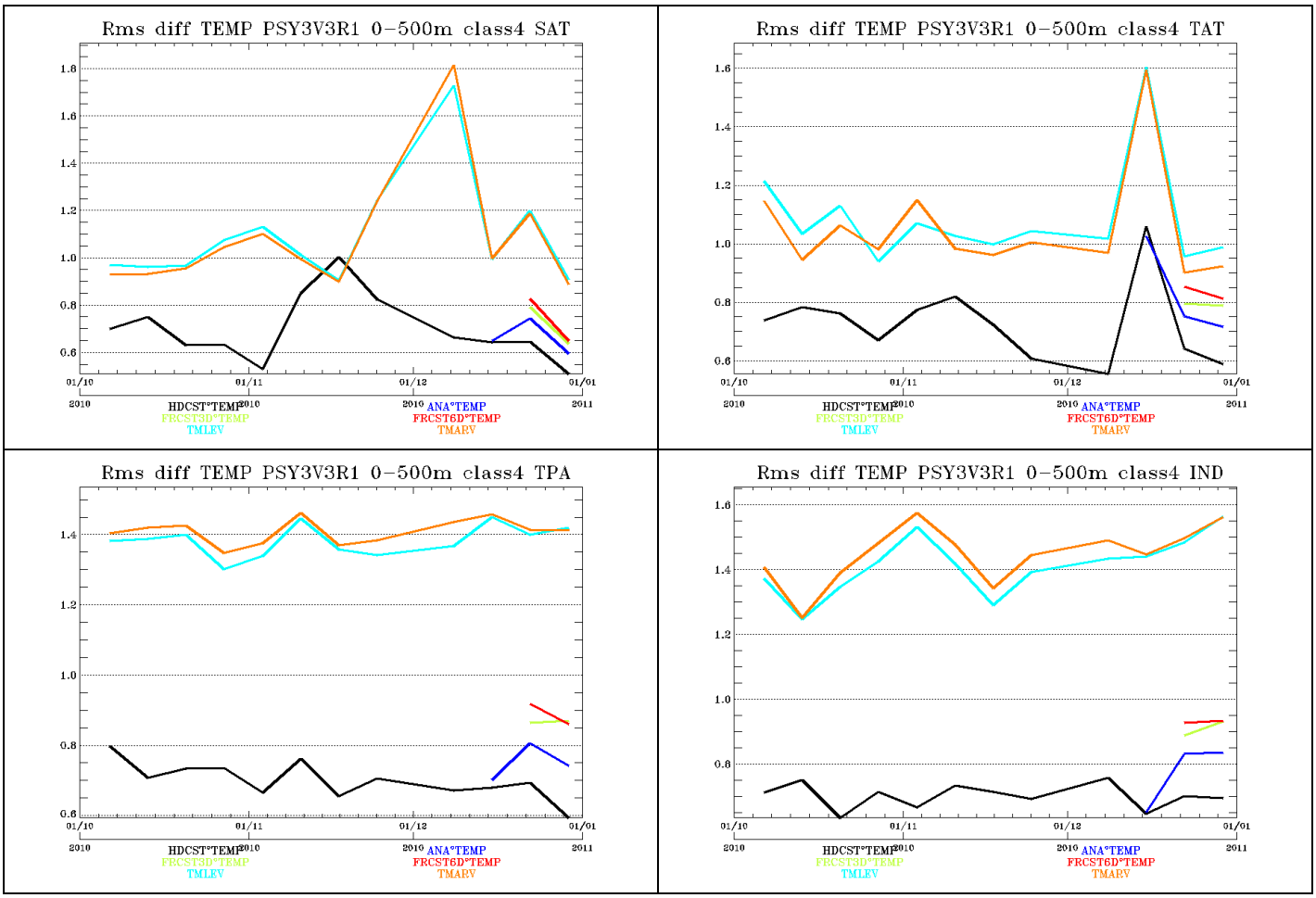

Figure 34: same as Figure 32 for temperature only in the 0-500m layer, the new PSY3 system and the South Atlantic Ocean (upper left panel), the Tropical Atlantic (upper right panel), the Tropical Pacific (lower left panel) and the Indian Ocean (lower right panel).

VI.2. Forecast verification: comparison with analysis everywhere

The Murphy Skill Score is described by equation 1 (cf Wilks, *Statistical Methods in the Atmospheric Sciences*, Academic Press, 2006). This score is close to 0 if the forecast is equivalent to the reference. It is positive and aims towards 1 if the forecast is more accurate than the reference.

$$SS = 1 - \frac{\sum_{k=1}^{n}\left[\frac{1}{M}\sum_{m=1}^{M}\left(Forecast_m - Obs_m\right)^2\right]}{\sum_{k=1}^{n}\left[\frac{1}{M}\sum_{m=1}^{M}\left(Ref_m - Obs_m\right)^2\right]}$$

equation 1

The Skill Score displayed on Figure 35 show the added value of PSY3 forecast with respect to the climatology (our reference here), but the relatively small sample of PSY3V3R1 forecast do not allow to conclude yet on the improvement of the skill score in PSY3V3R1 with respect to PSY3V2R2.

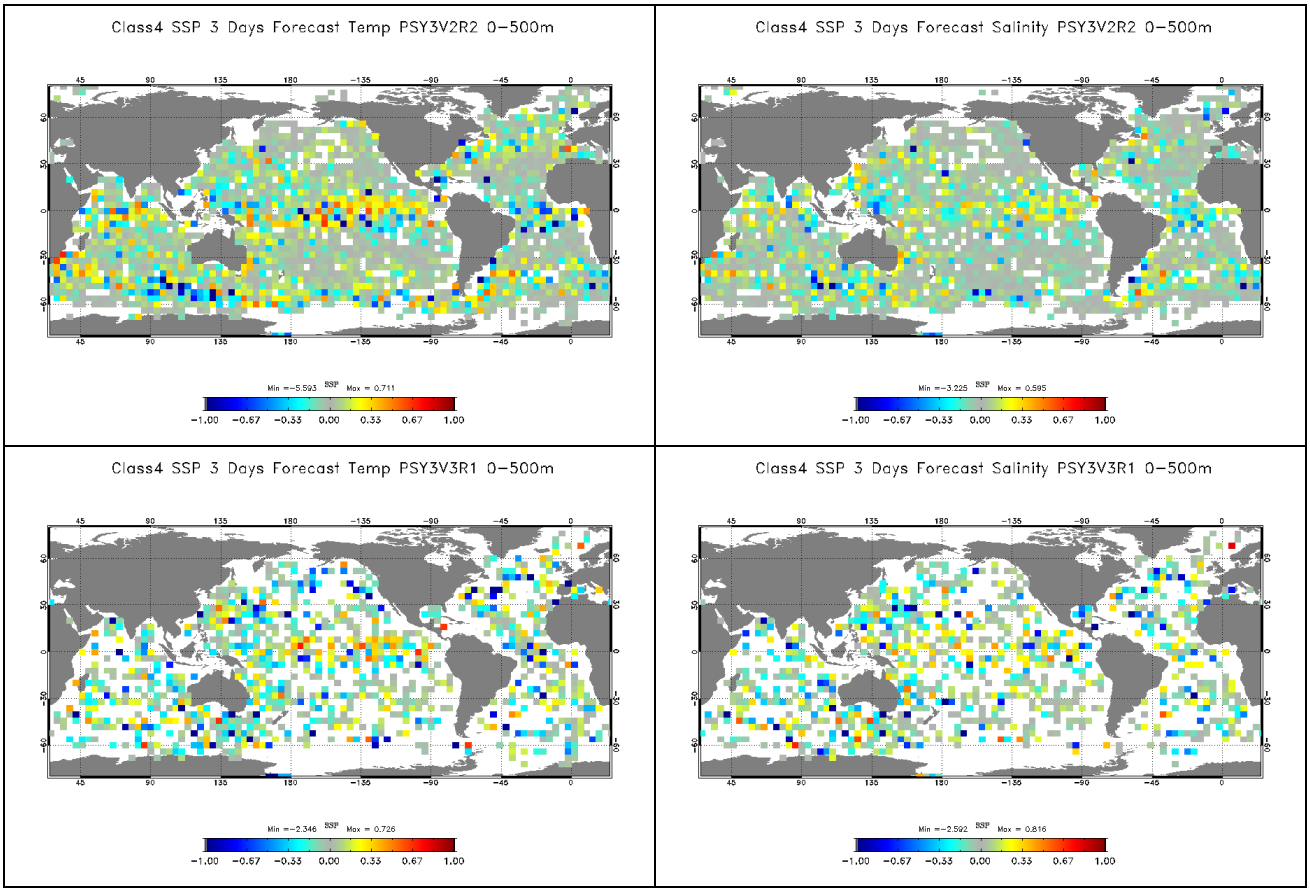

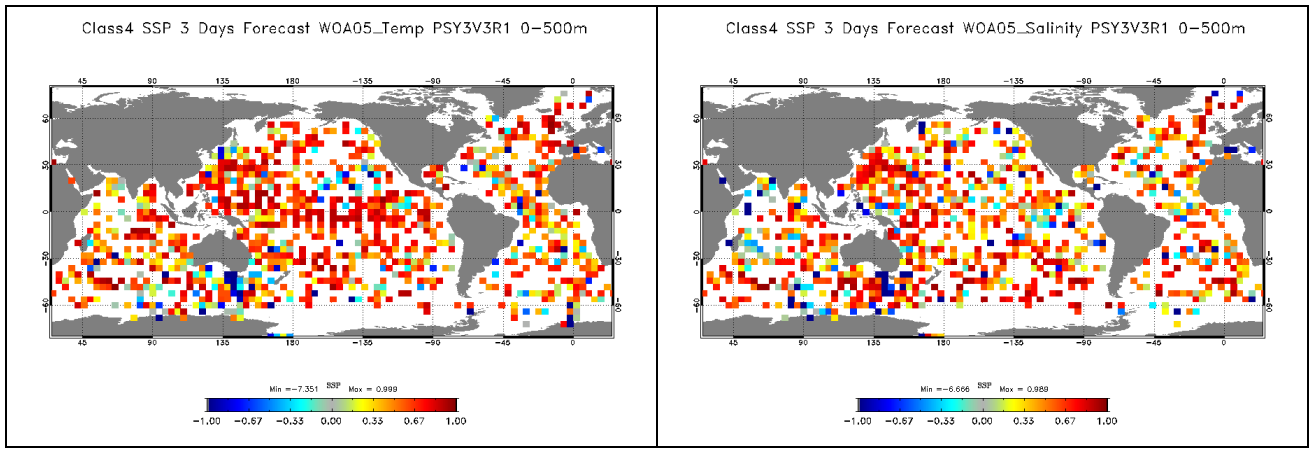

Figure 35: Skill score in 4°x4° bins and in the 0-500m layer, illustrating the ability of the 3-days forecast to be closer to in situ observations than a reference state (climatology or persistence of the analysis, *cf* formula below). Yellow to red values indicate that the forecast is more accurate than the reference. Upper panel: PSY3V3R2 (the reference is the persistence of the analysis), middle panel: PSY3V3R1 (the reference is the persistence of the analysis), and lower panel: PSY3V3R1 (the reference is the WOA 2005 climatology). Temperature skill scores are in the left column and salinity skill scores in the right column.

The PSY3V2R2 "forecast errors" illustrated by the sea surface height RMS difference between the forecast and the hindcast for all given dates of the season OND 2010 are displayed in Figure 36. The PSY3V3R1 sample is not large enough to produce these diagnostics with PSY3V3R1 outputs. The values on most of the global domain do not exceed 2 to 4 cm. In regions of high variability like the western boundary currents, Agulhas current and Zapiola eddy the errors reach around 20 cm, consistent with SLA innovation statistics.
High errors of more than 50 cm occur in the southern ocean (especially after two weeks), consistent with the drift of PSY3V2R2 SLA assimilation statistics in this region.

The results on the North Atlantic domain are very similar in PSY3V2R2 and PSY2V3R1 (not shown).

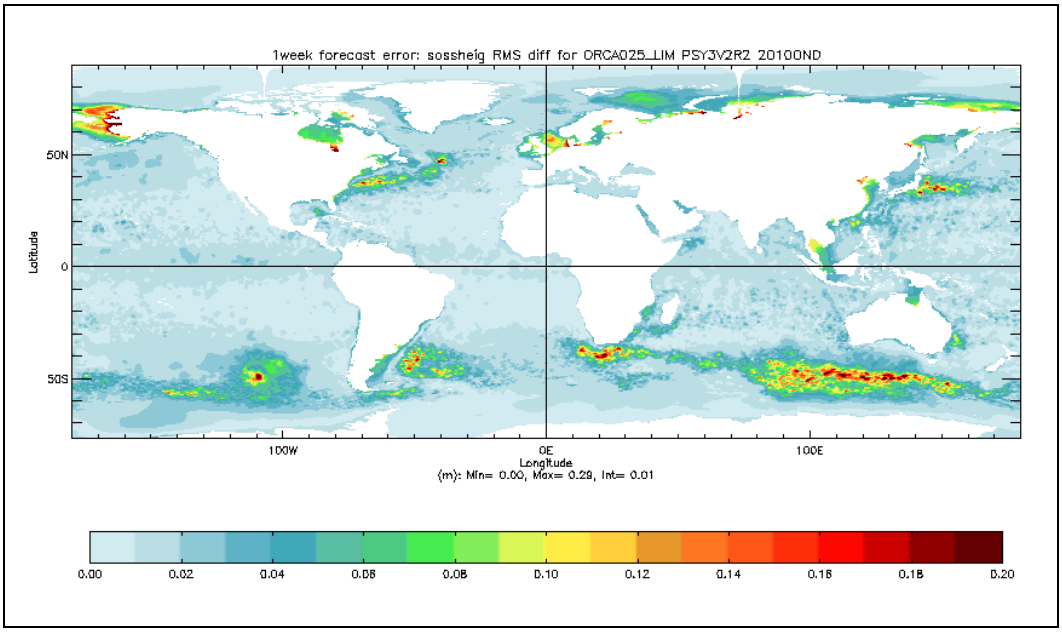

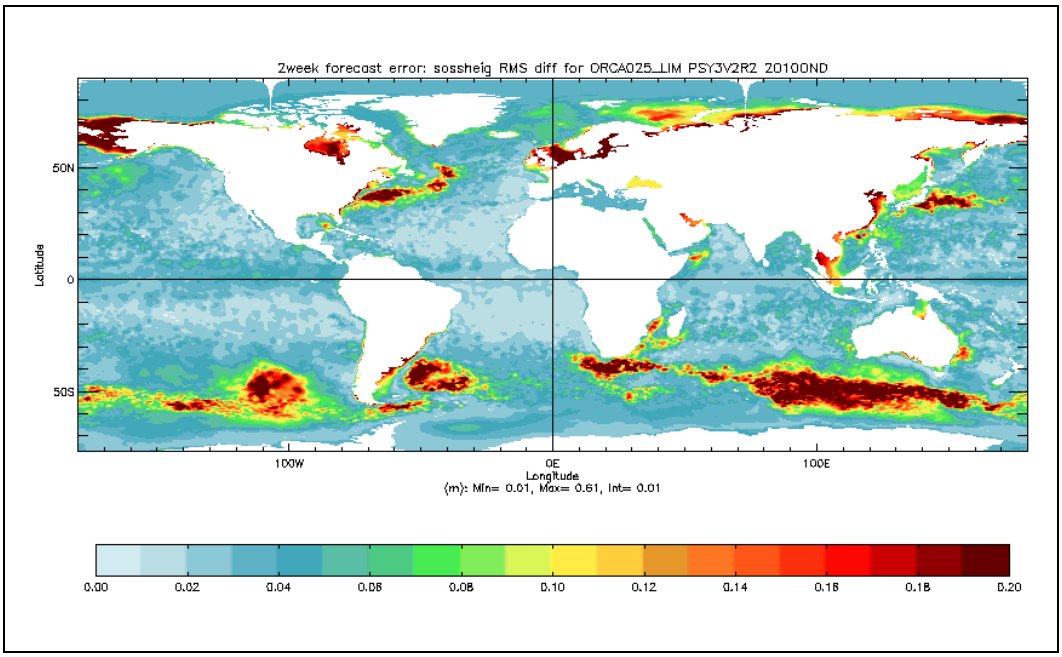

Figure 36: comparison of the sea surface height (m) forecast – hindcast RMS differences for the 1 week (upper panels) and 2 weeks (lower panels) ranges for the PSY3V2R2 system

Salinity forecast errors at all vertical levels show that the error is concentrated in the surface layer in the tropical regions, in the mesoscale variability regions like the Gulf Stream, at the sea ice limit and in regions of high runoff like the Amazon (Figure 37). The Skaggerak strait also exhibits salinity errors.

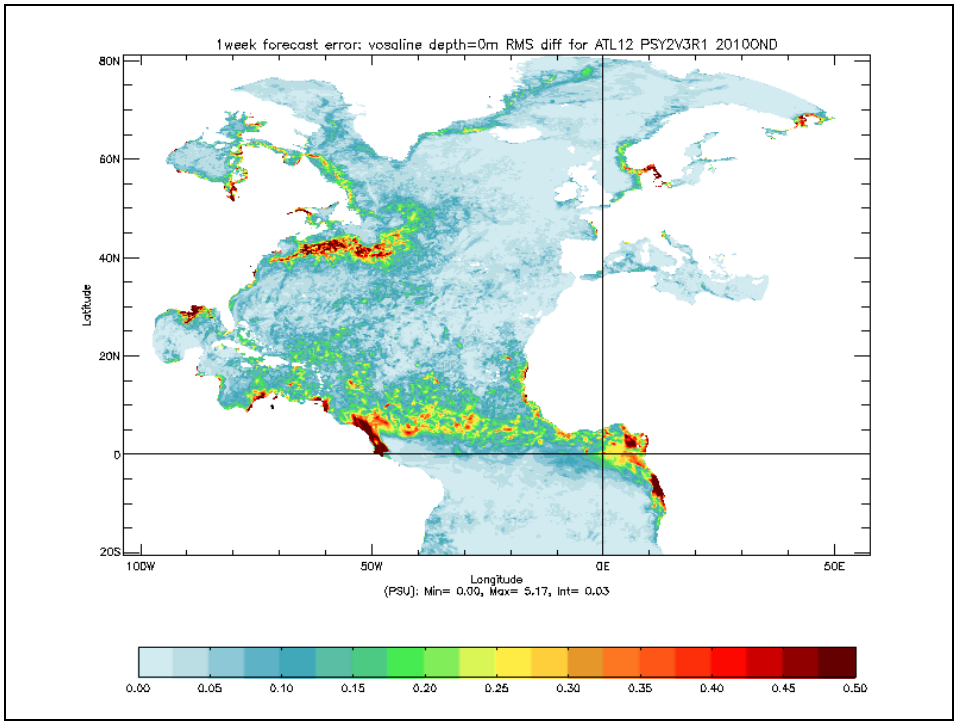

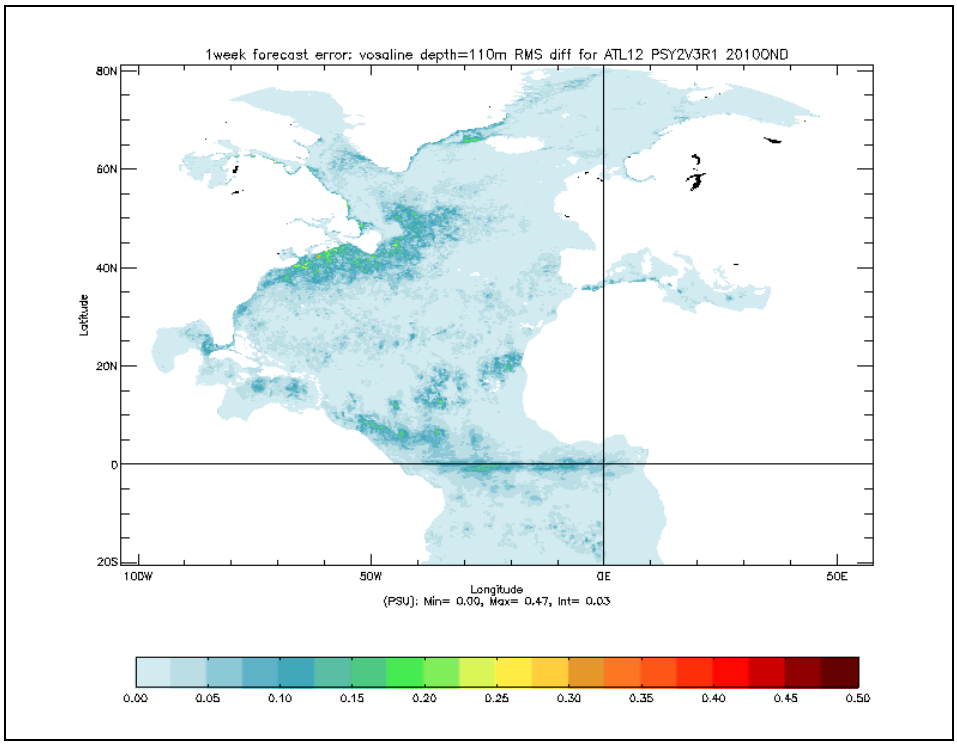

Figure 37: comparison of the salinity (PSU) forecast – hindcast RMS differences for the 1st week at surface (upper panels) and 110 m (lower panels), for the PSY2V3R1 system.

VIIMonitoring of ocean and sea ice physics

VII.1. Global mean SST and SSS

The spatial means of SST and SSS on the whole domains are computed for each day of the year, for both PSY2V4R1 and PSY3V3R1 systems. The mean SST is compared to the mean of RTG-SST on the same domain (Figure 38). The biases visible during summer and autumn tend to disappear during winter.

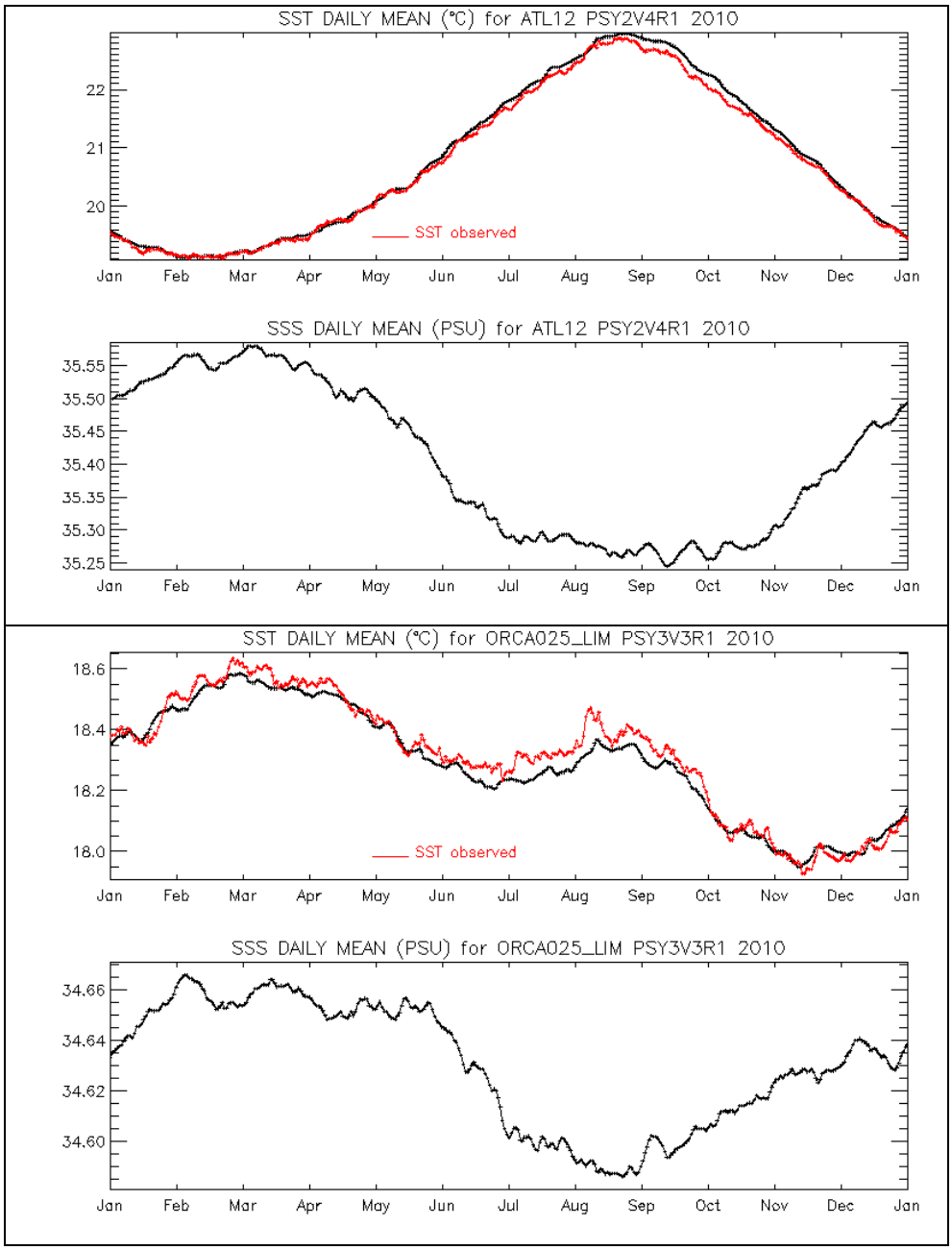

Figure 38: daily SST (°C) and salinity (psu) global mean for a one year period ending in OND 2010, for PSY3 (in black) and RTG-SST observations (in red). Upper panel: PSY2V4R1, lower panel: PSY3V3R1.

VII.2. Mediterranean outflow

As can be seen in Figure 39 the depth of the Mediterranean outflow in the Atlantic is more realistic in PSY2V4R1 than in PSY2V3R1, like in previous quarters. PSY3V3R1 similarly shows more realistic results than PSY3V2R2 (not shown).
We notice in Figure 39 a salty and warm bias in surface consistent with the biases diagnosed in the IBI region (see Figure 26and Figure 28 for instance).

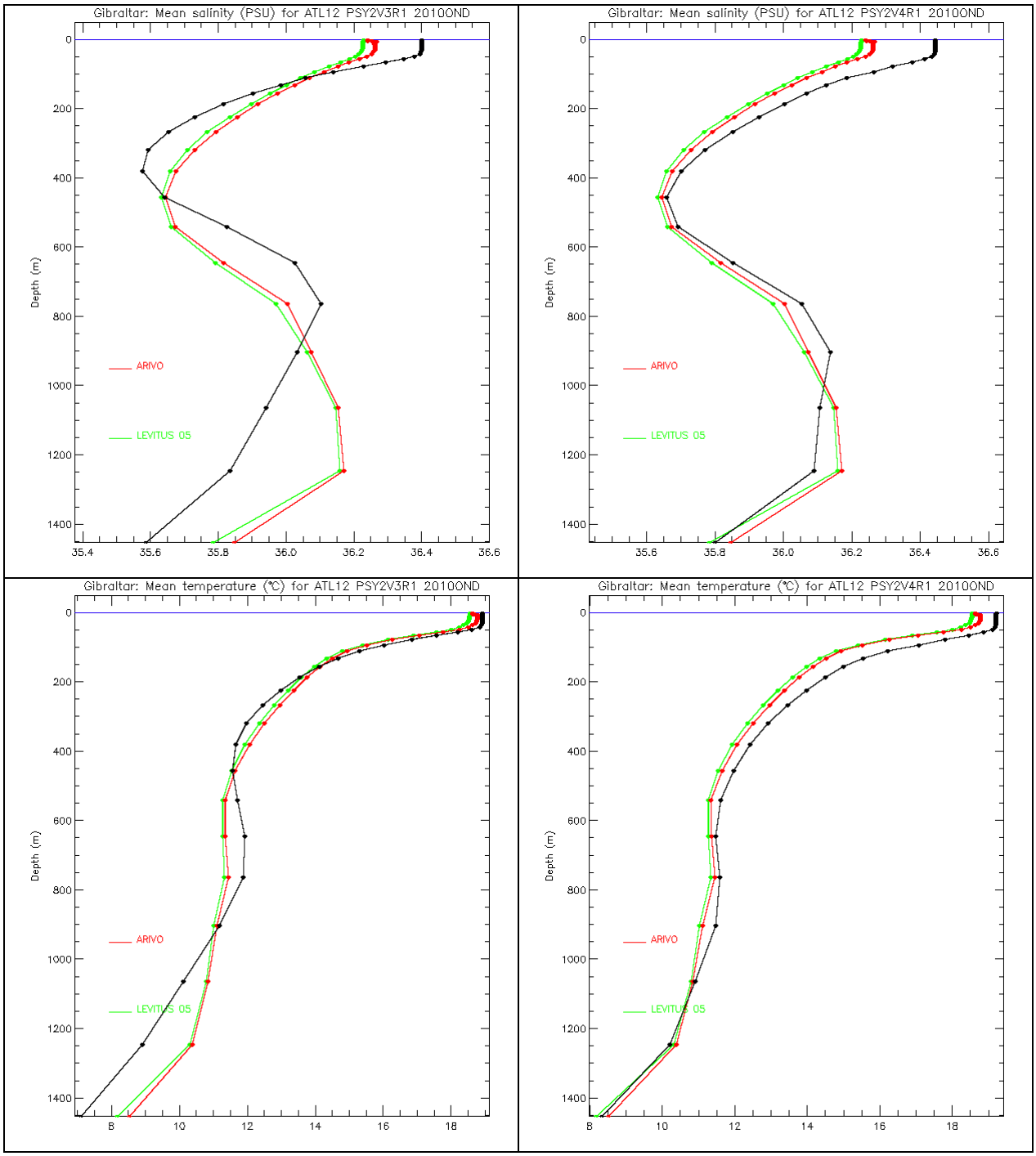

Figure 39: Comparisons between mean salinity (upper panel) and temperature (lower panel) profiles in PSY2V3 (left), PSY2V4 (right) and in the Levitus WOA05 and ARIVO climatologies.

VII.3. Surface EKE

Regions of high mesoscale activity are diagnosed in Figure 40: Kuroshio, Gulf Stream, Nino 4 box in the central Equatorial pacific (while it was Nino 3 during summer and autumn), Indian Equatorial current, Zapiola eddy, Agulhas current, East Australian current, Madagascar channel etc… The signature of the SLA drift in PSY3V2R2 is also visible in the circumpolar current in the RMS of SSH (Pacific and Indian quadrant). In the new systems PSY2V4R1 and PSY3V3R1, the EKE is slightly lower than in the former systems.

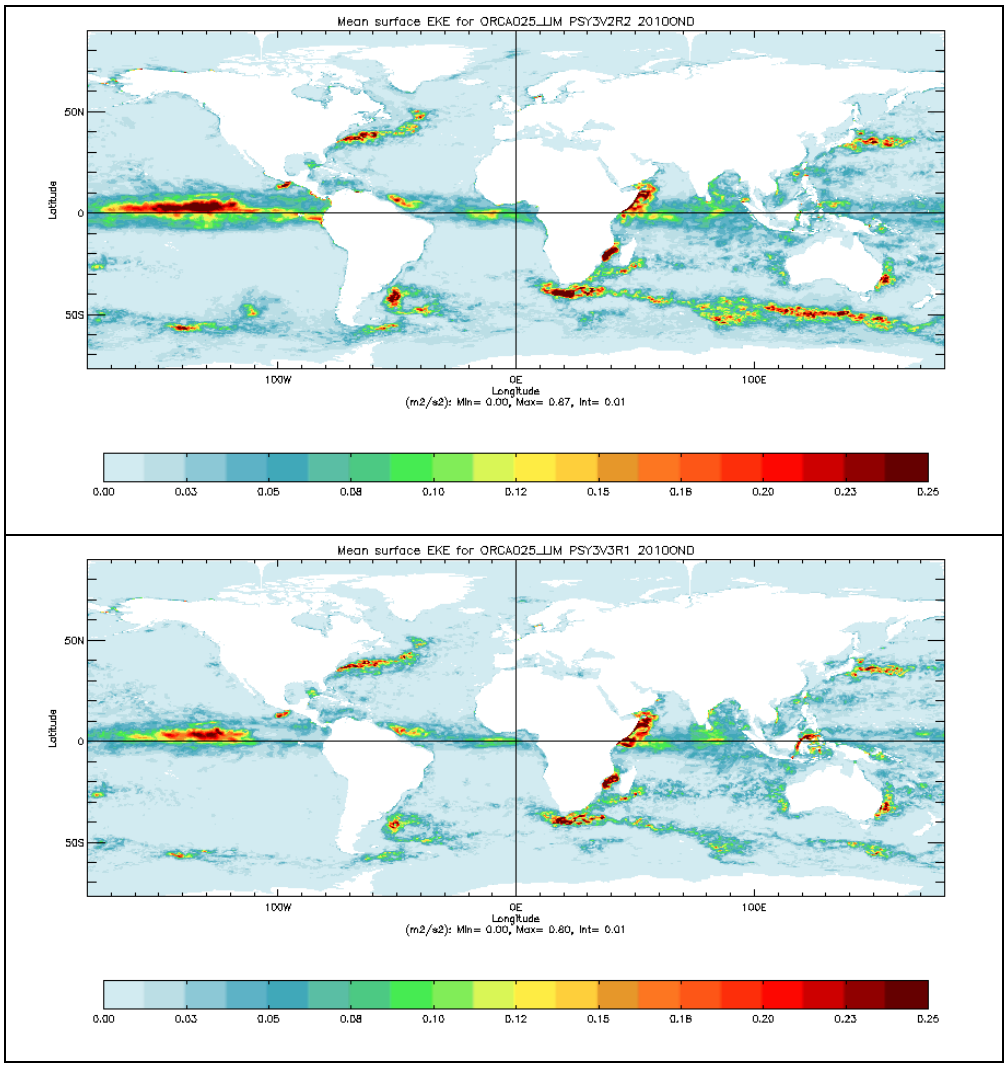

Figure 40: surface eddy kinetic energy EKE (m^2/s^2) for PSY3V2R2 (upper panel) and PSY3V3R1 (lower panel) for OND 2010.

VII.4. Sea Ice extent and area

The time series of monthly means of ice area and ice extent (area of ocean with at least 15% sea ice) are displayed in Figure 41 and compared to SSM/I microwave observations. Both ice extent and area include the area near the pole not imaged by the sensor. NSIDC web site specifies that it is assumed to be entirely ice covered with at least 15% concentration. This area is 0.31 million square kilometres for SSM/I.

These time series indicate that during winter, both PSY3V2R2 and PSY3V3R1 perform very well, with respect to observations. During summer, PSY3V3R1 reproduces the melting season better than PSY3V2R2 in the Arctic; in the Antarctic, PSY3V2R2 shows a higher area but PSY3V3R1's extent is closer to observations (see Figure 30 for details on distribution).

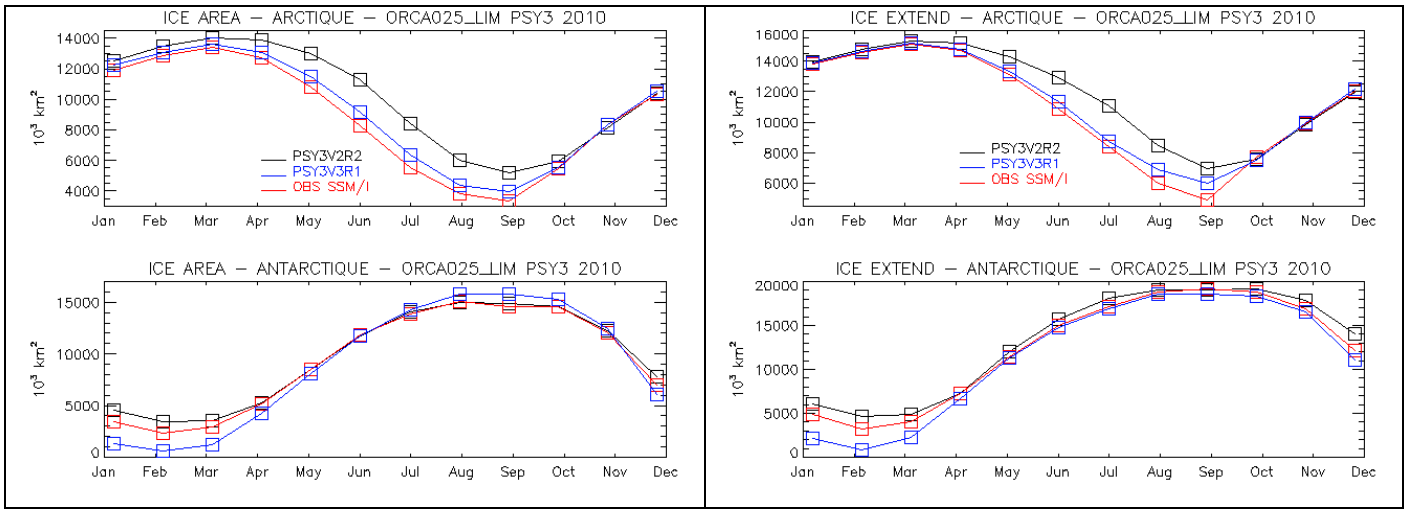

Figure 41: Sea ice area (left panel, 10^3 km^2) and extent (right panel, 10^3 km^2) in PSY3V2R2 (black line), PSY3V3R1 (blue line) and SSM/I observations (red line) for a one year period ending in OND 2010, in the Arctic (upper panel) and Antarctic (lower panel).

VIII Process study: Southern Ocean mesoscale activity in the high resolution system PSY4V1R3.

By Benoît Tranchant and Eric Greiner.

In this study, we focus on the Southern Hemisphere where the mesoscale eddies have a major role in the density structure and transport properties of the ACC (Antarctic Circumpolar Current). The ACC remains an insufficiently understood current in the ocean (mainly due to a lack of data), and the predicting circulation in the ACC is a key issue. The Antarctic Intermediate Water (AAIW), which is a key component of the upper branch of the global thermohaline circulation, has recently been studied by Lachkar *et al.* (2009). They argue on the need for ocean models to adopt higher resolution that properly represent the effects of eddies not only in the ocean interior but also in the deep mixed layers.

VIII.1. Jets and eddies in the ACC

The intrinsic dynamics of the ACC are mainly the effects of the mesoscale eddy field, and in a recent paper, Hurlburt *et al.* (2009) show that the 1/12° eddy-resolving Mercator Ocean forecasting systems depict much more mesoscale variability and smaller scale features than the 1/4° eddy permitting system. On Figure 42, the mean EKE calculated from the hindcast simulation of PSY4V1R3 compares well with data and previous studies using the same kind of spatial resolution (see Screen *et al.* 2009). The spatial pattern of mean EKE in the model shows a good agreement with that from altimeter data contrary to the magnitude which is too high (see PDF on Figure 42) except in the most energetic regions located near the ACC, in the Agulhas retroflection current, in the Brazil-Malvinas Current Confluence, and near the East Australian current separation.

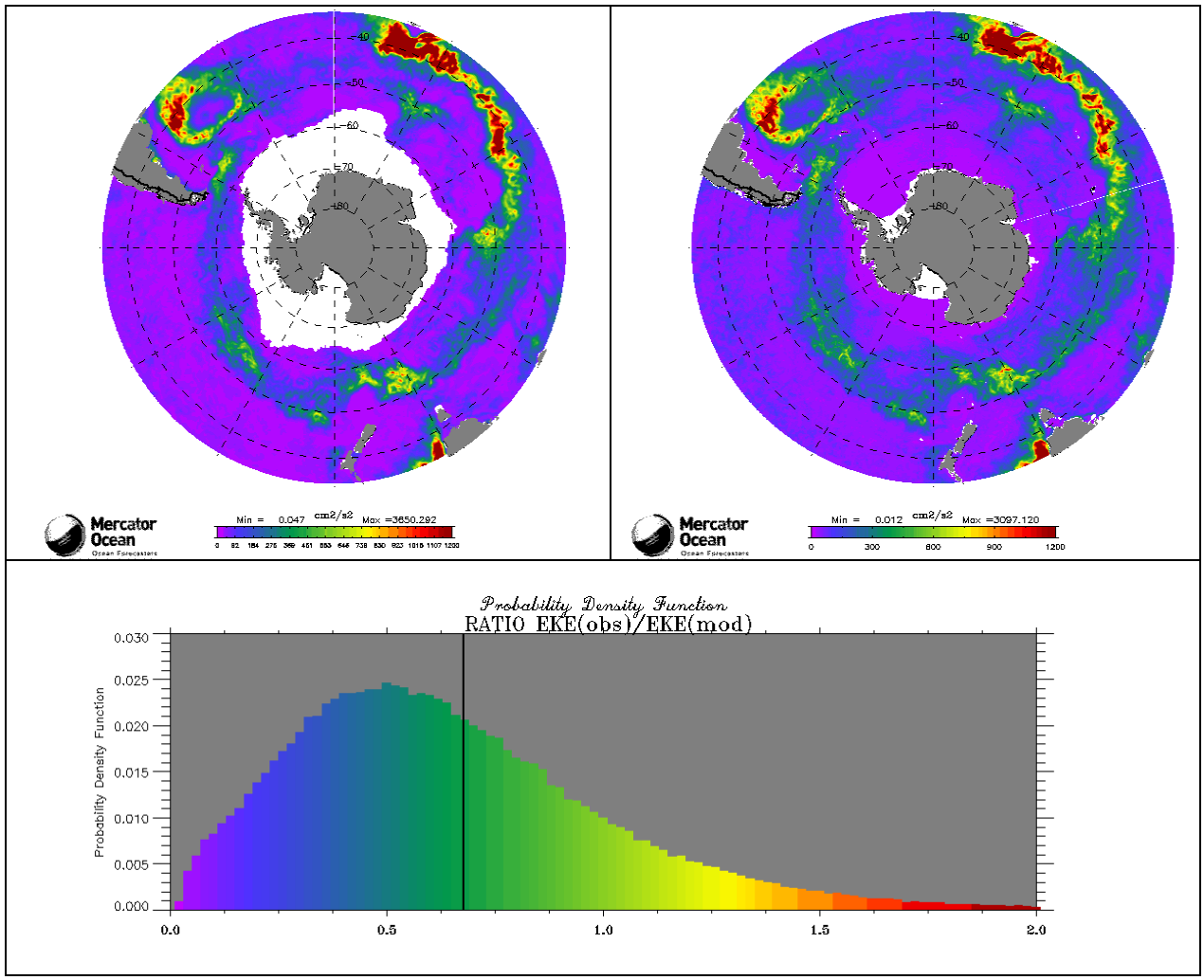

Figure 42: Mean EKE calculated between July 2009 and July 2010 in the South Hemisphere from altimeter data (left) and from the PSY4 hindcast simulation (right). Probability density function of the ratio between the observed EKE and the modelled EKE (the black bar indicates the median value=0.67).

The probability density function (Figure 42) refers to Sallée and Rintoul (2010). On the overall Southern hemisphere, the EKE magnitude from observations is approximately 30-40% smaller than that derived from the model (median value of 0.67). Sallée and Rintoul (2010) from a 1/6° ocean model (SOSE; Mazlof *et al.* 2008) using the Gent and McWilliams parameterization found that the observed EKE is approximately twice the intensity of the modelled EKE which is not the case with higher resolution models. Screen *et al.* (2009) show that the weakness of EKE in the lower resolution models could be due to the parameterization scheme. Moreover, they argue that such parameterization is unable to mimic the effects of change in the eddy field on Southern Ocean temperatures contrary to higher resolution models with the explicit resolved eddies. Based on many studies, Thompson (2008) assumes that the fact that eddies are parameterized or explicitly resolved plays a role on the relationship between the ACC's zonal transport and the changes in wind stress forcing.

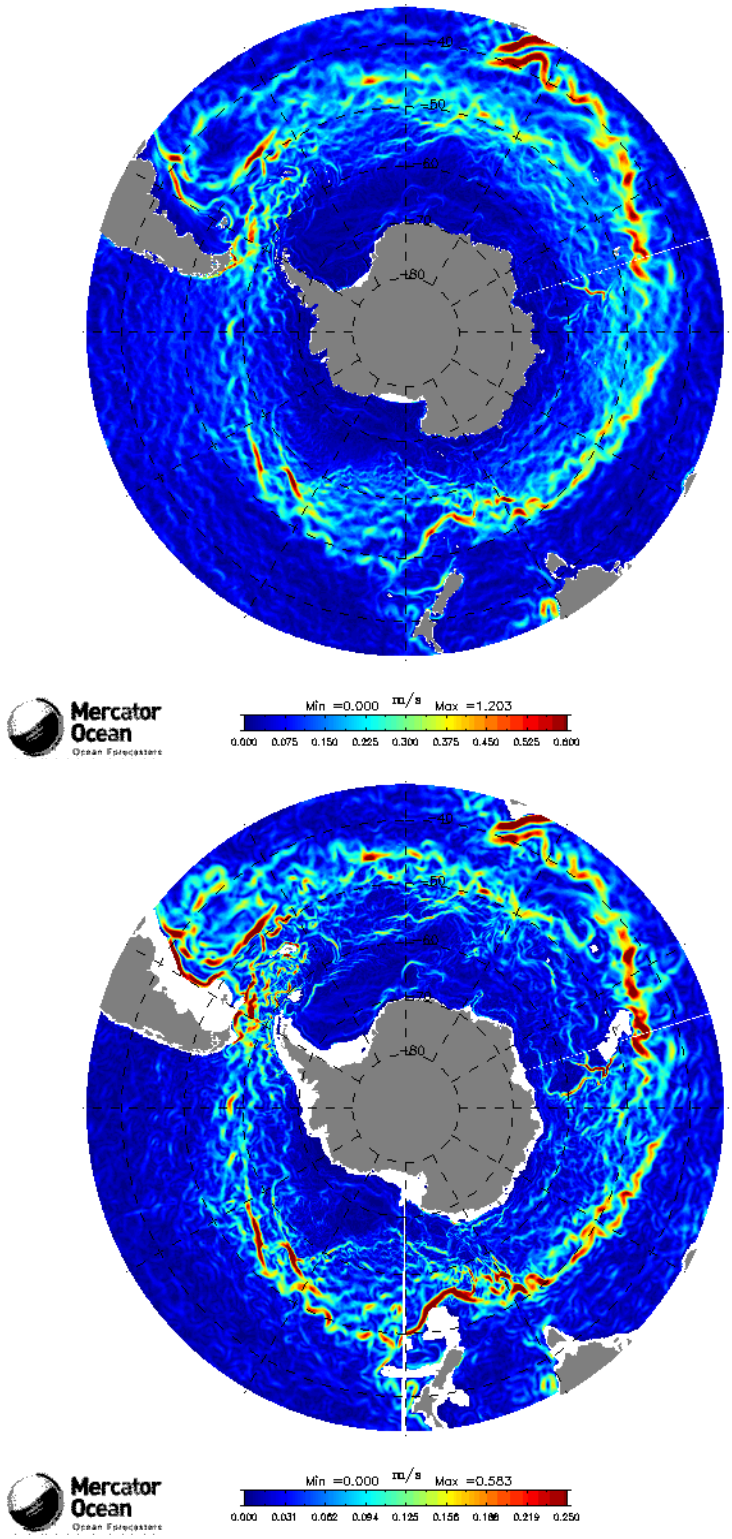

Figure 43: Mean current at surface (top) and 1000 m (bottom) from July 2009 to July 2010.

On Figure 43, mean currents at different depths are represented, and the filamentary structure within the ACC is clear. These structures can also be viewed from drifting buoys trajectories (see Figure 44) and tend to show that jets can also have an influence on transport in the ACC. In a recent study, Williams *et al.* (2007) concluded that ACC does

exhibit storm tracks characteristics. The jets and the EKE are well reproduced by the 1/12° system but the mean kinetic energy seems strongly underestimated.

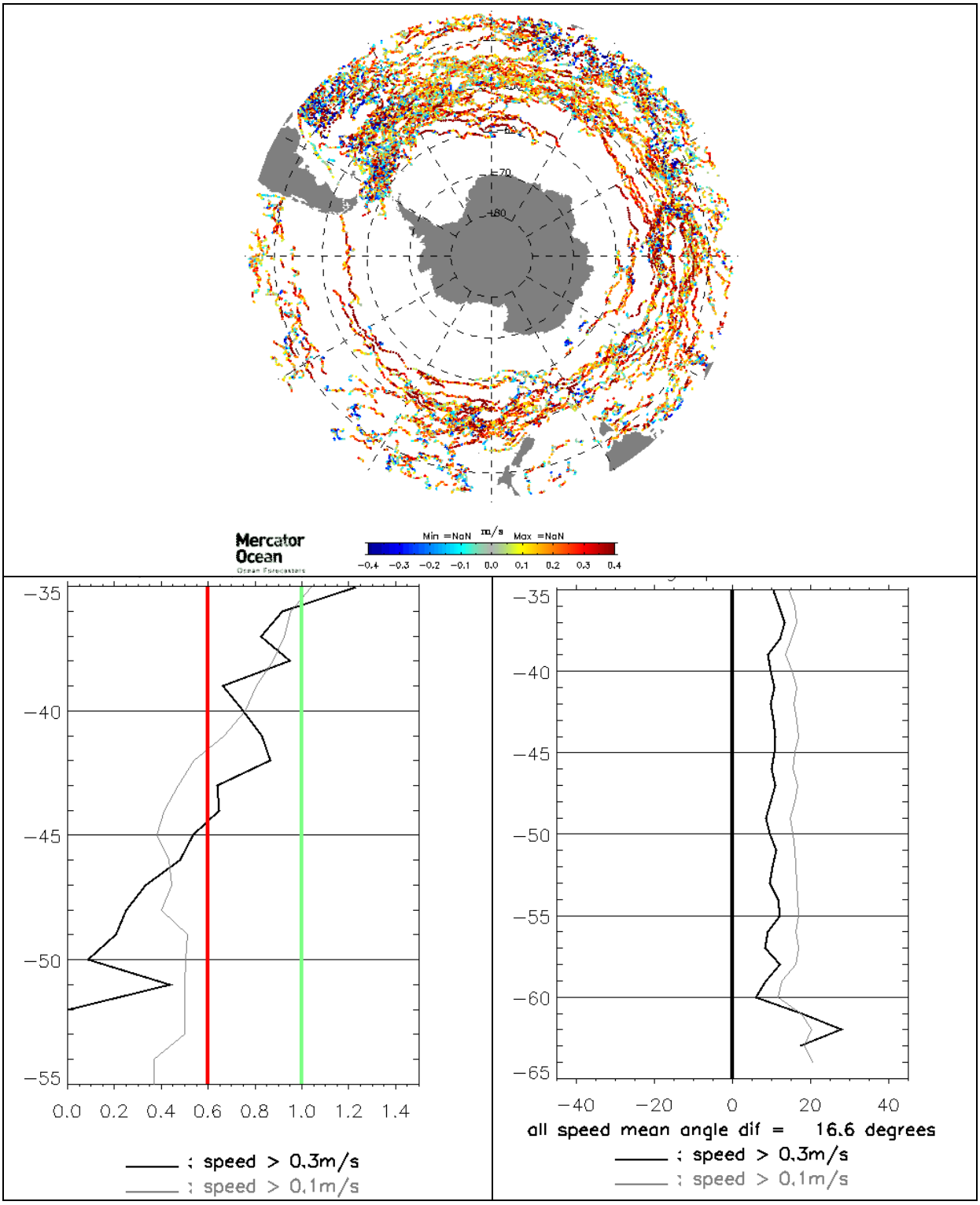

Figure 44: Mean annual difference (observation – model) of zonal velocity (m/s) [upper pannel], Ratio model/observation of module velocity per latitude [bottom left] and Angle of difference (observation – model) per latitude [bottom right]. Comparisons with surface drifters are done on a one year period (July 2009 - July 2010).

The mean annual difference between observations and model of the zonal surface velocity is shown on Figure 44. The surface velocity magnitude is underestimated by 40% near 45°S with a latitude dependency (stronger bias near the sea ice) and a slight angular bias of about 15° has been found. It questions the validity of the Ekman spiral in the model. The stokes drift and the coarse resolution of the MDT (Mean Dynamic Topography) also contribute to this weakness, see an example on Figure 45 that illustrates how a shift in space (MDT) and/or time (forcing, Stokes drift) can lead to a strong underestimation of the drift.

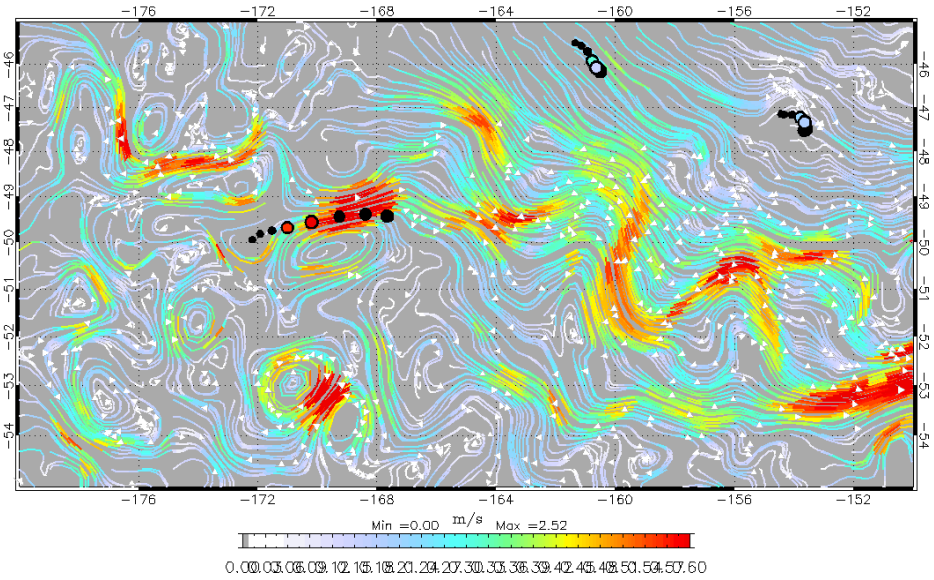

Figure 45: Surface velocity in the ACC region and surimposed drifters (amplitude and locations) where size of circles is proportional to the age of the data (2009/10/20)

Apparently, these biases do not affect the EKE level (Figure 42) which tends to show that the vertical structure of the currents may not be steep enough. In a recent paper, Allison *et al.* (2010) suggest that even if the ACC is mainly driven by winds over the circumpolar streamlines, the relationship between wind stress and ACC transport in an eddy-saturated regime is more complicated.

VIII.2. Conclusion

The new global ocean forecasting system offers a new perspective on the understanding of the role of eddies in the southern hemisphere from a hindcast simulation (near 2 years). **Further quantitative studies could improve our understanding of key mechanisms in this region. This system underestimates surface velocities but the energy level and the structures are well represented.**

References:

Allison L. C., H.L. Johnson, D.P. Marshall, and D.R. Munday, (2010) *Where do winds drive the Antarctic Circumpolar Current?*, Geoph. Phys. Lett., 37, L12605.

Biastoch, A., C. W. Böning, F. U. Schwarzkopf and J. R. E. Lutjeharms, *Increase in Agulhas leakage due to poleward shift of Southern Hemisphere westerlies*, Nature, Vol 462|26, November 2009.

Drillet et al., (2008). *The Mercator Ocean global 1/12° operational system: Demonstration phase in the MERSEA context*, The Mercator Ocean Newsletter #30, July 2008.

H.E. Hurlburt, G.B. Brassington, Y. Drillet, M. Kamachi, M. Benkiran, R. Bourdallé-Badie, E.P. Chassignet, G.A. Jacobs, O. Le Galloudec, J.-M. Lellouche, E.J. Metzger, P.R. Oke, T.F. Pugh, A. Schiller, O.M. Smedstad, B. Tranchant, H. Tsujino, N. Usui, and A.J. Wallcraft, (2009), *High-Resolution Global and Basin-Scale Ocean Analyses and Forecasts, Special Issue on the Revolution of Global Ocean Forecasting-GODAE : 10 Years of Achievement, Oceanography*, Vol 22, No 3, Sept 2009.

Lachkar Z., J C. Orr, J.C. dutay and P. Delecluse, *On the role of mesoscale eddies in the ventilation of Antarctic intermediate water*, Deep-Sea Research I, 56, 909-925., February 2009.
Mazloff M. R., P.Heimbach and C. Wunsh, (2008) *„An Eddy-Permitting Southern Ocean State Estimate*, J. Phys. Oceanogr., 40, 880-898.

Sallée, J.B.; and Rintoul, S.R. *Parameterization of eddy-induced subduction in the Southern Ocean surface-layer*, submitted to Ocean modelling, 2010

Screen, J.A., N. Gillett, D. P., Stevens, G. J. Marshall and H. K. Roscoe, The role of eddies in the Southern Ocean Temperature Response to the Southern Annular Mode, Journal of Climate, 22, 2009.

Thompson A. F., (2008) The atmospheric ocean: eddies and jets in the Antarctic Circumpolar Current, Phil. Trans. Soc. A (2008) 366, 4529-4541.

IX R&D study: improving the quality of the analysis and forecast with an update of the SAM2 error statistics from the ongoing operational production.

By Hélène Etienne.

The SAM2 assimilation scheme used in all Mercator Ocean operational systems is a multivariate multi data assimilation scheme. It is a version of the Singular Evolutive Extended Kalman filter (SEEK from D. T. Pham, J. Verron and M. C. Roubaud, *J. of Marine System*: A singular evolutive extended Kalman filter for data assimilation in oceanography. **16**, 323-340 (1998)) using multi-data sources: SLA from altimetry missions, ARGO profiles of temperature and salinity, SST from satellite.

The three dimensional background error matrix (**B**) is computed using an ensemble of anomalies called “historical base”. It is computed from an eight years experiment performed on a past period with no data assimilation. A spatial scale treatment is made to apply different corrections depending on the physical structures of the local ocean state. The correction is computed on a reduced space and finally the whole ocean volume is updated (barotropic height, temperature, salinity, and both components of the velocity).

The present study shows how the information coming from operational outputs can be used to enrich the actual ensemble based covariance matrix **B**. Each week on Wednesday (date J), a 14-day forecast is computed from the analysis of the day (nowcast). In order to obtain the best analysis possible (with the optimal number of input observations) the system starts 14 days back in time and performs a “hindcast” analysis at date J-7 days and then the nowcast analysis at date J. That is why for a given week, best analysis and forecasts are available (Figure 46).

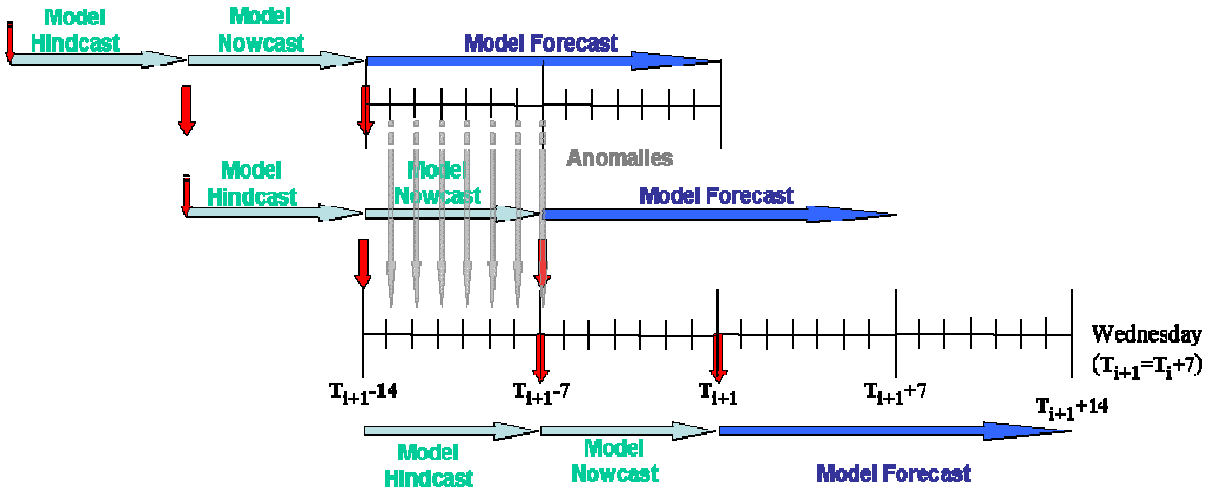

Figure 46: schematic description of the operational weekly schedule.

The differences between these two fields (forecast - hindcast) give some indications on the system error from both model (forcing fields, numerical schemes etc…) and assimilation scheme (choice of the reduced space, choice of **B** etc...) These anomalies are up-to-date information on the system error and we try to use it to improve the error covariance matrix and the assimilation scheme.

The study presented here is made using PSY3V2R2 operational outputs. We compute daily anomalies from 23-month operational PSY3V2R2 outputs of 2009 and 2010 including barotropic height, temperature, salinity, zonal and meridional velocities. Seven hundred anomalies (called modes) are available, corresponding to one to seven days system error information. Correlations obtained with the new set of modes are quite different depending on the anomaly. Figure 47 show an example of the correlation between SST and temperature or salinity on the vertical. The seven profiles (one for each forecast term) show a dispersion of the correlation increasing with depth for T below the mixed layer, whereas the S correlation profiles are already spread from the surface. Two profiles are shown for the historical base, because the corresponding anomaly time series is split into two parts due to discontinuity in the data. Considering this result, we can expect from the new ensemble an increase of the correction in the lower layers of the model.

Results for the 2D correlation are unchanged within the correlation radius (not shown). The difference is mainly observed on the secondary maxima, with a possible sign inversion of the correlation in some cases.

A four month simulation is performed, using different combinations of the two bases. Using only the new anomalies does not improve the assimilation results. We made a simulation in an operational way, by combining the historical base and the new base. Only anomalies previous to the analysis are used, completing the ensemble by the seven new anomalies computed from the previous seven days hindcast (Figure 46). The same number of historical and new anomalies is also maintained. So in this new simulation, we use a total of three hundred modes.

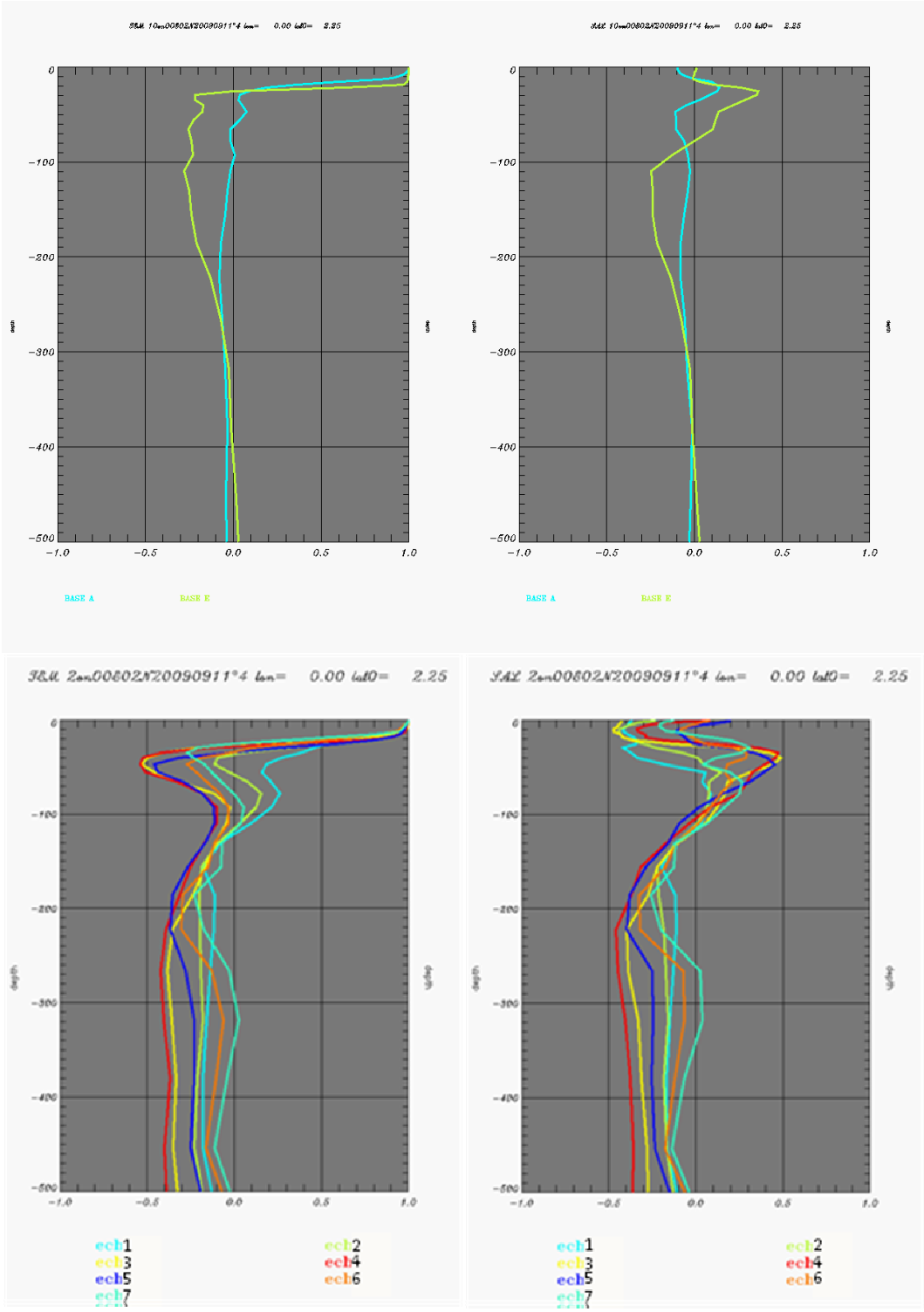

Figure 47: vertical correlation between SST and T (left) and S (right) computed from historical ensemble (upper) and new ensemble (lower).

This new ensemble improves the SLA statistics. The global SLA mean misfit is slightly reduced (0.2 to 0.3 cm) during the last month of the run (Figure 48), but the RMS misfit is improved of about 1 cm during the second half of the simulation (Figure 49). The increase of the SLA RMS misfit in the operational system near the end of May corresponds to a lack of Jason 1 data during 3 assimilation cycles (loss of about 50% of the data.) The operational system cannot deal with the decrease of SLA observation, whereas the new ensemble still

manages to constrain the model. The areas of greatest improvement of the SLA statistics are the Gulf Stream, the Irminger Sea, the Falkland current, Chile and Peru coast, the Indian Ocean and the California Current.

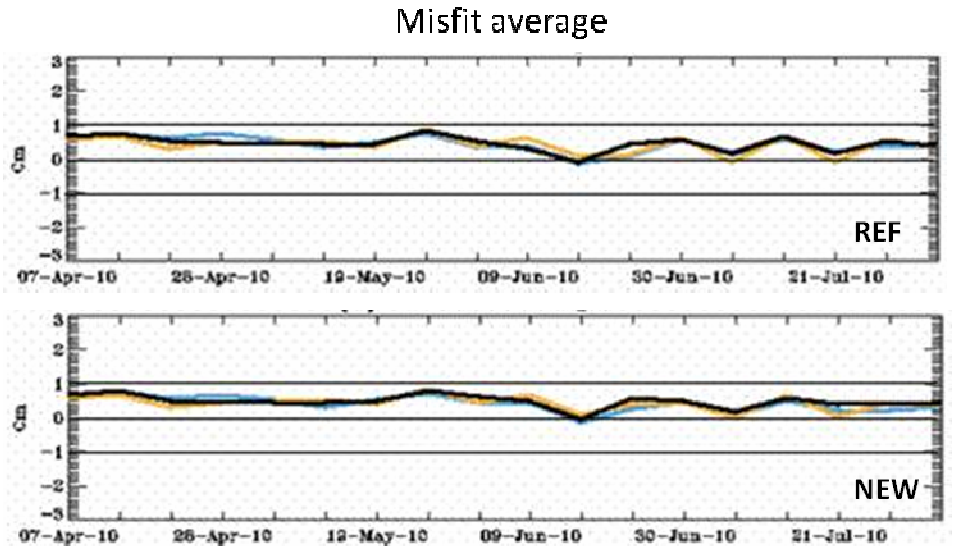

Figure 48: Average misfit of the reference simulation (operational system) and new simulation.

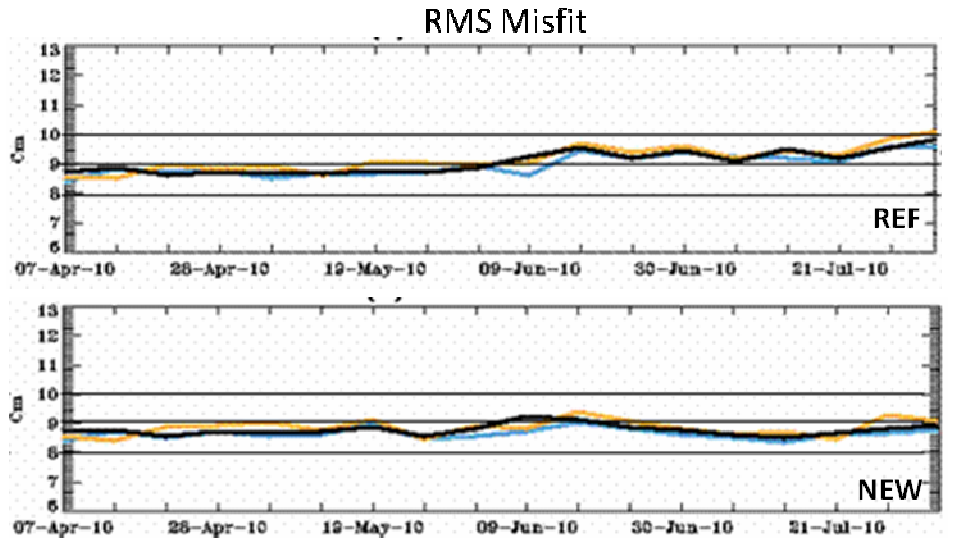

Figure 49: RMS misfit of the reference simulation (operational system) and new simulation.

The impact of the new **B** matrix is globally more important on the salinity than on the temperature field. This could have been expected, as the SST is already quite well observed (satellite SST and *in situ* profiles) whereas the salinity is only constrained by *in situ* profiles. Even if the salinity and temperature mean and RMS misfit are somehow reduced globally (mostly in the first 200m), regional improvements are more significant. 80% of the sub-regions show statistical improvement of the model against *in situ*. For example, this is the case for the Indian Ocean, Peru coast, the Mexico Gulf (Figure 50 and Figure 51) where salinity and temperature biases are clearly reduced below 50m.

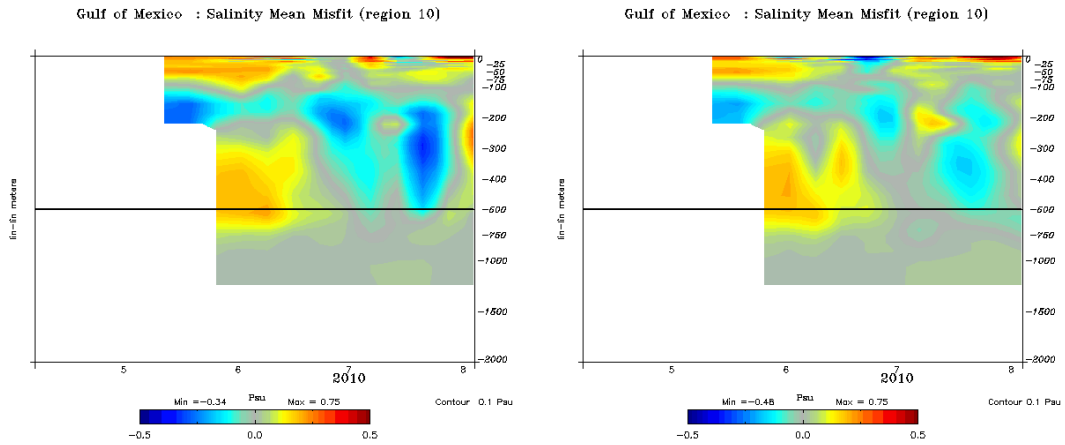

Figure 50: salinity mean misfits in the Gulf of Mexico for the reference (left) and new simulation (right).

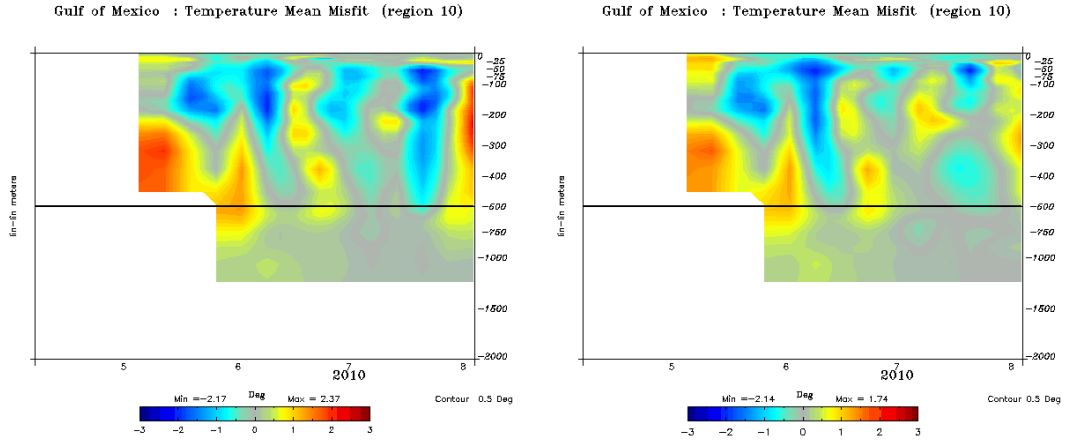

Figure 51: temperature mean misfits in the Gulf of Mexico for the reference (left) and new simulation (right).

IX.1. Conclusion

Updating the error information directly from the system outputs **improves the performance of the data assimilation scheme**. Diagnostics from both SLA and in situ data show a reduction of the mean and RMS misfits, with a significant impact on the salinity. Added to a balance of the background versus observation error covariance weight, this new ensemble could give some even better results.

X Annex A

Table of figures

XI Annex B

XI.1. Maps of regions for data assimilation statistics

XI.1.1. Tropical and North Atlantic

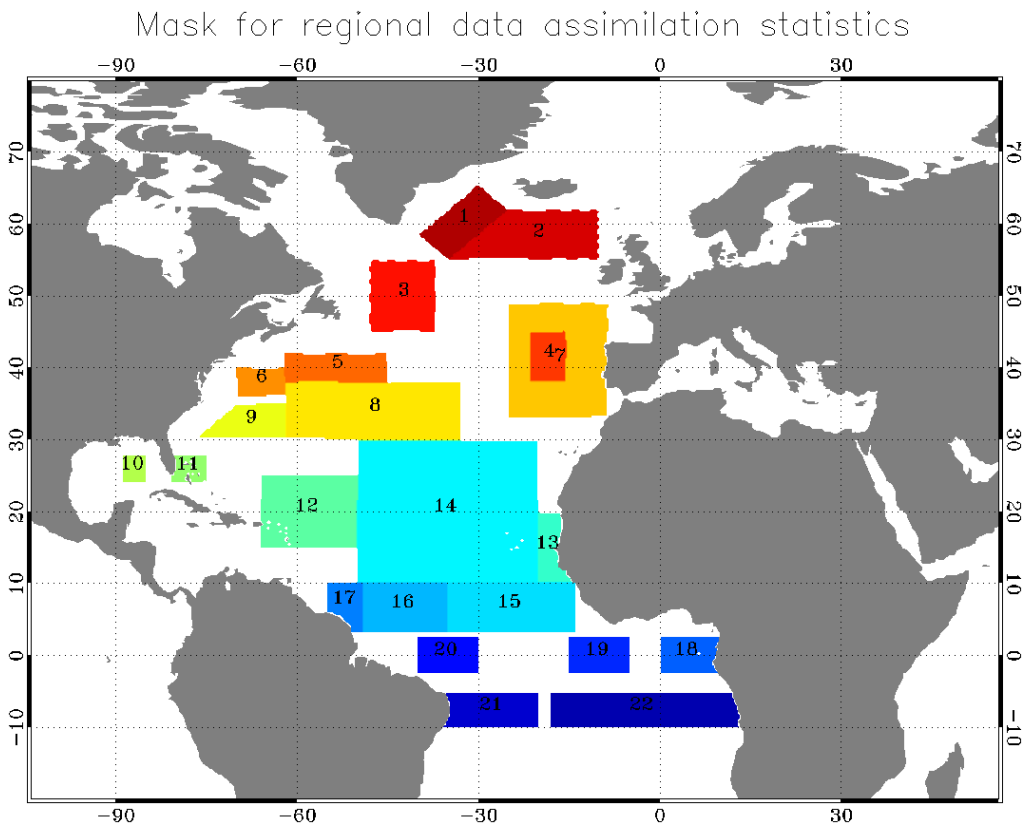

1	Irminger Sea
2	Iceland Basin
3	Newfoundland-Iceland
4	Yoyo Pomme
5	Gulf Stream2
6	Gulf Stream1 XBT
7	North Medeira XBT
8	Charleston tide
9	Bermuda tide
10	Gulf of Mexico
11	Florida Straits XBT
12	Puerto Rico XBT
13	Dakar
14	Cape Verde XBT
15	Rio-La Coruna Woce
16	Belem XBT
17	Cayenne tide

18	Sao Tome tide
19	XBT - central SEC
20	Pirata
21	Rio-La Coruna
22	Ascension tide

XI.1.2. Mediterranean Sea

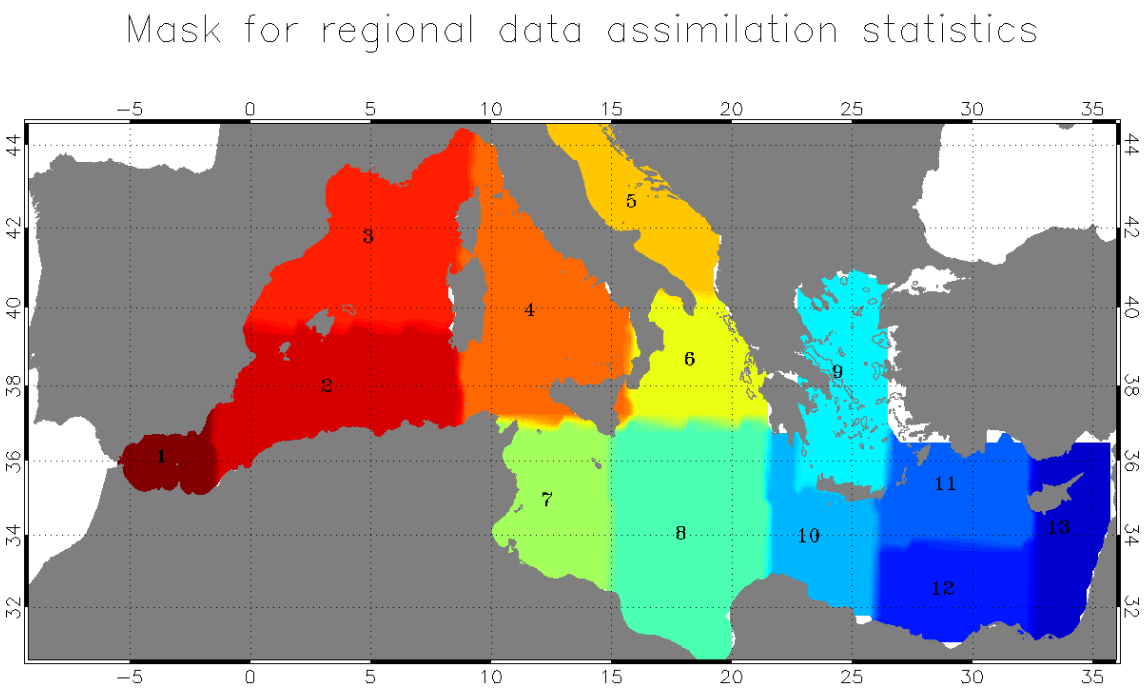

1	Alboran
2	Algerian
3	Lyon
4	Thyrrhenian
5	Adriatic
6	Otranto
7	Sicily
8	Ionian
9	Egee
10	Ierepetra
11	Rhodes
12	Mersa Matruh
13	Asia Minor

XI.1.3. Global ocean

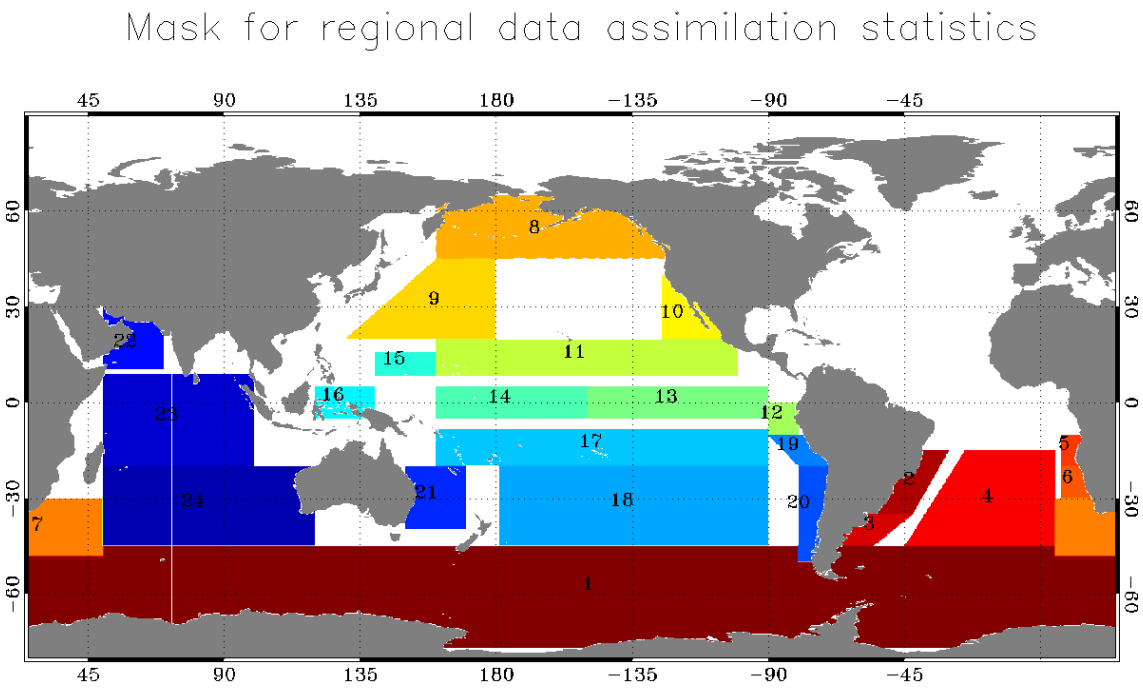

1	Antarctic Circumpolar Current
2	South Atlantic
3	Falkland current
4	South Atl. gyre
5	Angola
6	Benguela current
7	Aghulas region
8	Pacific Region
9	North Pacific gyre
10	California current
11	North Tropical Pacific
12	Nino1+2
13	Nino3
14	Nino4
15	Nino6
16	Nino5
17	South tropical Pacific
18	South Pacific Gyre
19	Peru coast
20	Chile coast
21	Eastern Australia
22	Indian Ocean
23	Tropical indian ocean
24	South indian ocean